



**Tomas Bata University in Zlín**  
**Faculty of Technology**

Doctoral Thesis

**The study of foodstuff rheological and thermal  
properties**

**Studium reologických a termických vlastností potravin**

Author: **Ing. Tomáš Valenta**

Degree programme: P2901 Chemistry and Food Technology

Degree course: 2901V013 Food Technology

Supervisor: doc. Mgr. Barbora Lapčíková, Ph.D.

Examiners: prof. Ing. Marián Valko, DrSc.  
doc. RNDr. Iva Burešová, Ph.D.

Zlín, November 2018

© Tomáš Valenta

The publication was issued in the year 2018.

*Key words: rheological properties, thermal properties, viscosity, moisture content, enthalpy, hydrocolloids, polysaccharides, kinetic models*

*Klíčová slova: reologické vlastnosti, termické vlastnosti, viskozita, obsah vlhkosti, entalpie, hydrokoloidy, polysacharidy, kinetické modely*

Full text of the doctoral thesis is available in the Library of TBU in Zlín.

## SUMMARY

The Doctoral Thesis deals with the issue of rheological and thermal properties of foodstuffs and additives based on polysaccharides and proteins which are widely used as food hydrocolloids.

Rheological analysis was used to determine intrinsic viscosity and flow parameters of polysaccharide solutions (guar gum,  $\kappa$ -carrageenan, xanthan gum) and gelatin/polysaccharide blends. Using suitable rheological models (Ostwald-de Waele and Herschel-Bulkley model), it was possible to define temperature and concentration dependency of flow parameters, the effect of solvent used and to examine the conformational transition of the dissolved polymers.

Rheological analysis of polysaccharides solutions both in distilled water and 0.07M KCl in the temperature range from 20 to 45 °C confirmed the concentration dependency of the solutions viscosities as reflected in observed changes of flow parameters. The consistency coefficient ( $k$ ) of the solutions increased with concentration, whereas the flow behaviour index ( $n$ ) decreased in all studied hydrocolloids except xanthan gum aqueous solutions. Temperature had an opposite effect in comparison to one obtained for concentration dependencies;  $k$  decreased with temperature, while  $n$  increased. However, xanthan gum both in water and KCl exhibited a different pattern of the flow parameters dependencies on temperature, and provided some specific properties, such as relatively viscous solutions at higher temperatures, and a noticeable yield stress in the whole studied temperature range. The transition from double helical polysaccharide structure to single coil conformation (in salt solution) and the disentanglement of coils' chains (in distilled water) promoted by elevating temperature were proved at temperature about 30 °C by a detectable change of the Kraemer constant temperature dependency.

Gelatin/polysaccharide blends in 0.07M KCl and 0.07M NaCl solutions were studied in the temperature range 25-45 °C by the same rheological models. Flow parameters of the blends were affected by the conformational change of the polysaccharide (helix-coil transition), as well as by the conformational ordering of gelatin, characterized by the dissociation of gelatin triple helices into flexible coils, and gel-sol transition. There was an evident change of the parameters at temperature about 35 °C. Rheological and other functional properties (conductivity) of the blends were substantially influenced by the type of salt solution. The type of salt solvent had also an effect on gelation properties of gelatin/ $\kappa$ -carrageenan blends; these mixtures in NaCl created a gel of high consistency at ambient temperature (20-25 °C), whereas in KCl did not gel in the studied temperature range, nor at refrigerated conditions (ca. 4 °C).

Thermogravimetric analysis and differential thermal analysis were employed to determine thermal properties of powder polysaccharides (guar gum,  $\kappa$ -carrageenan and xanthan gum). The results of thermal analysis showed that powder samples exhibit varying ability to bind moisture depending on their

structure. The temperature of the endothermic process (polysaccharide order-disorder transition) was determined at different heating rates. Peak temperature of the endotherm was found in the range 50-85°C, influenced by the applied heating rate and moisture content of the sample. Activation energy ( $E_a$ ) of the phase transition associated with the kinetics of water evaporation was calculated by several kinetic models (Friedman model, Kissinger model, and Model-free kinetics).

The Arrhenius model was used to evaluate the temperature resistance of the molecular structure of hydrocolloid water and salt solutions, prepared from the powders.  $\kappa$ -carrageenan provided the highest temperature resistance of its polymer network among all solutions, whereas xanthan gum was the least temperature dependent sample. Results of the Arrhenius model also indicate that energy necessary to promote viscous flow of solutions is higher for samples in distilled water than in 0.07M KCl, suggesting the ion-induced assembly of molecular chains in salt solution. In both cases,  $E_a$  was substantially reduced by application of higher shear rate.

## ABSTRAKT

Disertační práce se zabývá problematikou reologických a termických vlastností potravinářských látek a aditiv na bázi polysacharidů a proteinů, jež jsou hojně využívány jako potravinářské hydrokoloidy.

Reologická analýza byla využita ke stanovení vnitřní viskozity a tokových parametrů roztoků polysacharidů (guarové gummy,  $\kappa$ -karagenanu, xanthanové gummy) a směsí želatiny a polysacharidu. S využitím vhodných reologických modelů (Ostwald-de Waeleho a Herschel-Bulkleyho modelu) bylo možné určit teplotní a koncentrační závislost tokových parametrů roztoků, vliv použitého rozpouštědla a stanovit konformační přechod rozpuštěných polymerů.

Reologická analýza roztoků polysacharidů v destilované vodě a 0,07M KCl v teplotním rozmezí od 20 do 45 °C potvrdila závislost viskozity roztoků na jejich koncentraci, což se projevilo v pozorování příslušných změn tokových parametrů. Koeficient konzistence ( $k$ ) roztoků narůstal s rostoucí koncentrací, zatímco index toku ( $n$ ) klesal u všech studovaných vzorků s výjimkou vodných roztoků xanthanové gummy. Teplota vykazovala opačný efekt ve srovnání s koncentrační závislostí; hodnota  $k$  klesala s teplotou, kdežto hodnota  $n$  se s teplotou zvyšovala. Nicméně xanthanová guma ve vodě i v KCl poskytovala odlišné schéma závislosti tokových parametrů na teplotě, a vykazovala některé specifické vlastnosti, jako relativně viskózní roztoky při vyšších teplotách a poměrně značnou mez toku (prahové smykové napětí) v celém studovaném teplotním rozmezí. Přechod z polysacharidové struktury dvojšroubovic na konformaci jednoduchých klubek (v solném roztoku) a proces rozplétání řetězců klubek (v destilované vodě) stimulované zvýšením teploty byly prokázány při teplotě kolem 30 °C nárůstem teplotní závislosti Kraemerovy konstanty.

Pomocí stejných reologických modelů byly v teplotním rozmezí 25 až 45 °C studovány směsi želatiny a polysacharidu v 0,07M KCl a 0,07M NaCl. Tokové parametry směsí byly ovlivněny konformační změnou polysacharidu (přechod dvojšroubovice-klubko) i konformačním uspořádáním želatiny (přechodem z uspořádané do neuspořádané struktury, jenž je charakterizován disociací želatinových trojšroubovic do pružných klubek), a také gel-sol přechodem želatiny. Změna tokových parametrů byla patrná při teplotě kolem 35 °C. Reologické a jiné funkční vlastnosti (vodivost) směsí byly podstatně ovlivněny typem solného roztoku. Typ solného rozpouštědla měl též vliv na gelovatění směsí želatiny a  $\kappa$ -karagenanu. Uvedené směsi v NaCl vytvořily gel husté konzistence při okolní teplotě (20-25 °C), zatímco v KCl nenastal proces gelovatění ve studovaném teplotním rozmezí ani při ledničkových teplotách (cca 4 °C).

Pro stanovení tepelných vlastností práškových polysacharidů (guarové gummy,  $\kappa$ -karagenanu a xanthanové gummy) byla použita termogravimetrická analýza a diferenciální termická analýza. Výsledky termické analýzy ukázaly, že práškové vzorky mají různou schopnost vázat vlhkost v závislosti na jejich struktuře. Teplota endotermního procesu (přechodu polysacharidu z uspořádané do neuspořádané struktury) byla stanovena při různých rychlostech ohřevu. Teplota endotermního píku byla zjištěna v rozmezí 50-85 °C, a byla ovlivněna aplikovanou rychlostí ohřevu a vlhkostí vzorků. Aktivační energie ( $E_a$ ) fázového přechodu spojená s kinetikou odpařování vody byla vypočtena na základě několika kinetických modelů (Friedmanova modelu, Kissingerova modelu a Model-free kinetics).

Arrheniův model byl použit k vyhodnocení teplotní rezistence molekulární struktury vodných a solných roztoků hydrokoloidů, připravených z příslušných práškových polysacharidů.  $\kappa$ -carrageenan vykazoval nejvyšší teplotní odolnost polymerní sítě ze všech vzorků, zatímco xanthanová guma byla nejméně závislá (z hlediska zahájení viskózního toku) na teplotě. Výsledky Arrheniova modelu též naznačují, že energie potřebná pro viskózní tok roztoků je vyšší u hydrokoloidů v destilované vodě než v 0,07M KCl, což by mohlo implikovat vznik iontově-indukované struktury molekulárních řetězců v solném roztoku. V případě obou typů roztoků byla  $E_a$  podstatně redukována aplikací vyšší smykové rychlosti.

# CONTENT

SUMMARY.....	3
ABSTRAKT .....	4
CONTENT.....	6
ACKNOWLEDGEMENTS .....	8
INTRODUCTION .....	9
1. THE CURRENT STATE OF ART .....	12
1.1 Rheology of food products and additives .....	12
1.2 Thermal analysis of food products and additives .....	13
2. FOOD RHEOLOGY .....	16
2.1 Rheological properties of food products.....	17
2.1.1 Concentration regimes effect .....	17
2.1.2 Shear dependency of the viscosity.....	18
2.1.3 Significance of yield stress in food products.....	19
3. THERMAL ANALYSIS .....	20
3.1 Thermoanalytical methods and techniques.....	20
3.1.1 Thermogravimetric analysis .....	20
3.1.2 Differential thermal analysis .....	21
3.1.3 Differential scanning calorimetry.....	22
3.2 Thermal properties of food products.....	23
3.3 Kinetics study using thermal analysis.....	23
4. HYDROCOLLOIDS EXAMINED IN THIS STUDY .....	26
4.1 Guar gum .....	26
4.2 $\kappa$ -carrageenan.....	26
4.3 Xanthan gum.....	27
4.4 Gelatin.....	28
5. AIMS OF THE THESIS.....	30
6. MATERIALS AND METHODS .....	31
6.1 Rheological analysis of polysaccharide solutions .....	31
6.1.1 Materials .....	31
6.1.2 Preparation of solutions.....	31
6.1.3 Rheological analysis .....	31
6.1.4 Kraemer equation .....	32

6.2	Thermal and temperature dependency of polysaccharide hydrocolloids .....	33
6.2.1	<i>Materials and conditioning</i> .....	33
6.2.2	<i>Thermal analysis of powders</i> .....	33
6.2.3	<i>Kinetic models</i> .....	34
6.2.4	<i>Arrhenius model</i> .....	35
6.3	Functional properties of gelatin-polysaccharide blends.....	36
6.3.1	<i>Materials</i> .....	36
6.3.2	<i>Preparation of blends</i> .....	36
6.3.3	<i>Rheological analysis</i> .....	36
6.3.4	<i>Arrhenius model</i> .....	37
6.3.5	<i>Other analyses</i> .....	37
6.4	Statistical analysis of the data .....	37
6.4.1	<i>Statistical analysis of rheological parameters</i> .....	37
6.4.2	<i>Statistical analysis of thermal parameters</i> .....	38
7.	<b>RESULTS AND DISCUSSION</b> .....	40
7.1	Rheological properties of polysaccharide solutions.....	40
7.1.1	<i>Flow parameters</i> .....	40
7.1.2	<i>Intrinsic viscosity</i> .....	49
7.2	Thermal and temperature dependency of polysaccharide hydrocolloids .....	56
7.2.1	<i>Thermal analysis - endothermic transition and moisture content</i> .....	56
7.2.2	<i>Thermal stability of polysaccharide powders</i> .....	63
7.2.3	<i>Kinetic models</i> .....	64
7.2.4	<i>Arrhenius parameters</i> .....	70
7.3	Functional properties of gelatin-polysaccharide blends.....	76
7.3.1	<i>Rheological analysis</i> .....	76
7.3.2	<i>Arrhenius parameters</i> .....	83
7.3.3	<i>Other analyses</i> .....	86
8.	<b>CONTRIBUTION TO SCIENCE AND PRACTICE</b> .....	89
	<b>CONCLUSION</b> .....	91
	<b>REFERENCES</b> .....	93
	<b>LIST OF FIGURES</b> .....	102
	<b>LIST OF TABLES</b> .....	104
	<b>LIST OF SYMBOLS AND ABBREVIATIONS</b> .....	105
	<b>LIST OF PUBLICATIONS</b> .....	107
	<b>CURRICULUM VITAE</b> .....	108

## **ACKNOWLEDGEMENTS**

I would like to express my deep gratitude to my supervisor, doc. Mgr. Barbora Lapčíková, Ph.D., for her guidance, constant support and motivation throughout my Ph.D. study, which contributed to the completion of my doctoral thesis.

My thanks are also extended to my consultant prof. Ing. Lubomír Lapčík, Ph.D., for his abiding help.

Finally, I am grateful for material and technical support to the laboratory workers and administrative employees of the Department of Food Technology at Faculty of Technology, Tomas Bata University in Zlín.



## INTRODUCTION

Rheological and thermal character of food products and additives have a major impact on the food functional properties, shelf life, quality and sensory attributes. Rheological and thermal properties play an important role in the production and storage of many different foods and beverages, and these properties are also important in view of the consistency and overall attractiveness of the products for consumers.

Rheological analysis of food products is particularly important in the field of food quality management. Liquid and semi-solid foods (as the mixtures of biochemical compounds) show a great diversity in their rheological behaviour. Liquid foods, which contain a relatively high amount of dissolved low-molecular substances (e.g., simple carbohydrates) and no substantial amount of polymeric or solid insoluble particles, show Newtonian behaviour. However, even a small amount of dissolved polymer (an additive) about 1 % (w/w) can dramatically increase viscosity of the product and change its Newtonian behaviour (typical for water and diluted solutions) to non-Newtonian behaviour of water dispersions. For that reason, it is usually very difficult to predict the viscosity of liquid foods (Pavlínek et al., undated).

In recent years, a number of studies have reported on the functional aspects of hydrocolloids and their application within food systems. Many hydrocolloids are widely used in the food industry to extend food shelf life, improve rheological properties of food products and encapsulate flavour compounds. The principal reason for the extensive use of hydrocolloids in the food industry is their ability to bind with water and to modify the properties of food ingredients (Mohammadi et al., 2014; Silva et al., 2014; Varela & Fiszman, 2011).

Moreover, it seems to be only a matter of time before the physiological attributes of food hydrocolloids will be exploited in the new healthy products. So far, the physiological properties of individual hydrocolloids, particularly polysaccharides, have attracted relatively little attention from food scientists in contrast to their technological aspects. From a nutritional point of view, protein hydrocolloids also attract relatively little attention since the national diet in most industrialised countries is generally more than adequate in protein but high in fat and low in fibre and complex carbohydrates, i.e., in starch and non-starch polysaccharides (of small intestinal digestibility). A greater opportunity for the development of novel food combinations containing food hydrocolloids which are targeted at specific consumer groups (*functional foods*) could provide many positive physiological effects on the human health (e.g., reduction of plasma cholesterol, alteration of fat absorption, prevention of some degenerative diseases such as *diabetes mellitus*, coronary artery disease, cancer of the colon and others) (Topping, 1993).

From a chemical point of view, hydrocolloids are mainly polysaccharides obtained from different sources. They are present in various parts of edible

plants (starch, guar gum), of algae (carrageenan), of fungi and microorganisms (xanthan gum) (Rhein-Knudsen et al., 2017; Tomasik, 2004). In general, food hydrocolloids are a diverse group of long-chain polymers that are readily dispersive, fully or partially soluble, and prone to swell in water. They change the physical properties of the solution to form gels or enable thickening, emulsification, coating, and stabilization. More specifically, hydrocolloids are able to emulsify oil/water in water/oil systems (e.g., ice cream, yoghurt), enhance the food elasticity and thickness, and retain moisture. Hydrocolloids have also applications in crystallization inhibition (Shao et al., 2014; Viebke et al., 2014).

Although food hydrocolloids are usually present in the final products at concentration less than 1 % (w/w), they may significantly affect rheological, textural, organoleptic and other properties of many different foods. For example, guar gum provides relatively high viscosity to the liquid foods even at low concentrations, and this fact can be a limiting factor in the relevant production (Cevoli et al., 2013; Nor Hayati et al., 2016; Williams & Phillips, 2009).

According to the type of flow behaviour, most solutions of food hydrocolloids are shear-thinning, meaning their viscosity decreases when the shear rate is increased. Shear-thickening means that the viscosity increases with the increase of shear rate. An example of shear-thickening fluid is uncooked corn starch paste where shear stress squeezes the water from between the starch granules allowing them to grind against each other; this property is often used in sauces (e.g. tomato sauce) (Shao et al., 2014).

As stated above, food hydrocolloids have the ability to hold water and form a gel-like structure due to their specific properties. In other words, they can be dispersed in water forming viscous dispersions or gels, and thus, they are extensively used as thickening and gelling agents. The hydrophilic character of the hydrocolloids is based on the presence of a large number of hydroxyl groups which enhance the affinity of hydrocolloid chains to water molecules. In addition, food hydrocolloids provide the dispersions of a character between a true solution and a suspension, exhibiting colloidal properties (Chivero et al., 2015; Saha & Bhattacharya, 2010). The water holding capacity of hydrocolloids plays an important role in food industry and is tightly related to some processes such as syneresis. Syneresis depends on the type of solid and its concentration in the gel, and can be undesirable in some products (e.g., jelly) but may be useful, among others, in cheese production (Gyawali & Ibrahim, 2016; Li & Nie, 2016). This is of decisive importance for using the hydrocolloids in different food products, i.e., to overcome possible imperfections during food production. Moreover, the combinations and mixtures of several hydrocolloids can exhibit strong synergistic effects in the overall flow profile (BeMiller, 2011; Nor Hayati et al., 2016; Schorsch et al., 1997). In all cases, the influence of additives on the rheological and other functional properties of final products is necessary to determine before the beginning of mass production.

Besides rheology, other important method, which is now being used more and more in food applications to evaluate functional properties of food products and additives, is thermal analysis.

Thermoanalytical methods are widely performed to determine thermal stability, temperature effects, phase changes and chemical reactions of many different materials. In food industry, these methods enable to analyse the temperature changes which the food products are exposed to during their manufacture, transport, storage, kitchen preparation and consumption. Thermal analysis also contributes to optimization of food processing conditions, and is of considerable importance in food quality control management, regarding the fact that thermal properties of food products are directly related to the quality and durability of the food. The results of thermal analysis are very specific for each type of food, and any change in the composition, moisture content, conformation of chemical components, etc., provides different values of thermal parameters (Behlau & Widmann, 2003).

Before the initiation of thermal analysis, it is necessary to consider what types of food samples are studied, which thermal events can be expected and how can be demonstrated on the thermoanalytical curves. For example, the range of enthalpy changes and observation of endothermic or exothermic peaks should be reflected on. Considering these facts, it is necessary to decide in which temperature programme the expected changes will be adequately performed and which simultaneous methods can be used to detect the thermal events. The basic problem of all thermoanalytical methods, including thermal analysis of food, is the correlation between the data obtained and the thermal events which occur in the studied sample (Kloužková et al., 2012).

Thermoanalytical techniques can be used for the kinetic analysis of many different samples, including food materials. Knowledge of kinetic parameters, such as activation energy and degree of conversion, plays an important role in determining structural properties and reaction mechanisms of various products. The kinetic data are very useful for many technological processes, e.g., thermal decomposition of energetic materials, oxidation and combustion (degradation) of (bio)polymers, thermal transition and crystallization, etc.

For kinetics study, it is also important to set the right measuring conditions. Primarily, the isothermal and non-isothermal runs must be distinguished. Compared with isothermal kinetic experiments, non-isothermal runs are more effective and convenient to implement because it is not necessary to perform a sudden temperature jump of the sample at the beginning of heating/cooling procedure. For that reason, the isoconversional (non-isothermal) experiments are now being used to a much greater extent (Cai et al., 2018; Ramajo-Escalera et al., 2006; Vyazovkin & Wight, 1999).

# 1. THE CURRENT STATE OF ART

## 1.1 Rheology of food products and additives

Rheology of biopolymer solutions, particularly in a dilute form, has been extensively examined to gain insight into the structure and conformation of polymers in the solutions. In many technologies, (bio)polymers are nowadays used to control solution rheology, which provides information on the dynamics of individual polymer chains (Bock et al., 1994). The conformational properties play also an important role in food technology, and an increasing rheological research of the biopolymers, especially polysaccharides and proteins, can be expected in the following years.

The relevance of food rheology at the present time can be summarised into several categories: a plant design, quality control, sensory attributes of food products, and the research and development of food structure. The plant design, pumps and pipe sizing, heat and mass transfer calculations, as well as process engineering of mixers, coaters, homogenisers, etc., are based to a large extent on rheological data (McKenna & Lyng, 2003).

The quality control of raw material and products at different stages of the manufacturing process (including ingredient functionality determination and shelf life testing), and the evaluation of sensory attributes of these products also involve the rheological measurements. For instance, the correlation between sensory data and rheological data can be assessed. Last but not least, the investigation of rheological behaviour of food structure and conformation of its molecular components is very important aspect of the present research (McKenna & Lyng, 2003).

Overall, many areas of food industry require valuable scientific data on rheological behaviour of different food products and additives. Therefore, there is a great value in extending scientific research on the rheology of various solutions and mixtures, based on hydrocolloids. For instance, the assessment of structure and conformational changes in relation to the flow behaviour of polysaccharide/proteins solutions (the biopolyelectrolyte complexes) seems to be a promising research area.

The biopolyelectrolyte complexes (PECs), which are formed by oppositely charged polysaccharides and proteins, were largely investigated in the last years. The research was particularly focused on the physicochemical properties of the complexes, including rheological and gelation behaviour of food biopolymers employed in PECs (Derkach et al., 2015a; Derkach et al, 2015b; Kumbár et al., 2017; Viebke et al., 1994).

Other investigations in the field of biopolyelectrolyte complexes can bring great benefit in extending our knowledge of the protein/polysaccharide electrostatic complexation. Notably, the study of electrostatic interaction between gelatin and polysaccharides seems to have a significant importance for new practical applications of PECs in the food industry, i.e., for manufacturing

of various food products. Polyelectrolyte complexes of polysaccharides and proteins provide several unique properties (e.g., emulsion stabilization, flavour encapsulation, modification of low-calorie food products) which can be very useful in many food applications. These complexes can also be used as new types of emulsifiers (Cao et al., 2016; Derkach et al., 2015a), and possibly could serve as ingredients in dietary supplements. The production of dietary supplements and dietary food is one of the main trends in the food industry nowadays, particularly due to the fact that these products can substitute the diet based on high consumption of simple sugars. In other words, the consumption of dietary products involving PECs can prevent some diseases such as diabetes resulting from an unhealthy diet (Li & Nie, 2016).

It is also possible to obtain new modifications of rheological properties of gelatin-based products using gelatin-polysaccharide combinations of PECs. Gelatin in food production is limited by its rheological properties, thermal stability, etc., but the formation of polyelectrolyte complexes allows the compatibility of gelatin with different ionic polysaccharides, such as guar gum, xanthan gum and kappa-carrageenan. Moreover, the specific hydrophilic and polydisperse character of gelatin provides the electrostatic complexes a great nutritional value, favourable in the production of dietary food (Derkach et al., 2015a).

Structural and conformational properties of food matrices and their changes, depending on the physicochemical factors of production and storage conditions, can significantly affect flow behaviour and functional characteristics of the final products. From this point of view, the laboratory evaluation and scientific research of food rheological behaviour is an absolute necessity for the optimization of the production process.

## **1.2 Thermal analysis of food products and additives**

The application of thermal analysis (TA) in food technology is relatively new. Thermal analysis has been mainly used as a standard method for investigation of polymers. The processes of conversion in complex foods and pure food components (such as denaturation of proteins) exhibit, in many cases, only very low energy changes. This places very high demands on the measuring instruments and evaluation softwares; as found, TA techniques provide good performance standards. At present time, thermal analysis became generally accepted scientific method of food research and development. Above all, differential scanning calorimetry (DSC) is now being used in the food industry even for routine process analysis and quality control (Behlau & Widmann, 2003).

The results of thermal analysis of food products, additives and functional ingredients, dependent on their structure, conformation and transition processes, can bring new knowledge useful for practical application in food production.

Nowadays thermal analysis of food products is managed to reliably determine thermal stability of particular food complexes (Behlau & Widmann, 2003). Additionally, TA techniques enable to investigate the influence of changing heating/cooling rate, atmosphere, stress and other conditions on the transitions of individual food components. Using thermal analysis, it is also possible to determine how the previous treatment and conditioning of the sample (so-called *thermal history*) affect the physico-chemical properties of the foodstuffs. Based on thermal data, the quality of food products can also be assessed in terms of their structure and macromolecular composition.

In recent years, thermal properties of food hydrocolloids have been intensively studied. In particular, thermal behaviour of starch in relation to its gelatinization and glass transition temperature, swelling of starch granules, and ratio of amylose and amylopectin in these granules were characterized in detail (Bogacheva et al., 2002; Gryzkin et al., 2014; Homer et al., 2014).

However, there is a lack of knowledge about phase transition, thermal kinetics and temperature dependency of several food additives. First of all, there is clearly great value to extend previous studies about thermal properties of pure powder polysaccharides and the molecular sensitivity of their solutions to temperature. The future research can be also focused to explore structural and phase changes of hydrocolloids during their storage and various heating/cooling conditions.

For most additives, it is necessary to know their thermal stability, moisture content and water binding capacity, as well as structural and phase transition temperatures (i.e., temperatures of thermal events), which influence the manufacturing of the additives (Iqbal et al., 2013).

From practical point of view, the determination of transition temperatures becomes increasingly important in food technology. For instance, the glass transition temperature is closely connected to the stability considerations of sweets, other amorphous dried foods and deep-freeze processes (Behlau & Widmann, 2003).

An increasing number of scientific publications, which are focused on thermoanalytical evaluation of reaction kinetics, indicate the applicability of TA in the production processes. Obtaining kinetic data by thermal analysis brings practical problems of correct measurement and the necessity of data verification. Many factors can affect the kinetic parameters obtained by thermal processing (process conditions, heat and mass transfer restrictions, physico-chemical heterogeneity of the sample, etc.). Hence, the measurements are standardized and optimal evaluation of experimental data comes to the centre of scientific attention (Cai et al., 2018).

Non-isothermal (isoconversional) methods of TA are more suited for the calculation of activation energy and other kinetic parameters. Using these methods, it is possible to eliminate the uncertainty in determining kinetic parameters of the reaction. Because model-fitting approach can provide very

different values of kinetic parameters, the use of non-isothermal kinetic methods seems to be the best solution how to obtain reliable data. With respect to this problem, the scientists compare the equations for obtaining effective activation energies, the advantages and disadvantages of various isoconversional methods, as well as analytical methods for extracting reliable kinetic data from thermal experiments (Cai et al., 2018). For example, Saddawi et al. (2010) investigated the question of the most appropriate method for extracting kinetic data from thermogravimetric analysis of woody biomass decomposition; the authors also examined what kinetics are the most suitable forms for description of high heating rate thermal decomposition processes.

It could be possible to present many other questions and tasks related to the issue of kinetic parameters and mechanisms of thermal reactions, and it can be assumed that the research will be intensively focused on this topic in the future.

## 2. FOOD RHEOLOGY

Rheology is the branch of physics focused on the way in which materials deform or flow in response to applied forces or stresses. In the context of physics, “flow” can be defined as continuous deformation over time. The ability to flow is not only possessed by gases and liquids, but also by solids to a varying degree. Unlike solids, liquids flow under the shear stress caused by their own weight. A shear stress causes a continuously increasing strain, i.e., a constant shear rate which is the ratio between tangential velocity and radius of the applied rotation. Therefore, the fluids respond not only to an applied stress by the flowing, but also to the changes in stress by the changes in speed of their flowing (flow rate).

For liquids, the simplest rheological equation is Newton’s law of viscosity, according to which the stress is proportional to the rate of straining:

$$\tau = \eta \cdot \dot{\gamma} \quad (2.1)$$

where  $\tau$  is the shear stress,  $\eta$  - the dynamic viscosity,  $\dot{\gamma}$  - the shear rate (velocity gradient) (Macosko, 1994).

The Newtonian fluid is the basis for classical fluid mechanics. Most small molecules liquids like water and oils are Newtonian. However, many colloidal suspensions and (bio)polymer solutions do not obey the simple linear relation between shear stress and shear rate. Nearly all these non-Newtonian fluids provide a viscosity that decreases with increasing velocity gradient in shear. This *shear-thinning* (*pseudoplastic*) behaviour occurs in a wide range of materials, including hydrocolloid solutions. Some concentrated suspensions (e.g., starch-water suspensions) show *shear-thickening* (*dilatant*) behaviour, which is characterized by an increasing viscosity with increasing  $\dot{\gamma}$ .

Many important kinds of food products lie between the ideal elastic solid and ideal viscous fluid. For instance, mayonnaise is a typical example of shear-thinning substance. If mayonnaise is left on a piece of bread subject only to gravity stresses, it will barely move, but when sheared by a knife it spreads easily. In contrast, honey, which is more viscous than mayonnaise at high stresses, will slowly run through holes in the bread. The viscosity of honey is relatively constant, but the viscosity of mayonnaise is strongly dependent on the shear stress (Macosko, 1994).

A number of food products exhibit a rheological property called yield stress  $\tau_0$  which must be overcome in order to flow or to deform a substance. Also, the yield stress represents a minimum shear stress needed to be exceeded before the liquid (material) is able to flow (Figura & Teixeira, 2007).

Examples of several flow curves (various fluid types) are illustrated in Fig. 2.1.



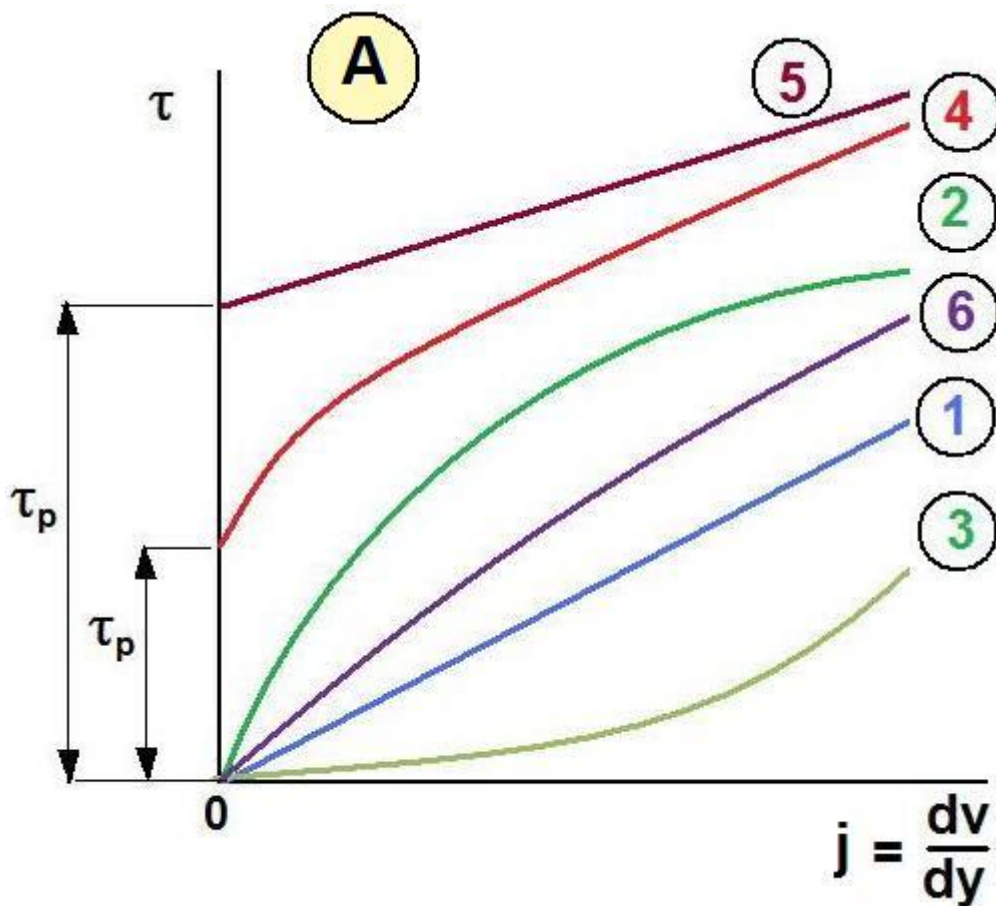


Fig. 2.1. Flow curves of shear stress  $\tau$  versus shear rate  $\gamma$  (with a yield stress  $\tau_p$ ) representing different fluids: 1 – Newtonian fluid; 2 – shear-thinning (pseudoplastic) fluid; 3 – shear-thickening (dilatant) fluid; 4 – real plastic fluid; 5 – Bingham ideal plastic fluid; 6 – Eyring model of fluid (Janalík, 2010).

## 2.1 Rheological properties of food products

### 2.1.1 Concentration regimes effect

Important factors of the rheological behaviour of food macromolecules involve molecular size, shape and flexibility. An appropriate parameter of macromolecular chain stiffness is the ratio of the contour length  $L$  of a chain to the length  $b$  of a statistical segment unit comprising  $n$  monomers. A ratio  $L/b > 10$  would be required for the polymer conformation to be regarded as a coil (Pruska-Kedzior & Kedzior, 2007).

Three concentration domains can be distinguished in biopolymer solutions: *dilute* regime at concentration lower than critical concentration  $c^*$  ( $c < c^*$ ), *semidilute* regime at concentration between two critical concentrations  $c$  ( $c^* < c < c^{**}$ ), and *concentrated* regime at concentration  $c > c^{**}$ .

In a very dilute solution, the volume available to each polymer molecule is much higher than that of the individual coil. The coils remain statistically far

from each other, and their contacts can be considered as infrequent. The coils maintain the dimensions of an isolated chain. In this low-concentration region, the hydrodynamic forces can be neglected (except only the Brownian motion which is acting against structural forces).

Above critical overlap concentration  $c^*$ , in semidilute regime, the polymer coils fill the volume of the solution. There is a progressive interpenetration of the coils, concomitant with a contraction of their individual volume. The solution becomes a transient network of entangled chains, although the coils still retain some degree of individuality. The progressive coil contraction and increasing entanglement density govern the rheological behaviour of semidilute solution, provided the molecular weight of the polymer above a critical value ( $M > Mc$ ). At the upper limit of the semidilute regime, the solution is about 100 times more viscous than the solvent because of the increase of entanglement density.

At higher concentrations above  $c^{**}$ , the polymer solution becomes an entanglement network where the chains have completely lost their individual character. Once the entanglement network is formed, the low-energy interactions develop between chains in the regions of entanglements, and the possibility of forming some junction zones appears. These junction zones exhibit lifetimes much longer than those of entanglements. The system has then shifted from the state of an entangled solution to the state of a *physical gel*.

Food polysaccharide solutions (e.g., guar gum, carrageenans) and food proteins (like whey proteins, collagen, etc.) as well as polysaccharide-protein mixtures exhibit this dependency of the molecule's state on solution concentration (Pruska-Kedzior & Kedzior, 2007).

### 2.1.2 Shear dependency of the viscosity

The non-Newtonian shear behaviour is typical for polymer solutions at concentration  $c > c^*$ . Below a critical shear rate value  $\dot{\gamma}_{crit}$ , the flow curve of the solutions shows the low-shear Newtonian plateau, where the viscosity holds a constant value  $\eta_0$ . Above  $\dot{\gamma}_{crit}$ , a shear-thinning region (where the viscosity decreases as shear rate increases) follows. At high shear rates, the viscosity tends to a second plateau, characterized by the value  $\eta_\infty$ . Due to instrumental limitations and flow instability, this high-shear Newtonian plateau is rarely observed experimentally, and it can be neglected in the most cases.

The flow curve of a concentrated biopolymer solution reflects the effect of shear rate on entanglement density. If  $\dot{\gamma}$  is low enough, the system remains in its equilibrium fully entangled state ( $\eta = \eta_0$ ). As  $\dot{\gamma}$  increases, the entanglement density and the viscosity decrease. Concentrated solutions are viscoelastic by nature; therefore, they do not respond instantly to the changes in shear rate or stress value. The constant equilibrium viscosity is reached at a given shear rate only after a long enough time, sometimes even after a few days (Pruska-Kedzior & Kedzior, 2007).

### **2.1.3 Significance of yield stress in food products**

Yield stress is a characteristic of plastic flow behaviour; it means that a liquid not begin to flow until a minimum shear stress is provided, and a solid material keeps its deformation as a permanent set after taking away the shear stress. A great example of this type of behaviour is butter, which looks like a solid, but can be deformed and keeps its plastic deformation. When a solid body is loaded with a shear stress below its yield stress, it can be deformed elastically, but will not flow.

In the case of liquids, the plasticity also stems from strong intermolecular interactions between the molecules within the molecular structure. The stronger are these interactions, the higher the yield stress. Yield stress also depends on the temperature. For instance, butter kept cold in the refrigerator will have a much higher yield stress than if we leave it out at room temperature (Figura & Teixeira, 2007).

Yield stress in food products may lead to some serious processing problems with significant economic losses, particularly in the manufacturing of coatings for enrobed food products. The coatings may range from chocolate enrobed confectionery to batter enrobed fish or meat products; all these products demand an enrobing material that exhibits a yield stress. If the yield stress is too low, the weight of enrobing liquid adhering to the sides of the product will induce a stress in excess of the yield stress, either on the vertical side or on a plane parallel to this within the enrobing material, and will cause the material to flow off the product. Conversely, too high a yield stress will lead to excessive thickness of enrobing material possibly attractive to the consumer of a chocolate bar, but with unfavourable economic consequences for the manufacturer (McKenna & Lyng, 2003).

In the preparation of certain meals, it is also important to achieve a needed yield stress. For example, whipped cream must have a sufficiently high yield stress in order to hold its shape as a decorative dessert topping (Figura & Teixeira, 2007).

### **3. THERMAL ANALYSIS**

According to the definition by ICTAC (International Confederation for Thermal Analysis and Calorimetry), thermal analysis is „*a group of techniques that study the relationship between a sample property and its temperature*“ (Wagner, 2009).

From a general point of view, thermal analysis is a term used for a range of thermoanalytical techniques which involve the measurement of physical and chemical properties of a sample as a function of temperature or time. The sample is subjected to a temperature program, which consists of a series of preselected segments in which the sample is heated or cooled at a constant rate or held at a constant temperature. A higher heating rate improves the sensitivity of the measurement, but on the other hand reduces the differentiation between simultaneous thermal events. In many experiments, the atmosphere of inert or oxidizing gases plays also an important role (Behlau & Widmann, 2003; Gorodylová et al., 2015; Kloužková et al., 2012).

The data produced in a thermal analysis experiment are displayed as a thermoanalytical curve in a thermoanalytical diagram. Frequently, several different measured signals are displayed at the same time (simultaneous measurements). The focus of the analysis is usually the interpretation of thermal effects in which the measured signal changes more or less abruptly (Wagner, 2009).

#### **3.1 Thermoanalytical methods and techniques**

##### **3.1.1 Thermogravimetric analysis**

Thermogravimetric analysis (TGA) is a method based on recording of sample mass as a function of temperature and time. For that reason, TGA is useful for the investigation of effects which involve mass changes, such as dehydration, decomposition, oxidation and others (Gorodylová et al., 2015).

Thermogravimetric measurement is performed in a defined atmosphere, usually in inert conditions (nitrogen) or in an oxidative environment (air or oxygen). The mass is measured with a highly sensitive electronic balance. Interfering buoyancy or gas flow effects are compensated by a blank curve correction. Thermogravimetric analysis provides information on the content of volatile components such as solvents or water, on decomposition behaviour, and also on the ash or filler content (Behlau & Widmann, 2003).

An example of a typical TGA curve of a polysaccharide sample is illustrated in Fig. 3.1.

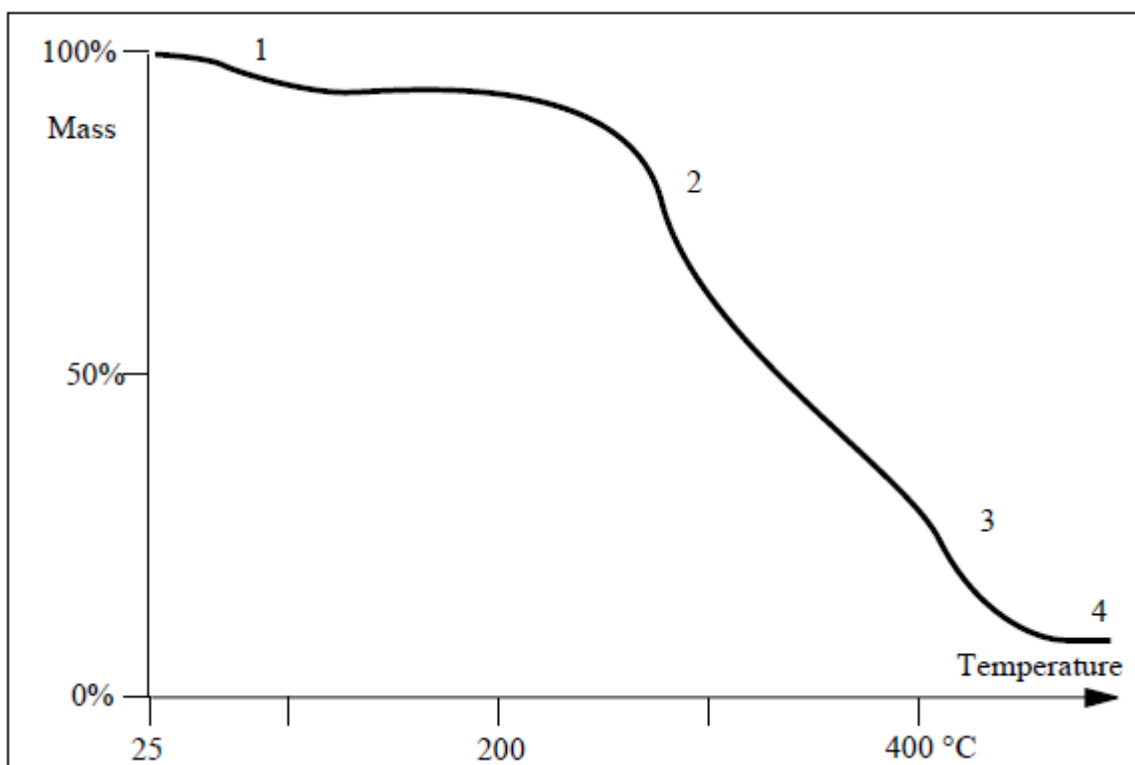


Fig. 3.1. A typical TGA curve of a polysaccharide thermally treated under air conditions. The numbers denote the following components or processes:  
 1 – volatile components (moisture); 2 – decomposition (dehydration);  
 3 – combustion of formed carbon black; 4 – residue (ash)  
 (Behlau & Widmann, 2003).

### 3.1.2 Differential thermal analysis

Differential thermal analysis (DTA) measures the difference in temperature between the sample and an inert reference material as a function of temperature, and detects changes in heat content. It is used to characterise thermal events, such as melting, decomposition, oxidation, phase transition, glass transition, etc. During these changes, the sample temperature either lags behind (if the change is *endothermic*) or leads (if the change is *exothermic*) the temperature of the reference (Gorodylová et al., 2015).

A very important factor for DTA measurements is the existence of the temperature gradient within the sample which causes that the heat is not absorbed or released at the same rate in all parts of the sample so that the peak area does not have to be a linear function of the reaction heat. This condition can be met in the samples which are small enough, but, on the other hand, for which it becomes difficult to accurately measure their temperature. In the case of decomposition reactions, which are associated with the release of gaseous products and changes in the atmosphere, the temperature effects are shifted depending on the heating rate because the peak temperature is related to the partial pressure of each gaseous product. The peak area corresponding to the

enthalpy change (reaction heat)  $\Delta H$  is not constant and increases with increasing partial pressure (Blažek, 1972).

In sum, DTA peak is related qualitatively to the magnitude of the enthalpy changes occurring, i.e., heat absorption or heat release. It is possible to calibrate DTA equipment so that reliable quantitative enthalpy values can be obtained. However, it is perhaps more convenient to use another thermoanalytical techniques, such as differential scanning calorimetry, for the precise measurement of the processes (Gorodylová et al., 2015).

Both DTA and TGA are very powerful techniques in investigation of the mechanism of different reactions. Simultaneous record of DTA and TGA curves helps to distinguish and identify processes which are connected with heat content changes and the mass loss during thermal processing of the reaction mixture. Besides very simple cases, DTA/TGA method does not provide sufficient information to make conclusions on nature of the chemical transformation occurring. If we want to know the step by step sequence of elementary reactions, it is possible to combine thermoanalytical techniques with X-ray diffraction (XRD). This combination can provide information about overall chemical change leading to the formation of final product (Gorodylová et al., 2015).

### 3.1.3 Differential scanning calorimetry

Differential scanning calorimetry (DSC) measures the difference between the heat flow to a sample and a reference which are subjected to the same temperature-time program. Only the signal representing the difference between sample and reference temperature is needed. DSC provides information on thermal effects characterized by an enthalpy change or change in heat capacity, such as melting, crystallization, solid-solid transition and chemical reactions (Behlau & Widmann, 2003; Figura & Teixeira, 2007).

There are two general principles of DSC hardware: the temperature difference  $\Delta T$ -measuring system, and the power compensation technique.

In the  $\Delta T$ -measuring system, the heat flow into the sample (reference) is calculated using  $\Delta T$  between oven and sample (reference). Thus, the temperature difference between sample and reference over time ( $\Delta T$  signal) is proportional to the heat flow into the sample.

The power compensation system is based on the heaters beneath the pans allowing independent control of heat flow in order to keep the same temperature in both sample pan and reference pan. The difference between the pans is kept at zero all the time; the transmitted power needed to keep this difference is recorded as heat flow in watts or milliwatts (mW). If the heat flow is integrated with respect to time then a quantity of energy is obtained which is expressed in relevant units (joules or millijoules, mWs=mJ) (Behlau & Widmann, 2003; Figura & Teixeira, 2007).

### 3.2 Thermal properties of food products

There are many important applications of thermal analysis (TA) in food industry. Various effects and properties of food products can be investigated by TA techniques. It is possible to study the process of melting (thawing) and freezing of meat and dough, to predict crystallization behaviour, as well as thermal and oxidation stability of different food products. The process of drying, sublimation and evaporation, denaturation and adsorption can be also examined. More specifically, for amorphous carbohydrates, a glass transition temperature, enthalpy change, and water plastication effects are determined (Behlau & Widmann, 2003; Figura & Teixeira, 2007).

In many food ingredients, the mass loss during thermal processing (e.g., roasting of coffee beans) is not only due to moisture, but also many gaseous components, such as CO<sub>2</sub> and volatile flavour and aroma compounds. To study this complex process, a suitable technique (TGA) should be coupled to other appropriate method, such as EGA (evolved gas analysis), and for extremely accurate measurements, the correction factors for buoyance effects should be involved in the calculations.

Additional information about food samples can be obtained from TGA by modification of atmosphere surrounding the sample in the heating oven chamber. For instance, by changing the atmosphere from low to high relative humidity, we can study at first desorption, then adsorption. Or, using aerobic and afterward anaerobic atmosphere, it is possible to study what part of the reaction depends on oxygen. Thermal applications under near vacuum of food materials are also realizable (Figura & Teixeira, 2007).

### 3.3 Kinetics study using thermal analysis

Thermal analysis enables to monitor the kinetics of a physico-chemical reaction and determine its kinetic constants (Blažek, 1972).

Assuming that the course of a reaction can be expressed by formal kinetic equation, it is possible to state the following relationship:

$$\frac{d\alpha}{dt} = k_i(1 - \alpha)^{n_i} \quad (3.1)$$

where  $\alpha$  is the degree of conversion,  $t$  - the time,  $k_i$  - the rate constant,  $n_i$  - the reaction order.

The temperature dependency of the rate constant  $k_i$  can be expressed on the basis of the Arrhenius equation:

$$k_i = A \exp\left(-\frac{E_a}{RT}\right) \quad (3.2)$$

where  $A$  is the preexponential factor (having the meaning of the kinetic process parameter),  $E_a$  - the activation energy,  $T$  - the thermodynamic temperature,  $R$  - the universal molar gas constant (8.3144598 J.K<sup>-1</sup>.mol<sup>-1</sup>) (Kejnar, 2009).

Kinetic transitions (evaporation, thermal decomposition, etc.) shift the temperature peaks to higher values at higher heating rates. Higher heating rates enhance the sensitivity, but, on the other hand, reduce the possibility to distinguish the simultaneous physico-chemical reactions within the sample (Kloužková et al., 2012).

In the case of DTA, the type of reaction can be estimated from the curve shape. For endothermic reactions, pure phase transition is manifested by the gradual increase of the descending branch of the curve to a sharp peak; in the case of a reaction whose speed is controlled by the diffusion, the endoeffect is contrariwise shallow and the peak is considerably rounded. The curve area corresponds to the reaction range, whereas the height of the effect represents the highest reaction rate. However, the temperature of the sample becomes in a certain sense uncontrollable during the reaction, and the temperature effect does not show a defined dependency on the degree of conversion, which makes it difficult to evaluate kinetic data from DTA curves (Blažek, 1972).

Using TGA to study the reaction kinetics, the degree of conversion ( $\alpha$ ) can be defined as the ratio of the weight loss at the time  $t$  to the maximal weight loss displayed on the thermogravimetric curve (Kejnar, 2009). The main advantage of TGA for kinetic experiments, in which a weight loss or gain is detected, is the fact that the temperature during thermogravimetric analysis can be controlled more accurately than by many other techniques, and the reaction temperature, particularly in rate studies, may be reached very quickly (Ramajo-Escalera et al., 2006).

There are two basic kinds of kinetic analysis: model-fitting and kinetic methods (isothermal and non-isothermal models). The use of model-fitting may reach analogous conclusions because almost any conversion function can satisfactorily fit experimental data at the cost of estimating considerably different kinetic parameter values. The uncertainty in estimating kinetic parameters caused by model-fitting can be avoided using isoconversional (non-isothermal) methods (Cai et al., 2018).

Isothermal and non-isothermal kinetic methods are basically different. The isothermal method, which was previously used to a great extent, is based on the determination of time dependency of the degree of conversion ( $\alpha$ ) at constant temperature. The non-isothermal method is based on the determination of time dependency of  $\alpha$  under dynamic conditions, i.e., at linearly increasing or decreasing temperature. The isothermal method is more suitable to obtain information about the driving (the slowest) process, i.e., to determine the reaction order and reaction mechanism. The non-isothermal method is more applicable to gain information about the reaction kinetics; the kinetic parameters can be determined on the basis of a single thermoanalytical curve at the whole temperature range and specific heating rate using only one sample (Kejnar, 2009).



The isoconversional and model-free kinetic methods are used to process thermoanalytical data in which the kinetic parameters (e.g., activation energy) are evaluated without explicit model for concentration dependency. These methods require analysis of several TGA (DSC) curves at different heating rates for the same value of conversion ( $\alpha$ ) to determine activation energy for each conversion point (Jain et al., 2016).

Activation energy ( $E_a$ ) is very important effective parameter in the processing of TA data. There are many reasons for the variations of  $E_a$  values calculated by the kinetic models. Some of the reasons in variations of kinetic parameters can be related to the temperature changes on account of the limited thermal conductivity of the sample (heat and mass transfer limitations) and thermal effects leading to sample self-heating/cooling. Other factors, which could affect the kinetic parameters, include physical and chemical heterogeneity of the sample, specific process and measuring conditions, and systematic errors (Cai et al., 2018; Vyazovkin et al., 2011).

It is also necessary to consider the fact that the concept of a reaction model as a representative of reaction mechanism is inconsistent with the multi-step nature of solid-state reactions. To overcome the discrepancy between the kinetic complexity of the reaction and the simplicity of its kinetic description, it is convenient to substitute the overall rate of the process by a set of rate equations for a given extent of reaction and temperature region (Vyazovkin, 2002). This approach is implemented in the non-isothermal (isoconversional) models.

The non-isothermal models enable to evaluate the activation energy of the process without determining the reaction model. However, the kinetic models can provide the mechanistic conclusions derived from the calculations of kinetic data in a specific way, which predetermine the kinetic parameters. To avoid the producing of method-dependent values, the results of kinetic parameters should be compared on the basis of different types of kinetic models.

## 4. HYDROCOLLOIDS EXAMINED IN THIS STUDY

### 4.1 Guar gum

Guar gum is a polysaccharide derived from seeds of legume plant, *Cyamopsis tetragonalobus*. It is a galactomannan having a 1,4- $\beta$ -linked-D-mannopyranosyl main chain with  $\alpha$ -D-galactopyranosyl units attached by (1 $\rightarrow$ 6) linkages on both sides of the backbone. Guar gum's mannose to galactose ratio can vary in specific range, e.g., the ratio can be 2:1. Due to its unique high viscosity properties, guar gum is an important food stabilizer used in a variety of food applications. First of all, it is widely used as thickener in food products such as sauces, syrups, ice cream, instant foods, beverages, confectionaries and baked goods (Li et al., 2005; Gupta et al., 2015).

Chemical composition of guar gum (guaran unit) is plotted in Fig. 4.1.

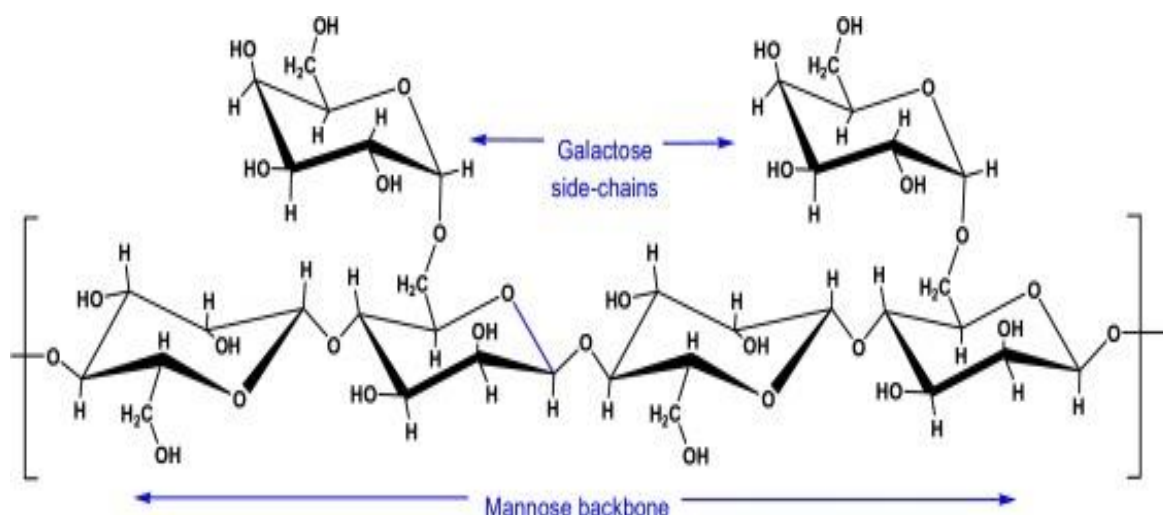


Fig. 4.1. Chemical structure of guar gum (Thombare et al., 2016).

### 4.2 $\kappa$ -carrageenan

Carrageenan is the generic name for the family of natural water soluble sulfated polysaccharides which are extracted from red seaweeds. The carrageenan fractions differ according to the number and position of the sulphate groups and to the possible presence of a 3–6 anhydrogalactose bridge. There are three main ideal carrageenan types: kappa ( $\kappa$ ), iota ( $\iota$ ) and lambda ( $\lambda$ ), which are extensively used in the food industry as a gelling, stabilizing and viscosity-building agent (Sen & Erboz, 2010).

Carrageenan is ranked among polysaccharides with specific functionalities. Recently, the demand for these types of hydrocolloids has been increased. Carrageenan is able to be kept at a solution state at high temperatures while turns to a gelation state when temperature is decreasing. This phenomenon (*cold-set gelation*) could be used to design gels able to improve food properties under specific physicochemical conditions (Shao et al., 2014).

$\kappa$ -carrageenan consists of an alternating linear chain of (1 $\rightarrow$ 3)- $\beta$ -D-galactose-4SO<sub>3</sub><sup>-</sup>-(1 $\rightarrow$ 4)-3,6-anhydro- $\alpha$ -D-galactose, as illustrated in Fig. 4.2. It is soluble in hot water (>75 °C) and even low concentrations (0.1 to 0.5 %) yield high viscosity solutions. Viscosity is stable over a wide pH range, because the semi-ester sulphates are always ionized even under strongly acidic conditions (Núñez-Santiago et al., 2011; Dunstan et al., 2001).

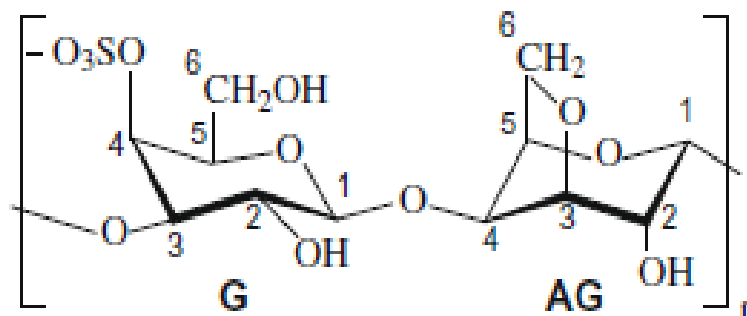


Fig. 4.2. Idealized structure of  $\kappa$ -carrageenan. G represents galactose, AG means anhydrogalactose (Sen & Erboz, 2010).

### 4.3 Xanthan gum

Xanthan gum is a branched, anionic microbial heteropolysaccharide produced by aerobic fermentation of the bacterium *Xanthomonas campestris*. Xanthan consists of pentasaccharide repeat units which comprise glucose, mannose and glucuronic acid in the molar ratio 2:2:1. Xanthan gum is widely and more extensively used as a food gum than any other polysaccharide (except starch) because of its unique and useful properties. Xanthan is soluble in hot or cold water and its solutions exhibit high viscosities at low concentrations and are highly pseudoplastic. This hydrocolloid shows excellent stability over a wide pH and temperature range, and is resistant to action of enzymes found in food systems (García-Ochoa et al., 2000; Viturawong et al., 2008).

Xanthan gum does not form gels. By adding a small amount of salt or reducing the temperature, it undergoes a conformational transition from disordered structure (the side chains here are not associated and project away from the backbone) to ordered form of 5-fold helices (a single- or double-stranded model) where side chains are folded in and associated with the backbone (Pelletier et al., 2001).

Structural formula of xanthan gum, illustrating the cellulosic backbone of (1,4)- $\beta$ -D-glucose residues, and a trisaccharide side chain of  $\beta$ -D-mannose-(1,4)- $\beta$ -D-glucuronic acid-(1,2)- $\beta$ -D-mannose, is shown in Fig. 4.3. The mannose residue attached to the backbone can be variably acetylated and the terminal mannose can contain a pyruvate group depending on the fermentation conditions (Pelletier et al., 2001).

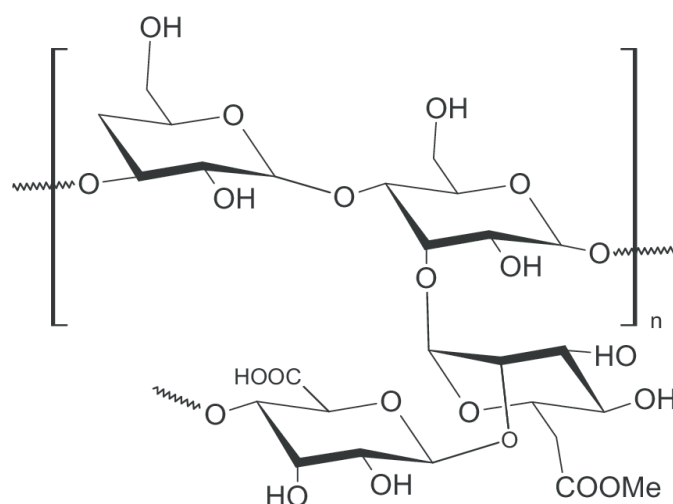


Fig. 4.3. Chemical structure of xanthan gum. Me – methyl group (Saboktakin, 2013).

## 4.4 Gelatin

Gelatin is a protein (polypeptide) extracted by denaturation of collagen from mammalian or fish tissues, using either acids (type A gelatin) or alkali (type B gelatin) (Fang et al., 2006; Roussenova et al., 2012). Even at high concentrations, gelatin exhibit the Newtonian behaviour in aqueous solutions, characterized by exponentially increasing viscosity with gelatin concentration (Gómez-Mascaraque et al., 2015).

In solution at moderate temperatures above 40 °C, gelatin is present in the form of flexible, disordered coils which associate into triple helices, similar to native collagen. In other words, the polypeptide chains of gelatin have a random coil conformation at higher temperatures; this conformation is slowly transformed into single helix by lowering temperature (Pelc et al., 2014; Sarbon et al., 2015).

By sufficient concentration (typically higher than 5 mg.mL<sup>-1</sup>), gelatin bonds with two other molecules to form a triple helix upon cooling. The triple helix is an insoluble semi-rigid rod partly consisting of collagen due to unfinished renaturation. Above the gelation temperature  $T_g$  (ca. 40 °C), gelatin behaves as a viscous liquid (*sol state*), under  $T_g$  as a thermoreversible weak gel (*gel state*). In the gel state, the gelatin oligomers are strongly intertwined, forming extended physical cross links resulting from the partial reversion of the polypeptide chains into ordered triple helical segments. These tropocollagen-like segments are joined along the chain contour by peptide residues in a random coil conformation, forming a transparent elastic network, as presented in Fig. 4.4 (Roussenova et al., 2012).

Gelatin exhibits the increase in the gel strength upon cooling to below 30 °C. However, at temperature above 35 °C, gelatin melts due to the dissociation of triple helices (Pelc et al., 2014; Sarbon et al., 2015).

In the food industry, gelatin due to its advantageous properties (neutral taste, ability to hold dye colour, processing convenience, and glossy appearance) has been applied as a stabilizer, thickener and texturizer for many years (Digenis et al., 1994). In addition to that, gelatin is commercially available at a relatively low cost (Gómez-Mascaraque et al., 2015). Owing to its ability of thermo-reversible gelation which occurs at temperatures close to the human body temperature, gelatin is extensively used for the manufacture of capsules and gelatin-coated tablets. These dosage forms are used to encapsulate labile active ingredients (e.g., essential nutrients and drugs) in order to protect them from external influences (in particular atmospheric oxidation), facilitate the retention of these active compounds and achieve their targeted release (Roussenova et al., 2012).

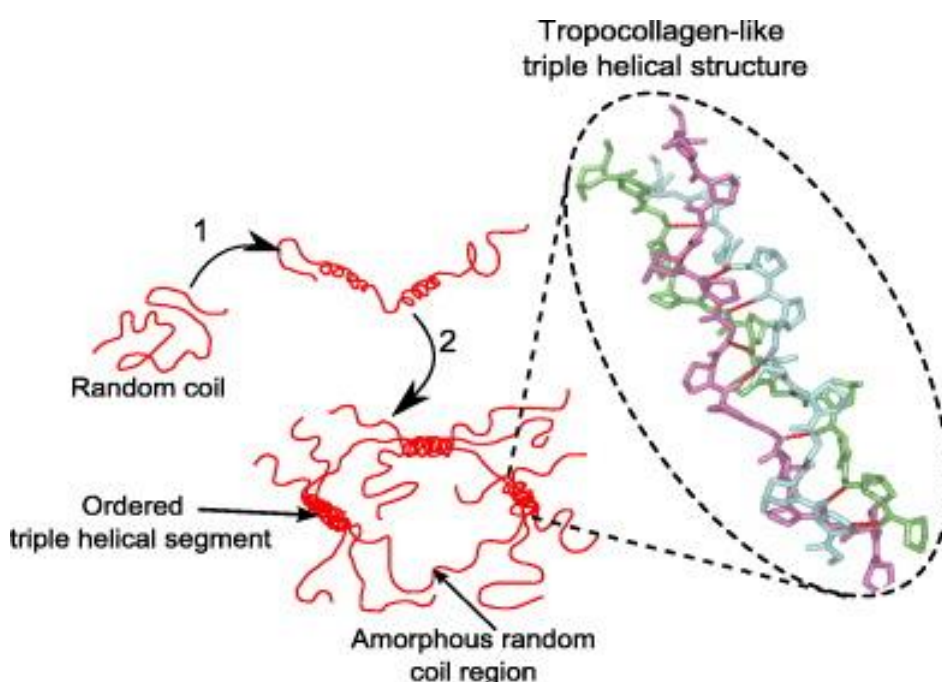


*Fig. 4.4. Spatial structure of gelatin. The numbers refer to the partial renaturation process in gelatin: 1 – forming of the “collagen fold” conformation after cooling an aqueous gelatin solution; 2 - association of polypeptide chains into a spatial network which is stabilized by lateral inter-chain hydrogen bonding within the helical regions (Roussenova et al., 2012).*

## **5. AIMS OF THE THESIS**

The main goal of the Doctoral Thesis is to examine rheological and thermal properties of selected food matrices, particularly polysaccharide and protein hydrocolloids which are used as food additives. The methods of the rheological and thermal analysis will be employed in this study.

The flow properties of model solutions of food hydrocolloids and their blends will be investigated using rheological analysis. Based on the rheological models, the flow parameters of the samples will be determined in relation to the concentration of the solutions, temperature and shear rate used. The influence of conformational transition of the dissolved polymers (polysaccharides, proteins) on flow properties of aqueous and salt solutions will be examined. The intrinsic viscosity (limiting viscosity number) of the solutions will also be determined, dependent on the specific physico-chemical conditions, and the temperature sensitivity of the samples will be evaluated by Arrhenius model.

Another aim of the Doctoral Thesis is to determine thermal properties of food samples, particularly of powder polysaccharides. As typical for food matrices, thermal analysis of the samples will be focused on the determination of their moisture content, on water release process, conformation and phase transition of individual chemical components, as well as components interaction with each other. In this context, the relationship between water (moisture) content, nature of interactions within the sample and observed endo/exothermic effects, i.e., the relationship between temperature peaks and weight loss of the sample during the thermal treatment (heating procedure) will be studied. Thermal analysis methods will also be used to evaluate the reaction kinetics, i.e., the evaporation of water from powder polysaccharide samples. On the basis of the most appropriate kinetic models, the reaction mechanism will be assessed, with a special focus on the activation energy of the thermal process.

## **6. MATERIALS AND METHODS**

### **6.1 Rheological analysis of polysaccharide solutions**

#### **6.1.1 Materials**

Powder samples of shear-thinning polysaccharides, guar gum (No. G4129),  $\kappa$ -carrageenan (No. 22048, viscosity of 0.3% solution at 25 °C reported as 5-25 mPa.s) and xanthan gum (No. G1253, viscosity of 1% solution reported as 800-1200 mPa.s) were purchased from Sigma-Aldrich Co. (St. Louis, USA).

All samples were stored in a dry laboratory place at room temperature (approx. 25 °C) and relative humidity of about 40 % (vol.).

#### **6.1.2 Preparation of solutions**

Solutions of studied polysaccharides were prepared in the concentration range of 0.25 %, 0.50 %, 0.75 % and 1.00 % (w/w) in two different solvents (distilled water and 0.07M KCl). The powder samples were dispersed in distilled water or 0.07M KCl and mixed by a magnetic stirrer. Because the polysaccharides were only partially soluble in cold water, the solutions (with equivalent amount of the solvent) were heated at higher temperature (above 50 °C), for a short time, to make easy the total dispersion. Prepared solutions were then kept at room temperature (ca. 25 °C) for 72 h to release air bubbles. Subsequently, the samples were stored in a refrigerator at temperature about 4 °C. Before the analyses, the solutions were gently and carefully mixed and shaken to ensure their homogeneous consistency.

#### **6.1.3 Rheological analysis**

Viscosimetric analysis of the solutions was performed using universal laboratory rheometer HAAKE RheoStress 1 (Thermo Scientific, USA) with automatic software RheoWin Job Manager and RheoWin Data Manager. The model type of measuring sensor geometry cylinder-cylinder (volume 40.1 mL) was used. Thermal control was ensured by Thermostat HAAKE AC 200 (Thermo Scientific, USA).

Prior to testing, the solutions were carefully mixed and gently shaken to ensure the homogeneous consistency and thermally equilibrated in the water bath. Values of shear stress and dynamic viscosity were determined at specific temperatures: 20 °C, 25 °C, 30 °C, 35 °C, 40 °C and 45 °C. Temperatures were kept constant with an accuracy of  $\pm 0.5$  °C using the heating circulator. Viscosimetric properties were measured in the range of shear rate between 2 and 200  $s^{-1}$ ; shear rate was rising and decreasing with the duration of one cycle 180 s. Measurement was performed three times for each sample of the studied concentration range. Experimental data were statistically analysed and fitted by suitable rheological models: the Ostwald-de Waele (power-law) model and the Herschel-Bulkley model.

The rheological models characterize the flow behaviour of the solutions. The Ostwald-de Waele relationship describes the effect of hydrocolloid concentration on apparent viscosity of the solution (Marcotte et al., 2001b) and the model has the following form:

$$\tau = k \cdot \gamma^n \quad (6.1)$$

where  $\tau$  is the shear stress (Pa),  $k$  the consistency coefficient (Pa.s<sup>n</sup>),  $\gamma$  the shear rate (s<sup>-1</sup>),  $n$  the flow behaviour index (dimensionless). In the case of Newtonian behaviour, Eq. (6.1) becomes Newton's law of viscosity, with viscosity equal to  $k$ . However, in the case of non-Newtonian behaviour with  $n \neq 1$ , the flow characteristic is described as the *shear-thinning* behaviour if  $n < 1$  (pseudoplastic fluids) and as the *shear-thickening* behaviour if  $n > 1$  (dilatant fluids) (Shao et al., 2014).

The Herschel-Bulkley model was used to describe the flow properties of the polysaccharide solutions above some yield point. It means that the Herschel-Bulkley model provides an extension of the Ostwald-de Waele model and contains an additional term which is the yield stress. This model has the following form:

$$\tau = \tau_0 + k \cdot \gamma^n \quad (6.2)$$

where  $\tau_0$  is the yield stress (Pa) (Figura & Teixeira, 2007).

#### 6.1.4 Kraemer equation

Polysaccharide solutions were characterized by viscosity intensifying effect, i.e., by the intrinsic viscosity of the solutions. The intrinsic viscosity  $[\eta]$  (limiting viscosity number) is possible to obtain as the intercept in a linear least-squares fit (Bourbon et al., 2010; Tomšič et al., 2008) and is defined as following:

$$[\eta] = \lim_{c \rightarrow 0} \frac{\eta_{sp}}{c} = \lim_{c \rightarrow 0} \frac{\eta_r - 1}{c} \quad (6.3)$$

where  $\eta_{sp}$  is the specific viscosity,  $c$  the concentration of the solution, and  $\eta_r$  the relative viscosity.

The specific viscosity, which can depict the polymer coil behaviour at the infinite dilution limit (Magny et al., 1994), was plotted and the reduced viscosity ( $\eta_{sp}/c$ ) was determined for each solution. Because the dependency of reduced viscosity versus concentration was not linear, the relationship of natural logarithm of relative viscosity divided by concentration ( $\ln \eta_r/c$ ) against concentration was used for the determination of intrinsic viscosity  $[\eta]$ . This relationship is called Kraemer equation:

$$\frac{\ln \eta_r}{c} = [\eta] - k_K [\eta]^2 c \quad (6.4)$$

where  $k_K$  is the Kraemer constant. In the Kraemer plot,  $[\eta]$  is the intercept, and  $-k_K[\eta]^2$  is the slope. The Kramer plot is linear only at sufficiently low concentrations (Garrec et al., 2013; Tomšič et al., 2008).



## **6.2 Thermal and temperature dependency of polysaccharide hydrocolloids**

### **6.2.1 Materials and conditioning**

Powder samples of polysaccharides, guar gum,  $\kappa$ -carrageenan and xanthan gum, as described in previous section (chapter 6.1.1), were delivered by Sigma-Aldrich Co. (St. Louis, USA).

Samples were stored at room temperature about 25 °C and relative air humidity of approx. 40 % (vol.). To adjust a constant moisture level of powders, one set of samples was conditioned in a desiccator at 25 °C for 72 hours, using potassium acetate (Sigma Aldrich, USA) as water activity standard which was dissolved at room temperature to prepare saturated aqueous solution of defined water activity, providing the atmosphere of saturated vapours of 22.5 % relative humidity. Another set of samples was conditioned in a desiccator at the same conditions, using potassium chloride (Sigma Aldrich, USA) as saturated solution to equilibrate the moisture level of the powders at 84.3 % relative humidity.

### **6.2.2 Thermal analysis of powders**

Thermal properties of powder samples were evaluated by automatic simultaneous thermal analyser DTG/60 (Shimadzu, Japan). Thermal effects characterized by reaction enthalpy were analysed by software ta60 Version 1.40 (Shimadzu, Japan). Measuring device was calibrated for temperature correction using indium and zinc standards. An equivalent amount of each polysaccharide was placed into an aluminium measuring pan (10 mg  $\pm$  0.5 mg). Pans were evenly filled with powder samples and placed into the analyser; an empty pan was employed as reference. Measurement was realized under nitrogen atmosphere (the flow rate of 50 mL/min). Thermal stability of powders was tested at 10 °C/min heating rate from 30 °C to 600 °C.

For kinetic parameters evaluation, the samples were heated from 30 °C to 200 °C at several different heating rates (5 °C/min, 10 °C/min, 15 °C/min and 20 °C/min). Afterwards, heat correction and baseline correction were performed for each set of data. Based on the results, values of peak temperature ( $T_p$ ), reaction enthalpy ( $\Delta H$ ), weight loss, and moisture content ( $\Delta m_w$ ), respectively, were determined.

All experiments were conducted three times for each sample and statistically analysed.

### 6.2.3 Kinetic models

Based on TGA data, activation energy ( $E_a$ ) was determined for thermally treated powder samples. Three different kinetic models (Friedman model, Kissinger model, and Model-free kinetics) which represent specific types of thermal kinetic evaluation were chosen to calculate the values of  $E_a$ . The activation energy was related to the water evaporation and phase transition of the polysaccharide samples occurred in the specified temperature range.

Degree of conversion  $\alpha$  can be defined as the degree of sample transition or degradation during thermal treatment, according to Eq. (6.5):

$$\alpha(t) = \frac{w_0 - w_t}{w_0 - w_{t\infty}} \quad (6.5)$$

where  $w_0$ ,  $w_t$  and  $w_{t\infty}$  represent the initial mass of the sample, the mass of the sample at a specific time  $t$  and the mass of the sample at the end of analysis, respectively (Berčič, 2017).

Reaction model  $f(\alpha)$  describes the dependency of the reaction on the extent of conversion. Many different forms of this reaction model had been published. In the case of my study, the reaction model was performed in the form which is relevant to the kinetics of homogenous reactions (Eq. 6.6):

$$f(\alpha) = (1 - \alpha)^{n_i} \quad (6.6)$$

where  $n_i$  is the reaction order.

Upon a constant conversion, the reaction rate is a function of the conversion, as stated by the isoconversional principle. Thus, according to this principle, the values of activation energy are not a function of temperature, but only function of the conversion (Berčič, 2017). The isoconversional methods, used in this study, are based on integral or differential analysis.

Friedman model belongs to differential isoconversional methods allowing the calculation of activation energy for the specified conversion range from the plot of  $\ln \frac{d\alpha}{dt}$  vs. reciprocal temperature  $\frac{1}{T_\alpha}$ . The numerical form of the Friedman method is presented by Eq. (6.7):

$$\ln \frac{d\alpha}{dt} = \ln A + n \cdot \ln(1 - \alpha) - \frac{E_a}{RT} \quad (6.7)$$

where  $A$  is the pre-exponential factor ( $\text{min}^{-1}$ ),  $E_a$  activation energy ( $\text{J}\cdot\text{mol}^{-1}$ ),  $R$  the molar gas constant ( $8.314 \text{ J}\cdot\text{K}^{-1}\cdot\text{mol}^{-1}$ ) and  $T$  the thermodynamic temperature (K). Values of activation energy can be determined from the slopes of isoconversional lines obtained at measured conversions, and pre-exponential factors from the intercepts of isoconversional lines with the ordinate axis (Cai et al., 2018; Berčič, 2017).

Kissinger model is integral non-isothermal method. It is described by Eq. (6.8):

$$\ln \frac{\beta}{T_m^2} = \ln \left[ \frac{n \cdot (1 - \alpha_m)^{n-1}}{E_a} \cdot RA \right] - \frac{E_a}{R} \cdot \frac{1}{T_m} \quad (6.8)$$

where  $\beta$  is the heating rate ( $^{\circ}\text{C}\cdot\text{min}^{-1}$ ),  $T_m$  is the peak temperature (K) recorded on derivative thermogravimetric curve ( $\text{mg}\cdot\text{min}^{-1}$ ), and  $\alpha_m$  is the degree of conversion corresponding to  $T_m$ .

To apply this Kissinger model, the samples were measured at four different heating rates (it is necessary to use at least three  $\beta$ ). To evaluate the values of activation energy, the respective dependency of  $\ln \frac{\beta}{T_m^2}$  vs.  $\frac{1}{T_m}$  was plotted, providing the straight lines with the slope of  $-\frac{E_a}{R}$ , and thus  $E_a$  was obtained as a function of sample conversion (Cai et al., 2018).

The last method, which was used to calculate the activation energy in this study, was Model-free kinetics. This isoconversional integral model is based on the postulate, that the activation energy (dependent on extent of conversion) may not be constant. Using several different heating rates,  $E_a$  was determined for various degrees of conversion, as stated by Eq. (6.9):

$$\ln \beta + \ln g(\alpha) = \ln k(T) + \ln \frac{RT^2}{E_a \alpha} - \frac{E_a}{RT} \quad (6.9)$$

where the value of  $g(\alpha)$  integrating up to the conversion degree  $\alpha$  provides following relation (Eq. 6.10):

$$\int_0^{\alpha} \frac{d\alpha}{f(\alpha)} = g(\alpha) = \frac{A}{\beta} \int_{T_0}^T e^{-E_a/RT} dT \quad (6.10)$$

where  $T_0$  is an arbitrary temperature at which a given conversion ( $\alpha$ ) will be reached (Ramajo-Escalera et al., 2006). According to the Model-free kinetics,  $E_a$  was calculated as a slope of the linear dependency  $\ln \beta$  versus  $\frac{1}{T}$  for specified degrees of conversion (Vyazovkin & Wight, 1999).

#### 6.2.4 Arrhenius model

Influence of temperature on the viscosity of polysaccharide solutions was evaluated by the Arrhenius model. Polysaccharide solutions were prepared from powder samples as described above (chapter 6.1.2). Dynamic viscosity of the solutions was measured on the laboratory rheometer at conditions specified for rheological analysis (chapter 6.1.3). Values of activation energy were reflecting the sensitivity of the molecular structure to temperature at specified shear rates ( $20 \text{ s}^{-1}$  and  $100 \text{ s}^{-1}$ ). The values of determination coefficient ( $R^2$ ) were calculated for all solutions.

The form of Arrhenius model is shown in Eq. (6.11):

$$\eta = A \exp\left(\frac{E_a}{RT}\right) \quad (6.11)$$

where  $\eta$  is the dynamic viscosity (Pa.s),  $A$  the pre-exponential factor (-),  $E_a$  the activation energy ( $\text{J}\cdot\text{mol}^{-1}$ ),  $R$  the molar gas constant ( $8.3144598 \text{ J}\cdot\text{K}^{-1}\cdot\text{mol}^{-1}$ ) and  $T$  the thermodynamic temperature (K) (Marcotte et al., 2001a). From the linear plot  $\ln \eta$  vs reciprocal temperature ( $T^{-1}$ ), it was possible to calculate  $E_a$  as a slope and  $A$  as an intercept (Wang et al., 2015).

## **6.3 Functional properties of gelatin-polysaccharide blends**

### **6.3.1 Materials**

Samples of powder polysaccharides, guar gum (No. G4129),  $\kappa$ -carrageenan (No. 22048) and xanthan gum (No. G1253) were delivered by Sigma-Aldrich Co. (St. Louis, USA), as specified above. Gelatin (No. 2111104), potassium chloride (KCl, No. 0163413) and sodium chloride (NaCl, No. 704212) were obtained by the Czech company IPL - Ing. Petr Lukeš (Uherský Brod, Czech Republic). All chemicals were of analytical grade.

The samples of hydrocolloids were stored in a dry laboratory place at room temperature (ca 25 °C) and relative humidity about 40 % (vol.).

### **6.3.2 Preparation of blends**

Solution of 1.0% (w/w) gelatin was prepared by dissolving the sample in 70mM KCl (the first sample set) or 70mM NaCl (the second sample set). Firstly, gelatin was swollen in a minor amount of the solvent. Afterwards, the solution was heated at 45 °C to dissolve completely. Then the solution was cooled under ambient temperature.

Polysaccharide solutions of 1.0% (w/w) concentration were prepared by dissolving the samples in 70mM KCl or 70mM NaCl and mixing by a magnetic stirrer. Since powder samples were only partially soluble in cold solvent, the solutions were mixed at room temperature (ca. 25 °C) for a long time and heated at higher temperature (above 50 °C) for a short time to make easy the total dispersion.

The salt mixtures of gelatin/polysaccharide were prepared by blending the equal amounts of 1.0% gelatin and 1.0% polysaccharide to achieve the final concentration of 0.5% (w/w). The dispersions of gelatin/polysaccharide were stirred at 45 °C for 10 min and afterwards kept at room temperature for 72 h to release air bubbles. The blends were then stored in a refrigerator at temperature about 4 °C, and immediately prior to analysis carefully mixed and shaken.

### **6.3.3 Rheological analysis**

Rheological analysis of the samples was performed by universal laboratory rheometer HAAKE RheoStress 1 (Thermo Scientific, USA) with automatic software. The model type cylinder-cylinder geometry was used. Thermal control was ensured by thermostat HAAKE AC 200 (Thermo Scientific, USA).

Prior to testing, samples were thermally equilibrated in the water bath. The measurements were performed at specific temperatures: 25 °C, 30 °C, 35 °C, 40 °C and 45 °C. The temperature was kept constant with an accuracy of  $\pm 0.5$  °C using the heating circulator. The viscosity was measured in the shear rate between 2 and 200 s<sup>-1</sup> with the duration of one cycle 180 s.

Flow parameters were obtained by fitting Ostwald-de Waele (power-law) model and Herschel-Bulkley model to the data. The models are described above by Eqs. (6.1) and (6.2), respectively.

### **6.3.4 Arrhenius model**

The effect of temperature on the apparent viscosity of gelatin/polysaccharide blends was tested at constant temperatures (20 °C, 25 °C, 30 °C, 35 °C, 40 °C and 45 °C) and evaluated using the Arrhenius equation at specified shear rates (20 s<sup>-1</sup> and 100 s<sup>-1</sup>). Viscosity of the studied solutions was measured on the laboratory rheometer HAAKE RheoStress 1 (three times for each sample), as described in the previous section. Determination coefficient ( $R^2$ ) was calculated for all blends to verify the appropriateness of the Arrhenius model. The Arrhenius relationship is described above by Eq. (6.11).

### **6.3.5 Other analyses**

Some additional characteristics of the blends were provided by conductivity measurement and zeta potential analysis.

Conductivity of the blends was determined by conductometer Mettler-Toledo (USA) in the temperature range 25-45 °C. Temperature of the samples was ensured by water bath Julabo MA-4 (Germany). Each sample was measured three times at specific temperatures: 25 °C, 27 °C, 29 °C, etc.

Zeta potential analysis of 0.5% gelatin/polysaccharide blends was measured by Zeta Potential Analyzer, Zeta Plus (Brookhaven Instruments Corporation, USA). The appropriate amount of the sample (1.6 mL) was poured into the polystyrene cuvette, and temperature of the samples was equilibrated at 25 °C by automatic software. Prior to testing, pH-values of the solutions were measured by pH meter Five Easy Plus FEP 20 (Mettler-Toledo, Switzerland); obtained results were entered as initial parameters for the analysis. The values of zeta potential of the solutions, as well as effective diameter of the particles were analysed by the software, each analysis was repeated ten times. The data were compared to evaluate the potential stability of the blends.

## **6.4 Statistical analysis of the data**

### **6.4.1 Statistical analysis of rheological parameters**

Rheological measurement of polysaccharide solutions was performed three times for each sample. Experimental data were statistically analysed and fitted by suitable rheological models, Ostwald-de Waele (power-law) model and Herschel-Bulkley model. Herschel-Bulkley parameters were evaluated with and without the extrapolation of yield stress values.

Herschel-Bulkley model was the most suitable model for all samples in terms of determination coefficient ( $R^2$ ). The high values of  $R^2$  obtained by fitting the Herschel-Bulkley model indicate a good fit of this model for polysaccharide solutions. However, for guar gum solutions and 0.25-0.50 % (w/w)  $\kappa$ -carrageenan in distilled water, Herschel-Bulkley model without extrapolation provided negative values of yield stress ( $\tau_0$ ), which is naturally meaningless. For that reason, the values of  $\tau_0$  were assumed to be zero in these cases, and thus the Herschel-Bulkley model was leading to the Ostwald-de-Waele model, as described in detail in the Discussion.

The same rheological approach was used for gelatin/polysaccharide blends. The Herschel-Bulkley model (without extrapolation of yield stress) was the most suitable model for all blends due to the high values of  $R^2$  (0.99) obtained by fitting this model.

Flow parameters were evaluated using the software SigmaPlot 2002 Version 8.0 (SPSS Inc., USA). The differences between the values of consistency coefficient ( $k$ ), flow behaviour index ( $n$ ) and yield stress ( $\tau_0$ ) were tested as statistically significant at significance level 95 %, based on two-way ANOVA statistical analysis (variability test) with repetition (evaluating three independent sets of data). The differences between the rheological parameters at various temperatures and concentrations of the solutions and interactions between the data were analysed. An alpha level of 5 % was used to define the statistical significance of the comparisons.

As evaluated by ANOVA testing, the values of the parameters at various temperatures, and at various concentrations were significantly different ( $p < 0.05$ ) in the studied temperature and concentration range. Thus, the null hypothesis  $H_0$  proposing that the differences between rheological parameters are given by the errors of the measurement can be rejected. Due to the p-values (significance values) less than 5 %, the alternative hypothesis  $H_1$  can be accepted. It means that the influence of two tested factors (temperature, concentration) on the results is verified. In other words, the effect of the factors on the data is sufficiently higher than the influence of the random measurement errors. Therefore, the differences between the results can be considered as statistically significant, as also demonstrated by the Fisher distribution (F-values) of the data.

#### **6.4.2 Statistical analysis of thermal parameters**

All thermal and kinetic experiments were conducted three times for each powder sample. To evaluate thermal properties of order-disorder transition and hydrocolloid-water interactions, as well as thermal stability of powders, the results of peak temperature ( $T_p$ ), reaction enthalpy ( $\Delta H$ ), and weight loss ( $\Delta m_w$ ) were calculated as means of triplicate determinations.

The kinetic study was based on TGA data obtained at four different heating rates. The degree of conversion ( $\alpha$ ), and the values of temperature  $T_a$  and  $T_m$  were calculated from the data (three times for each heating rate). According to the model used, activation energy ( $E_a$ ) was determined and expressed as a mean value.

The differences between the values of thermal parameters were tested as statistically significant at significance level 95 %, using one-way ANOVA statistical analysis or two-way ANOVA statistical analysis with repetition. As typical for physico-chemical measurements, an alfa level of 5 % was set as the probability that the differences between the parameters were caused by the random measurement errors.

In the case of powder thermal stability, one-way ANOVA test was employed to assess the null hypothesis  $H_0$  that the differences between tested parameters can be attributed to random errors. Due to sufficiently low significance value (p-value less than 5 %), the alternative hypothesis  $H_1$  can be accepted instead of  $H_0$ . Thus, the values of thermal parameters were statistically different, according to the type of sample.

For evaluation of thermal properties after different conditioning, and for analysis of kinetic parameters, two-way ANOVA test was used. The values were examined to assess the influence of conditioning conditions (temperature and relative humidity) or heating rate, respectively, on the final results. The second tested factor was the type of powder hydrocolloid, i.e., the ability of the hydrocolloid to bound water to a specific extent. As proved by ANOVA testing, the influence of random errors (hypothesis  $H_0$ ) can be considered as negligible, and the hypothesis  $H_1$  (significant effects of tested factors) can be accepted. Accordingly, it is possible to affirm with a high probability (95 %) that the values of thermal and kinetic parameters rank to the defined confidence interval. The differences between the results can be classified as statistically significant, and the data described by relevant Fisher distribution.

## 7. RESULTS AND DISCUSSION

### 7.1 Rheological properties of polysaccharide solutions

#### 7.1.1 Flow parameters

The polysaccharide solutions were prepared in two sets to compare the flow behaviour of samples in distilled water and samples in 0.07M KCl. The flow behaviour of the solutions was different due to relatively strong inter- and intramolecular hydrogen bonding present between individual macromolecular coils in distilled water, and, on the other hand, due to the presence of chaotropic cations in 0.07M KCl which eliminated the contributions to the viscosity from hydrogen bonding system and from intramolecular electrostatic repulsion (polyelectrolyte effect) of the polymer chains (Kupská et al., 2014).

Thus, it was possible to follow concentration effect of expanded stiffed macromolecular coil transition to random coil conformation, as well as temperature effect of conformational transition (based on flow parameters of the solutions), as induced by external stimuli, i.e., by changing temperature, polymer concentration and type of solvent. Flow parameters were obtained by fitting experimental data to the rheological models (Ostwald-de Waele and Herschel-Bulkley models) applied to the data of shear stress vs shear rate, because all the solutions exhibited shear-thinning behaviour.

Calculated flow curve model parameters for 25 °C temperature shear stress vs shear rate data are given in Tables 7.1 and 7.2. The Herschel-Bulkley model was the most suitable model for all samples in terms of the highest determination coefficient ( $R^2$ ) values. However, for guar gum samples (for whole studied concentration range and both solvents) and  $\kappa$ -carrageenan (for 0.25 and 0.50% w/w aqueous solutions), Herschel-Bulkley numerical non-linear regression modelling of the flow curves without extrapolation was giving negative values of the yield stress. This of course is from the physical point of view meaningless (Kelessidis et al., 2006; Razi et al., 2014). That is why in these cases the corresponding yield stress was assumed to be zero, and thus the Herschel-Bulkley model was leading to the Ostwald-de-Waele model. Such behaviour is typical with zero shear and infinity shear viscosities, and it is used for description of the viscoelastic flow patterns. To overcome the problem of negative yield stress optimized data modelling results, there was described a method by Kelessidis et al. (2006) in the literature.

It is possible to compare the data of the present study with a wide range of scientific works and reports on the relevant topic. On this place, it is worth to introduce some examples.

The flow parameters of guar gum aqueous solutions in the present study are comparable with the data obtained by Wang et al. (2015). For example, the flow parameters of 0.5% guar gum in distilled water at 20 °C were determined as 0.76 (flow behaviour index) and 73.4 mPa.s<sup>n</sup> (consistency coefficient), according to



the Ostwald-de Waele model. Wang et al. stated relatively close values of guar gum in deionised water at the same concentration and temperature: 0.86 and 82.3 mPa.s<sup>n</sup>, respectively.

The results of guar gum are also close to the data by Cevoli et al. (2013). The authors focused on the rheological properties of several food hydrocolloids in distilled water which were subjected to a shear rate 0-300 s<sup>-1</sup> at 25 °C. Their data were fitted using the Ostwald-de Waele model and Herschel-Bulkley model with and without extrapolation of the yield stress. The values of flow parameters of 1% guar gum in water at 25 °C in the present study were relatively consistent with the results by the authors, both for Ostwald-de Waele and Herschel-Bulkley models. For instance, the values of flow parameters in the present study for 1% guar gum in water at 25 °C (0.18, 21.85 Pa.s<sup>n</sup>, -17.74 Pa without extrapolation) were almost consistent with the results by Cevoli et al. for 1% guar gum at the same temperature (0.18, 27.41 Pa.s<sup>n</sup>, and -18.15 Pa). The Herschel-Bulkley parameters for xanthan gum solutions varied to a greater extent, e.g., the yield stress determined for 1% xanthan aqueous solution in the present study (9.32 Pa without extrapolation) was notably larger as compared to  $\tau_0$  by Cevoli et al. (6.90 Pa). The differences in the flow parameters may be explained by the different molecular weights of the samples and different measuring procedures applied to the hydrocolloid solutions.

The values of flow parameters of xanthan solutions in water are in compliance with the data by Figura and Teixeira (2007). The authors provided some exemplary results for xanthan aqueous solutions in the concentration range 0.125 - 1.0% (w/w). For instance, the flow parameters of 0.5% xanthan gum at 20 °C in the present study, 0.21 and 2.3 Pa.s<sup>n</sup> (the Ostwald-de Waele model), are in good agreement with the values by Figura and Teixeira, 0.24 and 3.0 Pa.s<sup>n</sup>, respectively.

### ***Effect of concentration***

As determined in the present study, concentration  $c$  had an obvious effect on the flow behaviour of polysaccharide solutions. As evident from the Kraemer plot (Fig. 7.2), there is a certain change at concentration about 0.5% (w/w) which can be associated to the process of conformational transition, i.e., to the process of chain entanglement and overlapping of macromolecular coils with increasing polymer concentration. For the solutions in distilled water, this process can be characterized as the transition from expanded stiffed macromolecular coils to the conformation of interpenetrating random coils. After addition of KCl (salt solution), the polysaccharide structure undergoes a coil-helix transition with increasing entanglement of polymer network at higher  $c$ . The change of the Kraemer plot at concentration about 0.5% (w/w) can also represent the transition from the dilute (0.25 %) to semi-dilute regime of the solutions.

The effect of concentration was also demonstrated by the change of flow parameters. The consistency coefficient calculated by the Ostwald-de Waele and Herschel-Bulkley model increased with the concentration, which is typical behaviour of hydrocolloid solutions (Cevoli et al., 2013).

On the other hand, the increase in concentration was accompanied by a decrease of flow behaviour index ( $n$ ), both for samples in water and KCl. In the case of guar gum and  $\kappa$ -carrageenan solutions, the flow behaviour index was decreasing with concentration and increasing with temperature. On the contrary, the consistency coefficient ( $k$ ) was increasing with concentration and decreasing with temperature.

Observed decrease of  $n$  with increasing polymer concentration for guar gum aqueous solutions reflected their increasing non-Newtonian rheological behaviour due to the higher mutual entanglement of the hydrogen bond stiffened individual guar macromolecules. After addition of the background salt (KCl) electrolyte into the guar aqueous solutions, the presence of strong chaotropic potassium ions induced organized water structure breakage, thus resulting in dissolution of the larger scale guar gum aggregates into individual molecules. This effect is clearly visible for the diluted systems; however, with increasing concentration it is diminishing due to the mutual macromolecular coils overlapping.

For  $\kappa$ -carrageenan in 0.07M KCl, the flow parameters were substantially influenced by the gelation of the samples (at concentration  $c \geq 0.50$  % w/w); therefore, the trend between the parameters was not possible to obtain by fitting the models (because of lower values of determination coefficient). In the case of 1%  $\kappa$ -carrageenan in KCl, the value of flow behaviour index (0.42) at 20 °C corresponds well to the lower value of  $n$  (0.34) of 1.5% carrageenan (i.e., of more concentrated sample) at the same temperature determined by Marcotte et al. (2001b). The authors investigated the flow behaviour of hydrocolloids with 1% salt addition at various temperatures and concentrations (at shear rate 0-300 s<sup>-1</sup>). However, the yield stress and consistency coefficient of 1.5% sample were higher than expected as compared with the parameters of 1.0% sample in this study. The discrepancies between the results can be related to the different molecular weight of the samples, as well as to different measuring procedure applied by Marcotte and co-workers.

In general, there was found a clear relationship between the concentration and flow parameters of hydrocolloid solutions. However, the samples of xanthan gum in distilled water exhibited changing behaviour of  $n$  versus concentration (after fitting the Herschel-Bulkley model). Obtained values of  $n$  fluctuated in a relatively narrow range; at 20 °C, the flow behaviour index was even increasing with concentration. This behaviour can be most probably related to the structural change of individual xanthan macromolecules due to the expansion/collapse of their macromolecular coils affected by the charged side chain groups, thus modulating their mutual electrostatic repulsions. This triggers ability of

individual xanthan macromolecules to entangle/disentangle as a function of the polymer concentration.

In the presence of salt (KCl), the charge screening effect causes the change of xanthan disorder conformation of macromolecular coils (present in the solution at low ionic strength) to order helical structure (Brunchi et al., 2014); this conformational transition undergone by increasing the ionic strength of the solution can be analogous to the coil to helix transition by lowering the temperature. Thus, xanthan solutions in KCl exhibited a prevalent decrease of  $n$  with concentration, probably due to a more stable polymer structure, in comparison to xanthan in distilled water. Moreover, the values of  $n$  and its change with concentration are strongly affected by the polymer molecular weight (Marcotte et al., 2001a).

### ***Effect of temperature***

Temperature had a direct effect on molecular motion in the studied solutions. As temperature increases, molecular motion takes place at a faster rate (molecules move with greater velocity) (Figura & Teixeira, 2007). Therefore, temperature affected the flow behaviour of the solutions. However, it was an opposite effect to that of concentration. The consistency coefficient of guar gum and  $\kappa$ -carrageenan solutions decreased with increasing temperature, whereas the flow behaviour index increased.

The effect of temperature on the flow parameters of Herschel-Bulkley model of 0.25 % (w/w) solutions is shown in Table 3. Flow curves of guar gum both in distilled water and in KCl at 25 °C are shown in Fig. 7.1. As reflected in flow index data dependencies, there is a change of the flow behaviour of studied solutions at temperature about 30 °C. This noticeable change could correspond to the conformational ordering of the shear-thinning polysaccharide, induced by the temperature change.

Nevertheless, the solutions of xanthan gum, particularly at lower concentrations (0.25 %, 0.50 % w/w), exhibited a different behaviour of  $n$  versus temperature, as compared to other studied samples. For the samples of xanthan in water and KCl, the flow behaviour index was decreasing until 30 °C, whereas the consistency coefficient was increasing. After 30 °C,  $n$  was fluctuated in a relatively narrow range, especially for the dilute solutions, as can be seen from data in Tables 7.1-7.3. This is in contrast to guar gum and  $\kappa$ -carrageenan which tend to less pseudoplastic behaviour at elevated temperatures. Overall, xanthan gum exhibited an evident change of its flow behaviour at temperatures around 30 °C, both for samples in water and KCl, which could demonstrate the transition of xanthan double helical structure to single coils conformation (in salt solution) or the disentanglement process of the coil chains (in distilled water), as shown in Table 7.3.

### *Significance of yield stress*

Xanthan gum exhibited a significant yield stress ( $\tau_0$ ) within the whole studied temperature range. The values of  $\tau_0$  were steeply increasing with concentration, both for samples in water and in KCl. Even at the highest temperature studied (45 °C) and the lowest concentration (0.25 % w/w), the yield stress was noticeable (0.21 Pa for the aqueous solution, and 0.27 Pa for the KCl salt solution, respectively). This fact is probably related to the ability of xanthan solutions to retain their stable viscosity and their three dimensional network structure at higher temperatures until reaching a specific “melting temperature”. The viscosity stability at elevated temperatures (relatively high at low-shear conditions) and the non-negligible value of yield stress result from the weak intermolecular associations of xanthan structure, even at very low hydrocolloid concentration. This rheological behaviour of xanthan gum is a consequence of the progressive alignment of the rigid xanthan molecules with the shearing force (Marcotte et al., 2001b).

Generally, higher yield stress values of xanthan solutions were determined at higher concentrations and lower temperatures. The values of  $\tau_0$  were substantially increasing with concentration. This is in agreement with expected hydrocolloids' yield stress behaviour. Although the yield stress of xanthan solutions was decreasing with the rising temperature only for dilute solutions; the more concentrated samples (0.75 %, 1.0 % w/w) showed an irregular change of  $\tau_0$ . The occurrence of a yield stress followed by shear thinning, which is caused by intermolecular association realized via acetate residues, is a typical behaviour of xanthan gum. The yield stress is a useful property of xanthan gum as a binder, since it helps to keep various components of a food composition in place (Marcotte et al., 2001a; Wang et al., 2017). The results obtained for xanthan gum aqueous solutions are in agreement with the observations by Marcotte et al. (2001a) who noticed a considerable value of yield stress for xanthan gum in distilled water at 20 °C and 40 °C.

$\kappa$ -carrageenan in water at higher concentration (1 % w/w) was characterized by a non-negligible yield stress in the temperature range of 20 to 35 °C. Flow parameters of  $\kappa$ -carrageenan obtained in my study are comparable with the results published by other authors (Cevoli et al., 2013; Marcotte et al., 2001a). As in the present study, Marcotte and co-workers (2001a) observed that carrageenan samples provided large values of yield stress at lower temperatures (20 °C).

Table 7.1. Flow parameters of hydrocolloid solutions in distilled water at 25 °C (upward curves).

Sample	$c$ (% w/w)	Herschel-Bulkley model without extrapolation				Herschel-Bulkley model with extrapolation			Ostwald-de Waele model		
		$\tau_0$ (Pa)	$k$ (Pa.s <sup>n</sup> )	$n$	$R^2$	$\tau_0$ (Pa)	$k$ (Pa.s <sup>n</sup> )	$R^2$	$k$ (Pa.s <sup>n</sup> )	$n$	$R^2$
Guar gum	0.25	-0.12	0.09	0.69	0.9999	0.003	0.23	1.0	0.07	0.74	0.9995
	0.50	-0.15	0.12	0.71	0.9999	0.020	0.31	1.0	0.09	0.76	0.9996
	0.75	-10.64	10.94	0.25	0.9998	0.620	7.30	0.9898	3.91	0.39	0.9939
	1.00	-17.74	21.85	0.18	0.9999	3.61	11.48	0.9967	8.14	0.30	0.9953
κ-carrageenan	0.25	-0.03	0.02	0.90	1.0	0.02	0.10	1.0	0.02	0.92	0.9999
	0.50	-0.09	0.06	0.85	0.9999	0.03	0.23	1.0	0.05	0.88	0.9997
	0.75	1.11	0.45	0.56	0.9995	1.11	1.46	0.9861	0.89	0.45	0.9969
	1.00	6.25	1.21	0.45	0.9993	6.20	3.68	0.9265	5.29	0.24	0.9875
Xanthan gum	0.25	0.68	0.24	0.48	0.9992	0.80	0.66	0.8817	0.61	0.34	0.9943
	0.50	3.04	0.31	0.49	0.9995	3.42	0.72	0.9904	2.32	0.21	0.9828
	0.75	6.42	0.43	0.47	0.9987	6.47	1.45	0.9992	5.27	0.15	0.9768
	1.00	9.32	0.55	0.43	0.9988	8.14	1.97	0.9948	8.11	0.11	0.9793

Note:  $c$  – concentration;  $\tau_0$  – yield stress;  $k$  – consistency coefficient;  $n$  – flow behaviour index;  $R^2$  – determination coefficient.

Table 7.2. Flow parameters of hydrocolloid solutions in 0.07M KCl at 25 °C (upward curves).

Sample	<i>c</i> (% w/w)	Herschel-Bulkley model without extrapolation				Herschel-Bulkley model with extrapolation			Ostwald-de Waele model		
		$\tau_0$ (Pa)	<i>k</i> (Pa.s <sup><i>n</i></sup> )	<i>n</i>	<i>R</i> <sup>2</sup>	$\tau_0$ (Pa)	<i>k</i> (Pa.s <sup><i>n</i></sup> )	<i>R</i> <sup>2</sup>	<i>k</i> (Pa.s <sup><i>n</i></sup> )	<i>n</i>	<i>R</i> <sup>2</sup>
Guar gum	0.25	-0.03	0.02	0.85	1.0	7.0x10 <sup>-4</sup>	9.5x10 <sup>-2</sup>	1.0	0.02	0.87	0.9999
	0.50	-1.32	1.18	0.42	0.9997	0.02	1.47	0.9894	0.61	0.52	0.9971
	0.75	-7.03	8.08	0.24	0.9999	0.95	5.60	0.9925	3.26	0.36	0.9955
	1.00	-33.23	39.77	0.13	0.9999	5.99	14.31	0.9975	11.68	0.26	0.9938
κ-carrageenan	0.25	0.14	0.31	0.45	0.9992	0.20	0.90	0.9020	0.37	0.42	0.9991
	0.50	6.04	0.40	0.60	0.9608	7.47	9.76	0.9776	3.29	0.29	0.9521
	0.75	-	-	-	-	-	-	-	-	-	-
	1.00	-	-	-	-	-	-	-	-	-	-
Xanthan gum	0.25	0.49	0.25	0.44	0.9992	0.48	0.74	0.9525	0.53	0.33	0.9962
	0.50	2.01	0.90	0.35	0.9995	2.04	2.07	0.9678	2.35	0.22	0.9948
	0.75	5.51	1.86	0.29	0.9985	6.55	2.67	0.9830	6.44	0.14	0.9922
	1.00	8.58	2.44	0.30	1.0	8.74	4.84	0.9443	9.38	0.15	0.9942

Note: *c* – concentration;  $\tau_0$  – yield stress; *k* – consistency coefficient; *n* – flow behaviour index; *R*<sup>2</sup> – determination coefficient. The hyphen means that no relevant value was possible to determine by the fitting of the model.

Table 7.3. Effect of temperature on the flow parameters of Herschel-Bulkley model (without extrapolation) for 0.25% (w/w) solutions.

Solvent	$T$ (°C)	Guar gum			$\kappa$ -carrageenan			Xanthan gum		
		$\tau_0$ (Pa)	$k$ (Pa.s <sup>n</sup> )	$n$	$\tau_0$ (Pa)	$k$ (Pa.s <sup>n</sup> )	$n$	$\tau_0$ (Pa)	$k$ (Pa.s <sup>n</sup> )	$n$
Distilled water	20	-0.15	0.12	0.67	-0.04	0.03	0.88	0.86	0.20	0.51
	25	-0.12	0.09	0.69	-0.03	0.02	0.90	0.68	0.24	0.48
	30	-0.07	0.06	0.74	-0.03	0.02	0.89	0.57	0.30	0.44
	35	-0.08	0.06	0.73	-0.02	0.02	0.92	0.50	0.30	0.45
	40	-0.07	0.05	0.74	-0.02	0.02	0.95	0.31	0.35	0.43
	45	-0.06	0.05	0.76	-0.01	0.02	0.94	0.21	0.35	0.43
0.07M KCl	20	-0.04	0.03	0.80	0.43	0.31	0.47	0.72	0.19	0.49
	25	-0.03	0.02	0.85	0.14	0.31	0.45	0.49	0.25	0.44
	30	-0.03	0.03	0.81	0.38	0.17	0.54	0.32	0.31	0.41
	35	-0.02	0.02	0.84	0.36	0.13	0.56	0.34	0.32	0.40
	40	-0.02	0.02	0.85	0.27	0.13	0.55	0.34	0.28	0.41
	45	-0.02	0.02	0.87	0.30	0.10	0.59	0.27	0.30	0.40

Note:  $T$  – temperature;  $\tau_0$  – yield stress;  $k$  – consistency coefficient;  $n$  – flow behaviour index.

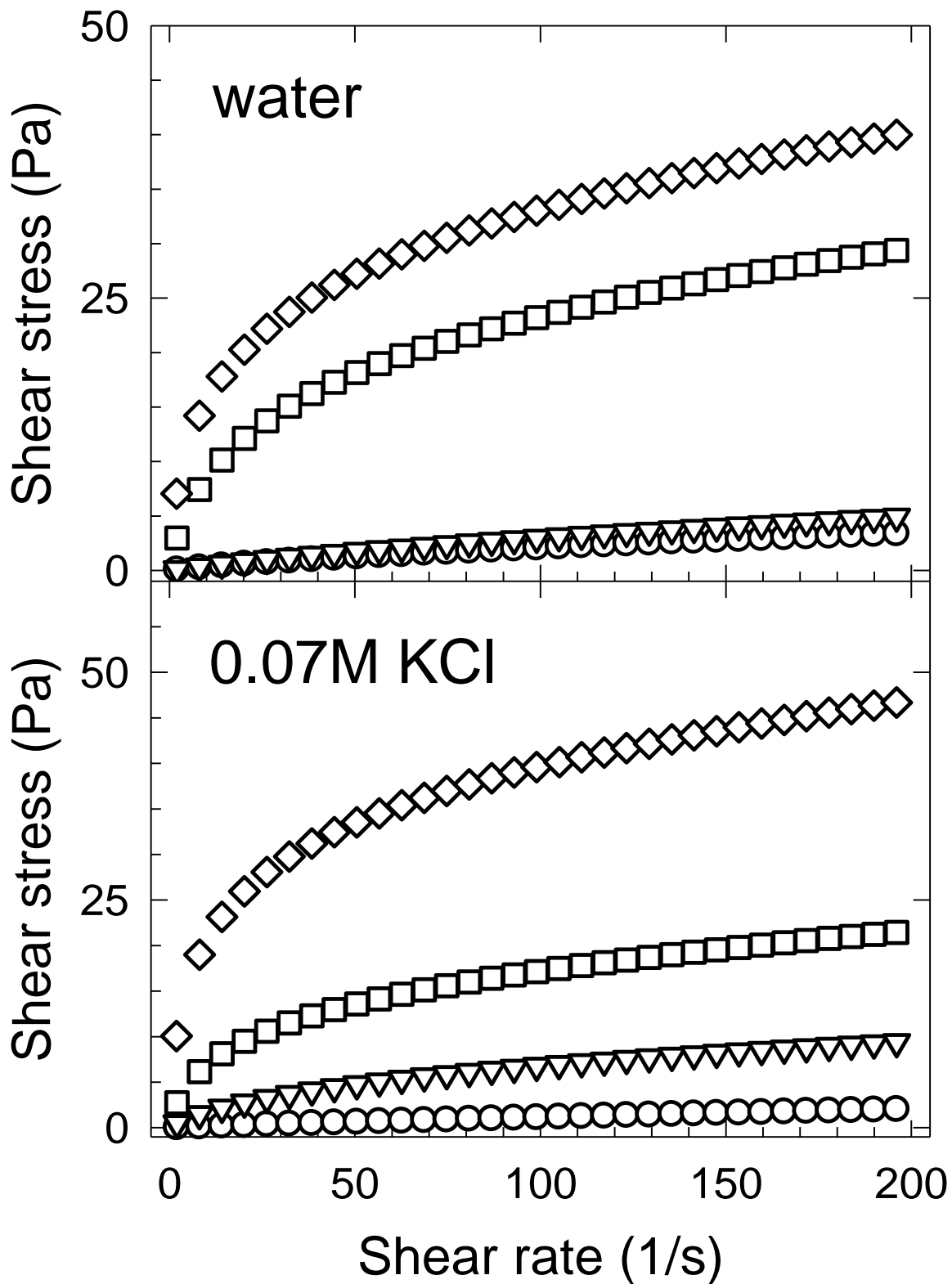


Fig. 7.1. Concentration dependent flow curves of guar gum solutions at 25 °C (increasing shear rate): circle – 0.25 w.%, triangle – 0.50 w.%, square – 0.75 w.%, diamond – 1.0 w.%.



### 7.1.2 Intrinsic viscosity

Polysaccharide solutions in distilled water and 0.07M KCl were characterized by the intrinsic viscosity  $[\eta]$  calculated according to the Kraemer equation (Eq. 6.4). The values of  $[\eta]$  were also tested by the Huggins equation without correct results, because the plot of  $\eta_{sp}/c$  versus concentration ( $c$ ) was not linear. The Kraemer plots of the studied samples at 25 °C are presented in Fig. 7.2.

Values of intrinsic viscosity of guar gum and xanthan gum in KCl solutions are moderately lower in comparison with  $[\eta]$  of these polymers in distilled water at the same temperature ( $T$ ), as evident from data given in Tables 7.4 and 7.5. For comparison, the intrinsic viscosity of guar gum at 20 °C in water was 14.47 dL/g, while  $[\eta]$  of guar gum in KCl was 12.77 dL/g (at 20 s<sup>-1</sup>). This fact can be related to a partial dissolution of colloidal polymer aggregates due to the presence of potassium cations. As stated by Ma and Pawlik (2007) for dilute guar gum solutions with salt addition, the chaotropic electrolytes such as KCl are able to accelerate the dissolution of colloidal aggregates which are ordinarily present in polysaccharide solutions under ambient conditions. This dissolution of colloidal polymer aggregates consequently results in a decrease of intrinsic viscosity.

In the case of guar gum, the obtained results of intrinsic viscosity of salt solutions are in accordance with the data in literature. For example,  $[\eta]$  of guar gum in KCl at 25 °C was 12.23 dL/g (at 20 s<sup>-1</sup>). This value corresponds very closely to  $[\eta]$  obtained by Wang et al. (2015) for guar gum dissolved in seawater (12.53 dL/g, according to the Higiroy et al.'s equation).

From a structural point of view, hydrogen bonding-induced network of guar gum structure (Li et al., 2006) is more likely to collapse at higher temperatures; as a consequence, the viscosity of guar gum solutions decreases with increasing temperature. Intrinsic viscosity of guar gum in water was slightly decreasing within temperature range 20-45 °C (at 20 s<sup>-1</sup>), due to increasing intramolecular distance between the molecules in the solution. However, the change of  $[\eta]$  at higher shear rate (100 s<sup>-1</sup>) was not so extensive, suggesting a lower temperature dependency of intrinsic viscosity at higher shear rates, probably due to the breakage of the original molecular arrangements. For guar gum solutions in KCl, the intrinsic viscosity fluctuated in a relatively narrow range (see Tables 7.4 and 7.5).

Intrinsic viscosity of xanthan gum is strongly dependent on its macromolecular structure. As compared to other polysaccharides, xanthan is relatively rigid, probably due to the interactions between the trisaccharide side chains and polymer backbone, resulting in a greater conformational constraint. The presence of ionizable groups on side chains, which dissociate in water, affects xanthan solution properties. Backbone of xanthan in water at room temperature (20-25 °C) is extended by the electrostatic repulsions between the charged groups on the side chains; at 25 °C, the addition of salt causes the collapse of side chains onto the backbone because of the charge screening effect,

and xanthan chains tend to adopt a stable helical conformation. This screening effect leads to a decreased intrinsic viscosity in the salt solution (Brunchi et al., 2014).

Obtained results confirmed the fact that intrinsic viscosity of xanthan gum in distilled water is higher than in KCl solution, although the differences between the samples were only moderate. For instance, the value of  $[\eta]$  for xanthan in water at 20 °C was 20.10 dL/g, whereas for xanthan in KCl 19.52 dL/g (at 20 s<sup>-1</sup>). Thus, the intrinsic viscosity of xanthan gum was influenced by its specific conformations in various solutions. Secondary structure of xanthan gum depends not only on solvent and salinity, but also on temperature. As temperature increases, a new transition to disordered random coil conformation occurs; the polymer macromolecules are dissociated, and therefore the observed rheological properties of the solution are changed (Brunchi et al., 2014). Values of intrinsic viscosity of xanthan gum both in water and KCl solution were decreasing with increasing temperature; the increase was relatively constant, although the change was larger at higher shear rate (100 s<sup>-1</sup>), as compared to  $[\eta]$  at lower shear rate (20 s<sup>-1</sup>).

As evident from the results, xanthan gum undergoes an order-disorder transition on heating at temperature about 30 °C. The disordered form is characterized by the random coils, but the precise nature of the ordered helix form is still in debate. The thermal transition is reversible and the original state is recovered upon cooling. The addition of electrolyte promotes the ordered state as demonstrated by an increase in the conformational heterogeneity at a given temperature, which is described in many scientific studies (Viebke & Williams, 2000; Mannion et al., 1992).

Viebke and Williams (2000) performed the order-disorder transition of xanthan gum aqueous solutions. The transition was broad, in the temperature range of ca. 30-70 °C, as measured by DSC. In the same way, Williams et al. (1991) found that the midpoint transition temperature ( $T_{mid}$ ) of xanthan gum mixed with konjac mannan or locust bean gum in water was 51 °C, whereas in 0.04 mol.dm<sup>-3</sup> NaCl the  $T_{mid}$  even increased to 84 °C. In general, the value of xanthan transition temperature changes with concentration of salt solution (of different ionic strength), and is naturally dependent on the character of hydrocolloid and feasible combinations of dissolved polymers (Pelletier et al., 2001). Moreover, a suitable technique (such as DSC) enables to determine a thermoanalytical curve with a  $T_{mid}$  value of the solution, whereas the rheological approach in this study was focused on the change of solution flow behaviour, represented by a specific change related to the temperature of conformational transition.

The transition from ordered macromolecular structure stabilized by relatively strong hydrogen bonding system to a collapsed random coil conformation of studied aqueous solutions (in distilled water) and helix-coil transition (in KCl) were demonstrated by the plots of Kraemer constant ( $k_K$ ) versus temperature, as

presented in Fig. 7.3. The presence of chaotropic ions  $K^+$  in KCl solutions leads to a small increase of Kraemer constant of guar gum in KCl as compared to water. Generally, the increasing values of  $k_K$  indicates a better solubility of the polymer in the solution. When compared guar gum in water with one in salt solution, the Kraemer constant (at  $20\text{ s}^{-1}$ ) mildly increased at the lowest temperature ( $20\text{ }^\circ\text{C}$ ), as well as at the highest temperature ( $45\text{ }^\circ\text{C}$ ). It means that salt solution ( $0.07\text{M KCl}$ ) point to be a better solvent for guar gum than distilled water.

Observed differences in  $k_K$  between the samples of xanthan gum in water and KCl were only minor. On the other hand, the values of intrinsic viscosity and Kraemer constant of  $\kappa$ -carrageenan were substantially different for samples in salt solution than for samples in distilled water. This rheological behaviour of  $\kappa$ -carrageenan solutions is consistent with the observations of many other authors (Brenner et al., 2014; Chen et al., 2002; Núñez-Santiago et al., 2011; Piculell et al., 1997), and it can also be the conformation of better solubility of studied polysaccharide types (of shear-thinning character) in KCl solution as compared to distilled water.

As can be seen in Fig. 7.3,  $\kappa$ -carrageenan showed a conformational transition at temperature about  $30\text{ }^\circ\text{C}$ . Viebke and Williams (2000) determined by DSC technique the order-disorder transition of  $\kappa$ -carrageenan in  $0.1\text{M}$  sodium iodide at  $37\text{ }^\circ\text{C}$  ( $T_{mid}$ ). Iodide salts stabilised the helical conformation of  $\kappa$ -carrageenan (the ordered state), but prevent aggregation. As stated by Plashchina et al. (1986), the concentration of solution ions strongly affects the midpoint temperature of  $\kappa$ -carrageenan helix to coil transition. In the case of  $\kappa$ -carrageenan in KCl solution, the authors define the temperature of  $\kappa$ -carrageenan conformational transition as linearly increasing function of the logarithm of potassium cations concentration.

$\kappa$ -carrageenan even at low concentrations ( $0.1\text{-}0.5\text{ \% w/w}$ ) provides high viscosity solutions; it forms strong *gels* with potassium ions. The mechanism of gelation involves coil-helix transition of carrageenan molecules (Dunstan et al., 2001). Gel is an intermediate state of hydration between solid and sol, and has a continuously three dimensional network in which solid matrix encloses a delicately separated liquid phase and immobilizes the liquid within it to form a rigid structure. This structure is resistant to flow. From rheological aspect, gel is a viscoelastic system with the storage (elastic) modulus ( $G'$ ) larger than the loss (viscous) modulus ( $G''$ ). The textures of hydrocolloid gels vary extensively, from the elastic gel to the brittle gel. As far as brittle gels are concerned, they may be generated when carrageenans are involved, which is the case of my study. Gel structure of  $\kappa$ -carrageenan is easy to shrink and prone to syneresis (Li & Nie, 2016).

As confirmed in the present research, it is possible to yield carrageenan gels upon cooling depending of the presence of specific cations. This is in agreement with the research of other authors who characterized  $\kappa$ -carrageenan gels as hard

and brittle, and the formation and aggregation of carrageenan helices to be strongly dependent on the identity of alkaline cations (Brenner et al., 2014; Núñez-Santiago et al., 2011).

In the case of this study,  $\kappa$ -carrageenan in 0.07M KCl provided hard gels, except at concentration of 0.25 % (w/w) which exhibited an unstable gelation at room temperature (approx. 25 °C). Intrinsic viscosity of these polymer-salt solutions was evidently higher than that of samples in water, particularly at lower shear rates. The less negative values of Kraemer constant determined for  $\kappa$ -carrageenan in KCl also indicate a better affinity of carrageenan chains to this salt solvent as compared to distilled water, as discussed above.

Table 7.4. Intrinsic viscosity and Kraemer constant at 20 s<sup>-1</sup> and 100 s<sup>-1</sup> for samples in distilled water.

Sample	T (°C)	Kraemer equation (20 s <sup>-1</sup> )		Kraemer equation (100 s <sup>-1</sup> )	
		$[\eta]_K$ (dL/g)	$k_K$	$[\eta]_K$ (dL/g)	$k_K$
Guar gum	20	14.47	-0.03930	13.17	-0.04600
	25	14.36	-0.03882	13.19	-0.04544
	30	13.74	-0.03836	12.82	-0.04501
	35	13.61	-0.03806	12.75	-0.04454
	40	13.58	-0.03789	12.84	-0.04426
	45	13.62	-0.03778	12.86	-0.04396
$\kappa$ -carrageenan	20	11.37	-0.04407	11.46	-0.05383
	25	11.59	-0.04339	11.78	-0.05299
	30	12.01	-0.04762	12.09	-0.05406
	35	12.45	-0.05272	12.35	-0.05633
	40	13.07	-0.05457	13.08	-0.05604
	45	13.52	-0.05429	13.32	-0.05568
Xanthan gum	20	20.10	-0.03717	15.18	-0.04872
	25	20.46	-0.03644	15.62	-0.04739
	30	20.98	-0.03567	16.05	-0.04620
	35	21.27	-0.03508	16.49	-0.04510
	40	21.55	-0.03457	16.91	-0.04410
	45	21.66	-0.03422	17.25	-0.04321

Note: T – temperature;  $[\eta]_K$  – intrinsic viscosity according to the Kraemer equation;  $k_K$  – Kraemer constant.

Table 7.5. Intrinsic viscosity and Kraemer constant at 20 s<sup>-1</sup> and 100 s<sup>-1</sup> for samples in 0.07M KCl.

Sample	<i>T</i> (°C)	Kraemer equation (20 s <sup>-1</sup> )		Kraemer equation (100 s <sup>-1</sup> )	
		$[\eta]_K$ (dL/g)	$k_K$	$[\eta]_K$ (dL/g)	$k_K$
Guar gum	20	12.77	-0.03503	11.65	-0,04359
	25	12.23	-0.03311	11.48	-0.04236
	30	12.87	-0.03400	11.83	-0.04210
	35	12.83	-0.03328	11.92	-0.04141
	40	12.82	-0.03278	12.01	-0.04086
	45	12.77	-0.03239	12.06	-0.04036
κ-carrageenan	20	19.71	-0.03205	15.98	-0.04317
	25	19.59	-0.03162	15.52	-0.04264
	30	19.49	-0.03099	15.51	-0.04271
	35	20.05	-0.03107	15.95	-0.04226
	40	19.87	-0.03120	15.78	-0.04233
	45	19.82	-0.03156	15.77	-0.04281
Xanthan gum	20	19.52	-0.03638	14.40	-0.04759
	25	19.76	-0.03612	14.74	-0.04672
	30	20.01	-0.03552	15.12	-0.04573
	35	20.51	-0.03499	15.49	-0.04487
	40	20.73	-0.03469	15.77	-0.04420
	45	20.97	-0.03426	16.07	-0.04347

Note: *T* – temperature;  $[\eta]_K$  – intrinsic viscosity according to the Kraemer equation;  $k_K$  – Kraemer constant.

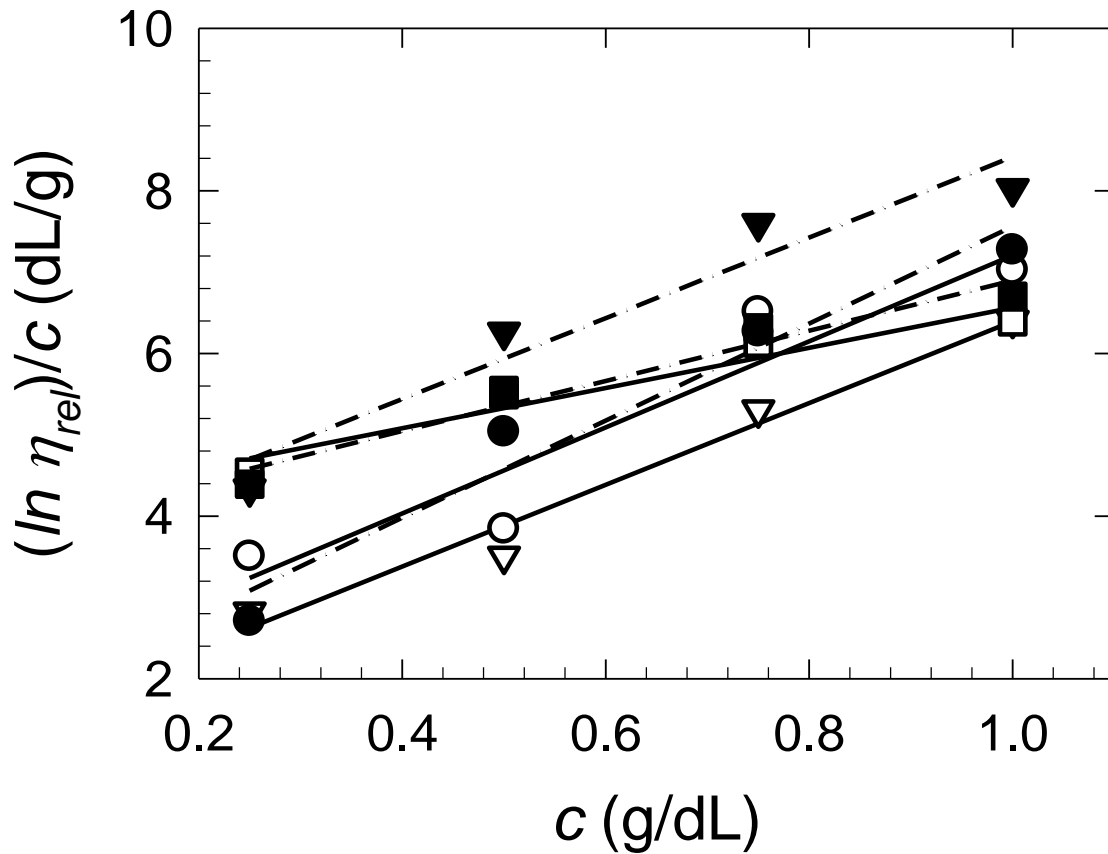


Fig. 7.2. Kraemer plot of studied hydrocolloids samples in water (empty symbols) and in 0.07M KCl (full symbols) at 25 °C (viscosities read at shear rate 20 s<sup>-1</sup>): circle – guar gum, triangle – κ-carrageenan, square – xanthan gum. Linear regression curves: full line – in water, dash-dot line – in 0.07M KCl.

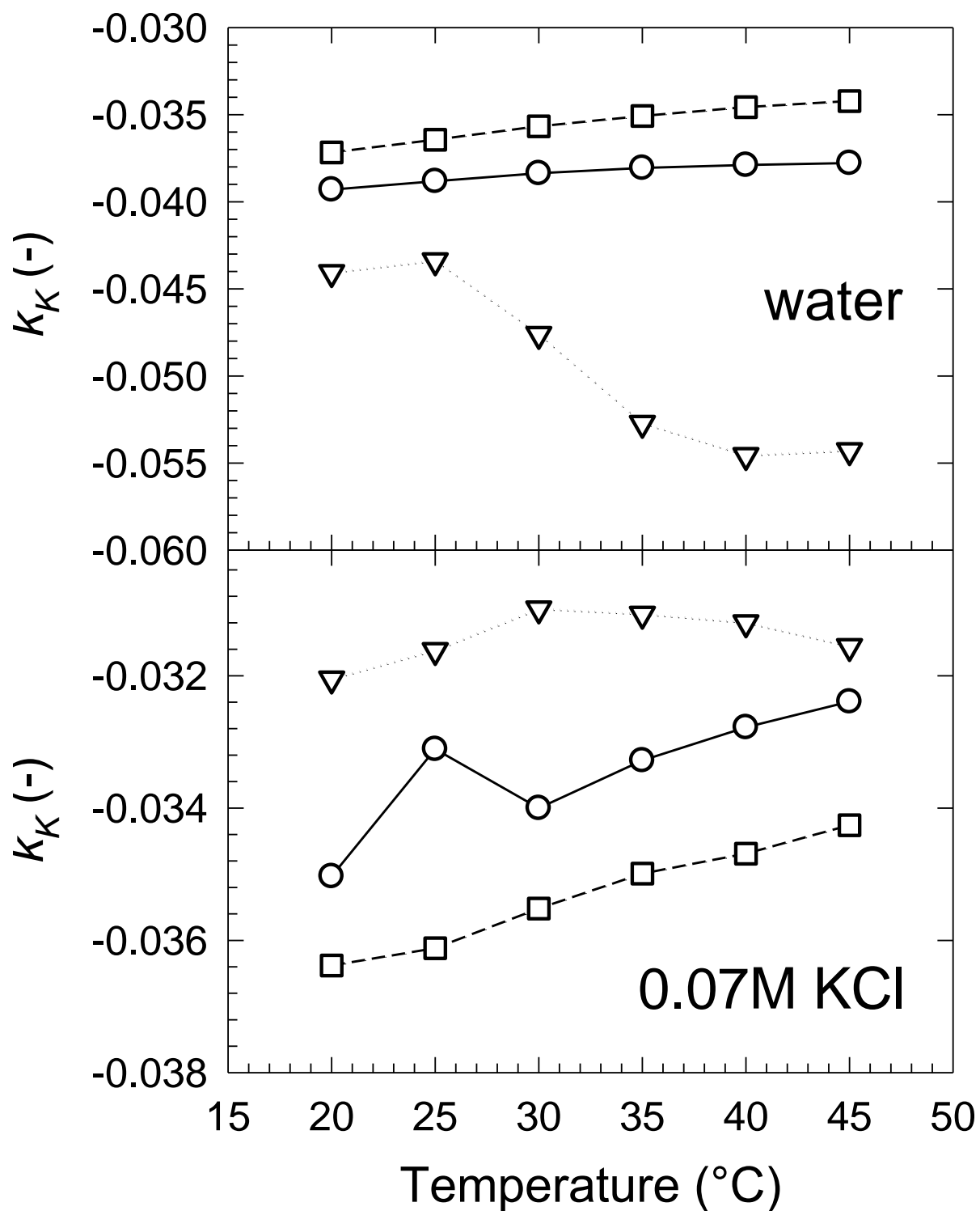


Fig. 7.3. Temperature dependency of the Kraemer constant ( $k_K$ ) of studied samples in water and in 0.07M KCl (at shear rate  $20 \text{ s}^{-1}$ ): circle – guar gum, triangle –  $\kappa$ -carrageenan, square – xanthan gum.

## 7.2 Thermal and temperature dependency of polysaccharide hydrocolloids

### 7.2.1 Thermal analysis - endothermic transition and moisture content

Thermogravimetric analysis (TGA) and differential thermal analysis (DTA) of powder polysaccharide hydrocolloids were used to investigate the hydrocolloid-water interactions. TGA and DTA curves of studied samples are shown in Figs. 7.4 and 7.5. Measured values of peak temperature ( $T_p$ ), reaction enthalpy ( $\Delta H$ ), weight loss, and moisture content ( $\Delta m_w$ ), respectively, were determined at different heating rates with regard to the kinetics of phase transition and water evaporation. According to the ability to bind water in different amount, the hydrocolloids showed different values of  $\Delta H$  and  $T_p$ , as given in Tables 7.6 and 7.7.

As listed in the tables, different moisture content of the samples after their conditioning proved the ability of hydrocolloids to bind water to different extent, i.e., the role of polysaccharide structure to equilibrate the moisture content of powders was evident. After the conditioning by saturated vapours, guar gum was able to bind relatively low moisture content, as compared to other hydrocolloid samples (e.g., 27.3 % w/w by potassium acetate conditioning). This fact can be related to the unique structure of guar gum, consisting of galactomannan chains of various mannose to galactose ratio. This ratio can vary in specific range (e.g., 2:1) (Gupta et al., 2015; Li et al., 2005), and it can be the reason of different sample solubility (affinity to water). From a structural point of view, guar gum is a galactomannan of which the twofold guaran helix is stabilized by periodic intramolecular hydrogen bonds between the galactosyl side chains and mannan main chain (Li et al., 2006), which can be responsible for the lower affinity of guar structure to water molecules in comparison to other hydrocolloids examined.

On the other hand, xanthan gum was able to bound relatively high moisture content (e.g., 38.7 % w/w using potassium acetate standard) which indicates the higher affinity of its polymeric structure to water molecules. Xanthan gum is a branched hetero-polysaccharide built up from sugar nucleotides precursors (Viturawong et al., 2008) and it can be assumed that the water molecules may be included in the complex structure of xanthan pentasaccharide repeating units. Character of xanthan order-disorder transition is dependent on the degree of ionization of xanthan carboxyl and acetyl residues (Bilanovic et al., 2015; Pelletier et al., 2001), and this fact may be related to the obtained values of thermal parameters.

In the case of  $\kappa$ -carrageenan, the moisture content ranged between 9.0 and 34.1 % (w/w) within the conditioning regime used.  $\kappa$ -carrageenan consists of an alternating linear chain of  $\beta$ -D-galactose and 3,6-anhydro- $\alpha$ -D-galactose (Dunstan et al., 2001), and it is conceivable that the number and position of the



sulphate groups attached to the galactose units (Sen & Erboz, 2010) can be related to the ability of powder hydrocolloid to bind moisture.

Observed results confirmed the ability of powder hydrocolloids to bind moisture in varying degrees, depending on their chemical configuration and higher-order conformational structure. This mode of behaviour seems to be characteristic for the polysaccharide hydrocolloids examined in this study. It means that the course of phase transition is controlled by water availability in the system. This availability is related not only to the ability of particular hydrocolloids to hold water molecules, but also to their conformational changes, and can be used for the identification of individual samples (Baranowska et al., 2008), as evidenced by the fact that the same mode of hydrocolloids' behaviour was found for all tested moisture content regimes.

In general, as given in Table 7.7, there was obtained higher values of reaction enthalpies with increased moisture content in the whole relative humidity conditioning regime started from 22.5 % up to 84.3 % of relative humidity (RH). It seems reasonable to assume that the application of the different relative air humidity conditioning affected the saturation of powders by means of initiating their swelling at higher relative humidity of the air/powder interface. Hence, this triggered at the higher relative humidity the decrease of total surface available for water sorption. Therefore, there was a higher saturation of polysaccharide powders during potassium acetate conditioning (providing relatively low values of air humidity) than using potassium chloride conditioning of relatively high RH (84.3 %) but accompanied by the process of powder swelling, which didn't allow an "adequate" saturation of conditioned powders.

As already mentioned, the hydrocolloids with increasing moisture content (at the same heating rate) provided higher values of reaction enthalpy (regardless of the hydrocolloid type), suggesting that the endothermic transition is fully completed at higher moisture level in the system. The comparison of different saturated hydrocolloids also enables the evaluation of the relations between the results of thermal analysis and Arrhenius parameters (see chapter 7.2.4), considering the fact that an "intermediate" water content usually occurs in the real food systems during practical food applications.

As obvious from the graphs (Figs. 7.4 and 7.5), the first thermal transition is an endothermic process initialized at the beginning of heating procedure (30 °C). This process can be related to the change of hydrocolloid structure analogous to the gelatinization of starch (Ai and Jane, 2015; Coral et al., 2009; Liu et al., 2006; Zobel and Stephen, 2006). Reaction enthalpy provides energy required to change the structure of powder samples, thus  $\Delta H$  illustrates the order-disorder transition reflecting changes on molecular scale of tested samples. This fact is in accordance with the moisture weight loss at temperatures ranging between 30 to 200 °C. This is demonstrated by the first step on TGA curves in the above mentioned temperature range (Fig. 7.4), corresponding to the phase transition observed on DTA curves (Fig. 7.5).

The drop of system enthalpy proved the fact that the underlying process deals with the water vaporization from the powders, corresponding to the process of water diffusion and, at higher temperatures, water desorption from the samples. These two steps of water release are closely related to the molecular mobility and binding of water to polymer network. When the sample is heated, water rearranges its partition over the system, and the more tightly bound water becomes less free to move away, thus requiring higher temperatures to be evaporated by the desorption process (Appelqvist et al., 1993; Fessas and Schiraldi, 2001).

The observation of order-disorder transition with characteristic peak temperature coheres with the moisture content of the samples because water molecules promote the beginning of the transition process in the polysaccharide powders. In other words, water molecules have a function of plasticizing agents in the polymer molecular network (Roos, 1995), and for that reason without presence of water as a plasticizer, the transition in polymeric structure (which is induced by thermal changes) could not be possible to occur and powders would be thermally decomposed at higher temperatures without any phase transition.

In spite of this important role of water, there was no obvious relationship between moisture content (weight loss) and peak temperature of the samples, as evident from the experimental data. The endothermic process, centred in the temperature range between 50 and 85 °C, showed no systematic change with the moisture content due to the fact, that the values of  $T_p$  provided apparently non-systematic variations with  $\Delta m_w$ . Therefore, it was impossible to generalize the relationship between these parameters, which is in accordance with the results by Appelqvist et al. (1993) for polysaccharides at low moisture content. As stated by the authors, the peak temperature variations may reflect thermal histories of the samples, i.e., the maximal temperatures encountered during their storage. Appelqvist and co-workers investigated the polysaccharide samples containing 5-25 % (w/w) water (conditioned at room temperature), as a general probe of water-carbohydrate interactions. Except for a few materials of very low moisture content (less than 5 % w/w), all polysaccharides showed an apparent endothermic event centred in the temperature range 50-80 °C (except those above their glass transition temperature), which corresponds to the data of my research.

As obvious from the results in the present study (Table 7.6), a shift of thermal peak to higher temperatures was observed using larger heating rate. The higher heating rate also leads to a higher value of reaction enthalpy, determined during the *faster* thermal treatment of the sample. This is typical thermal behaviour based on the fact that the diffusing elements (water molecules) cannot immediately react to the driving force imposed, i.e., to the increase of temperature, requiring some time to relax (Fessas and Schiraldi, 2000; Fessas and Schiraldi, 2001).

Thus, reaction enthalpy, related to the order-disorder transition and water evaporation, was evidently affected by the moisture content and heating rate used. Although each polysaccharide family may have a different water dose-response relation (Appelqvist et al., 1993), there was found a clear dependency between reaction enthalpy and moisture content of different polysaccharide samples. As can be seen in Table 7.6,  $\kappa$ -carrageenan with the lowest moisture content (after room conditioning) provided the lowest values of reaction enthalpy. On the other hand, xanthan gum exhibited the highest  $\Delta m_w$  corresponding to the highest  $\Delta H$  among the studied samples. Obtained values determined for xanthan gum (relatively large peak temperatures and reaction enthalpies) can be related to the specific structure of this polymer, as discussed above.

Table 7.6. Thermal analysis of powders (conditioned at room conditions) in the temperature range 30-200 °C at different heating rates.

Sample	$\beta$ (°C.min <sup>-1</sup> )	TGA	DTA	
		Weight loss (% w/w) (30-200 °C)	Temperature $T_p$ (°C)	Enthalpy $\Delta H$ (Endo) (J.g <sup>-1</sup> )
Guar gum	5	10.9	52.4	169.0
	10	10.0	64.4	216.0
	15	9.9	72.1	236.3
	20	9.4	77.4	221.1
$\kappa$ -carrageenan	5	9.5	49.6	94.0
	10	9.0	64.5	139.3
	15	8.7	70.7	137.9
	20	8.4	82.1	154.4
Xanthan gum	5	11.3	56.7	171.7
	10	12.1	69.2	259.6
	15	11.9	76.6	264.0
	20	11.9	83.1	298.5

Note:  $\beta$  – heating rate; TGA – thermogravimetric analysis; DTA – differential thermal analysis;  $T_p$  – peak transition temperature;  $\Delta H$  – reaction enthalpy.

Table 7.7. Thermal analysis of powders at constant moisture level (adjusted at different conditions) in the temperature range 30-200 °C at heating rate 10 °C/min.

Sample	Type of conditioning								
	Room conditions (25 °C, 40 vol.% RH)			Potassium chloride conditioning (25 °C, 84.3 % RH)			Potassium acetate conditioning (25 °C, 22.5 % RH)		
	$\Delta m_w$ (% w/w)	$T_p$ (°C)	$\Delta H$ (J.g <sup>-1</sup> )	$\Delta m_w$ (% w/w)	$T_p$ (°C)	$\Delta H$ (J.g <sup>-1</sup> )	$\Delta m_w$ (% w/w)	$T_p$ (°C)	$\Delta H$ (J.g <sup>-1</sup> )
Guar gum	10.0	64.4	216.0	18.4	53.2	231.5	27.3	52.1	363.3
$\kappa$ -carrageenan	9.0	64.5	139.3	20.1	55.5	267.3	34.1	57.8	481.0
Xanthan gum	12.1	69.2	259.6	24.6	57.9	369.0	38.7	72.6	670.9

Note: RH – relative humidity;  $\Delta m_w$  – moisture content;  $T_p$  – peak transition temperature;  $\Delta H$  – reaction enthalpy.

TGA (%)

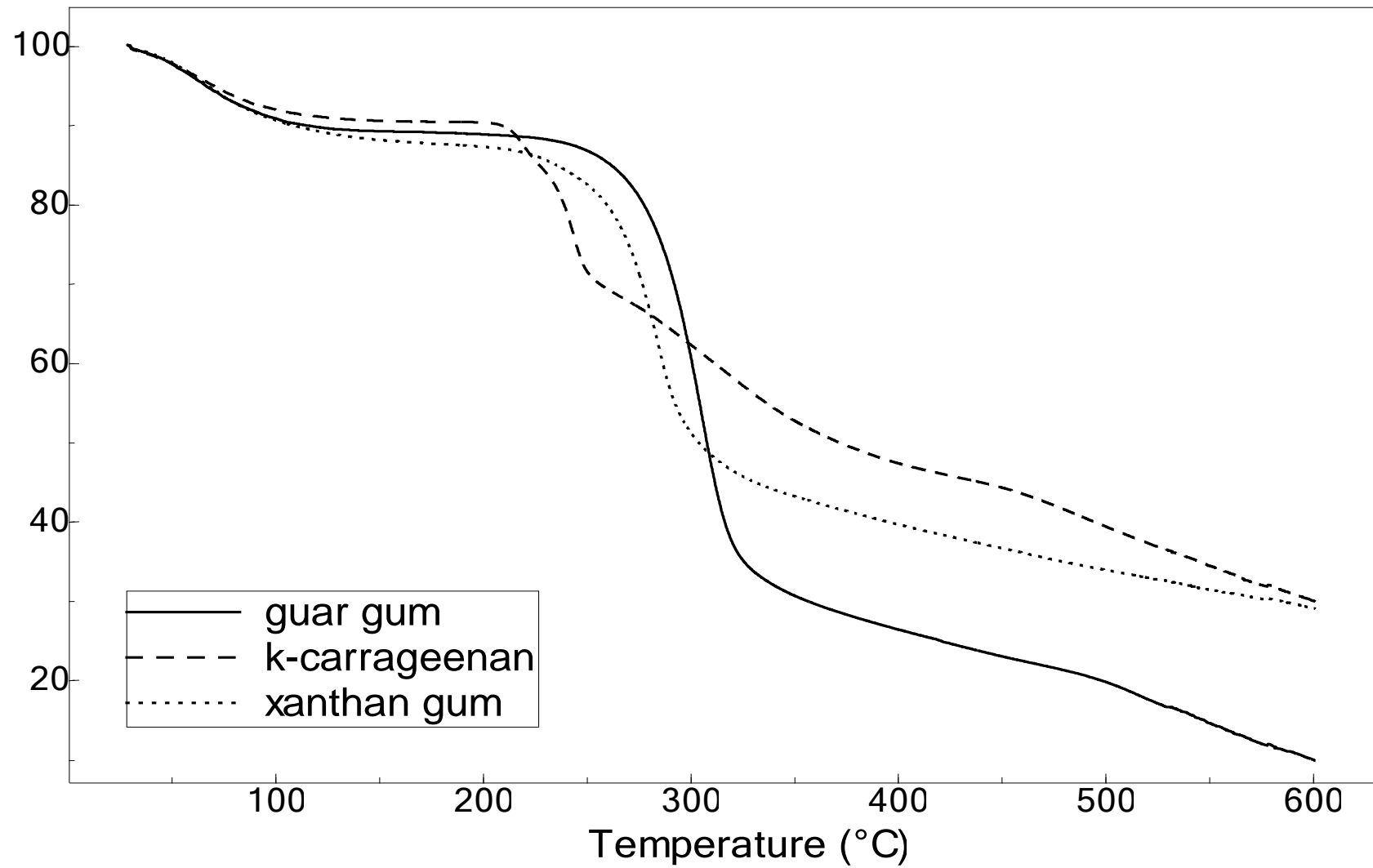


Fig. 7.4. TGA curves of powder samples (conditioned at room conditions) in the range 30-600 °C (heating at 10 °C/min).

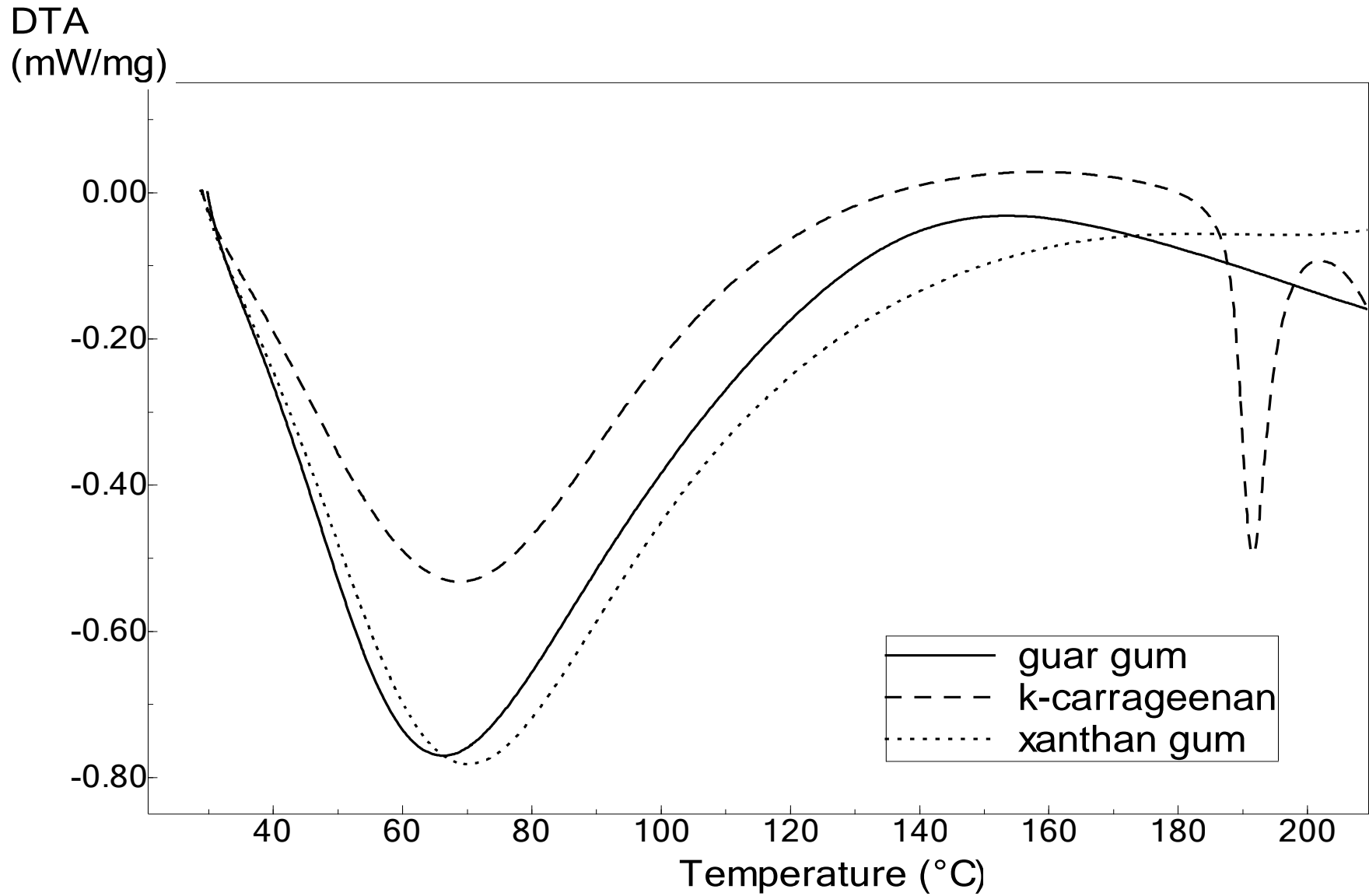


Fig. 7.5. DTA curves of powder samples (conditioned at room conditions) in the range 30-200 °C (heating at 10 °C/min).

### 7.2.2 Thermal stability of polysaccharide powders

Thermal stability of powder samples was found to be restricted to the temperature range between 200 and 230 °C. Exceeding this temperature limit, there was a noticeable decrease in the weight of each sample. As can be seen in Fig. 7.4, there was observed a second step on TGA curves in the temperature range from 200 to 400 °C. This weight loss represents thermal decomposition of polysaccharide chains and is different with the type of studied hydrocolloid (Table 7.8).

For all studied samples, the weight loss on TGA curves was accompanied by the second peak (exothermic) as observed on DTA curves (the peaks are not shown) which was assigned to thermal decomposition (burning profile) of the powders. In the studied temperature range (between 200 and 400 °C, at heating rate 10 °C/min), samples of  $\kappa$ -carrageenan showed a multi-step degradation, which was characterized by relatively low weight loss about 43 % (w/w), i.e.,  $\kappa$ -carrageenan exhibited the highest thermal stability of all powders under study. This specific degradation can be associated with the peak observed on DTA curve at approx. 240 °C.

In comparison to other samples, guar gum exhibited the most rapid decline of TGA curve (as shown in Fig. 7.4), corresponding to relatively high weight loss of 62.4 % (w/w). It means that thermal stability of guar gum powder was relatively low. Xanthan gum was characterized by one-step symmetric degradation with the weight loss of 47.6 % (w/w).

Table 7.8. Thermal stability (burning profile) of powders (conditioned at room conditions) in the temperature range 200-400 °C at heating rate 10 °C/min.

Sample	TGA	DTA	
	Weight loss (% w/w) (200-400 °C)	Temperature $T_p$ (°C)	Enthalpy $\Delta H$ (Exo) (J.g <sup>-1</sup> )
Guar gum	62.4	345.6	124.2
$\kappa$ -carrageenan	42.9	244.4	85.8
Xanthan gum	47.6	284.2	152.6

Note: TGA – thermogravimetric analysis; DTA – differential thermal analysis;  $T_p$  – exothermic peak temperature;  $\Delta H$  – enthalpy of thermal decomposition.

### 7.2.3 Kinetic models

Three different kinetic models were used to evaluate the process of water evaporation and order-disorder phase transition as induced on heating of powder samples (in the temperature range from 30 to 200 °C after room conditioning). The non-isothermal models used in this study enable to evaluate the activation energy of the process without determining the reaction model. To avoid the producing of method-dependent values, the results of  $E_a$  were compared on the basis of three different model types.

Values of activation energy ( $E_a$ ), representing the energy barriers which has to be overcome to attain sample transition, were determined based on TGA results. According to the kinetic model used,  $E_a$  values varied in a specific range, as can be seen in Table 7.9. Using Friedman model, activation energy was found to range between 10 and 30 kJ/mol. In the case of guar gum,  $E_a$  fluctuated in the range about 25 to 30 kJ/mol. For  $\kappa$ -carrageenan, activation energy was generally increasing with rising heating rate until 15 °C/min (the maximum value was approx. 31.4 kJ/mol). By Kissinger model, activation energy was determined in the range from 25 to 45 kJ/mol for samples studied at specified heating rates (Fig. 7.6).

To discuss the results obtained in my study, it is necessary to compare different model types. Friedman model (built on differential calculation of activation energy at different heating rates) is the most universal differential kinetic model because it is applicable to wide range of temperature programs. However, the use of this method requires the derivative conversion data which can be numerically unstable and noise sensitive (Cai et al., 2018).

Kissinger model as an integral method (based on integral calculation of a summary  $E_a$  value for all heating rates) can accomplish the same degree of multiple-heating rate universality as Friedman model but it has some important limitations. A main limitation of Kissinger model is the fact that produces a single value of  $E_a$  for the reaction process regardless of its actual kinetic complexity. Thus, activation energy determined by this model adequately represents only single-step kinetics. Moreover, because the degree of conversion  $\alpha_m$  may significantly vary with heating rate  $\beta$ , the determination of accurate  $E_a$  value requires the reaction model to be independent of  $\beta$ . Otherwise, the Kissinger plot would deviate systematically from a straight line, resulting in a systematic error in activation energy (Vyazovkin et al., 2011). For that reason, the Kissinger estimations of multi-step mechanism should be verified by other non-isothermal methods.

In my study, the values of  $E_a$  calculated by Friedman and Kissinger models match relatively closely in the case of  $\kappa$ -carrageenan and xanthan gum powders. Besides, the plots of Kissinger model in the present study (Fig. 7.6) confirmed a satisfactory accuracy of linear regression determined for all samples examined (no less than 95 % of  $R^2$ ).



Model-free kinetics was used to provide information about the relation between degree of conversion ( $\alpha$ ) and activation energy; this energy may not be constant at the same heating rate and is a function of sample conversion (Ramajo-Escalera et al., 2006). The dependency of  $\alpha$  on temperature for xanthan gum is plotted in Fig. 7.7. Model-free kinetics for the calculation of  $E_a$  values of  $\kappa$ -carrageenan is illustrated in Fig. 7.8. This method demonstrated an evident decrease of activation energy (from 180 to 60 kJ/mol) during heating of powders with increasing  $\alpha$ , particularly between 5 and 20 % of sample conversion. The largest decrease of  $E_a$  values was obtained for  $\kappa$ -carrageenan, the lowest for xanthan gum (as given in Table 7.9).

The decrease of activation energy with  $\alpha$  can be related to the loss of moisture and increasing disordering of powder system. The energetic associations between water molecules and polysaccharide chains (hydrophilic moieties) are disrupted during thermal treatment (Dranca & Vyazovkin, 2009) and the energy necessary to overcome the energy barriers of the system drop continually until 60 % of sample conversion. Above this limit, there was no systematic change of activation energy with  $\alpha$ ; an increase or fluctuation of  $E_a$  values was observed, which can be related to the process of thermal equalization.

Model-free kinetics is free of any temperature integral approximations. It allows even complex chemical reactions to be analysed using a few TGA measurements without making any assumptions about a particular reaction model (Cai et al., 2018; Jing, 2005). This kinetic approach reveals the reaction complexity as a dependency of the effective activation energy on  $\alpha$ ; it means that  $E_a$  varies with  $\alpha$  in multi-step kinetics (Vyazovkin, 2002). Compared to other methods used in this study, the values of  $E_a$  calculated for powder samples by Model-free kinetics were obviously higher due to the multi-step character of the reaction process, providing a total value of activation energy based on energy barriers of individual steps.

Table 7.9. Activation energy of powders (conditioned at room conditions) calculated by kinetic models in the temperature range 30-200 °C.

Sample	Friedman model				Kissinger model	Model-free kinetics							
	$\beta$ (°C/min)					$\alpha$ (%)							
	$E_a$ (kJ/mol)												
	5	10	15	20		5	10	20	30	40	50	60	
Guar gum	29.9	28.3	25.3	31.5	43.3	148.7	138.2	110.2	99.2	90.6	86.6	85.7	
$\kappa$ -carrageenan	11.0	18.7	31.4	26.7	26.4	179.8	146.0	78.2	69.7	64.2	61.7	60.5	
Xanthan gum	24.2	20.9	28.0	24.3	32.4	123.4	109.5	90.8	88.7	87.0	86.3	86.2	

Note:  $\beta$  – heating rate;  $E_a$  – activation energy;  $\alpha$  – degree of conversion.

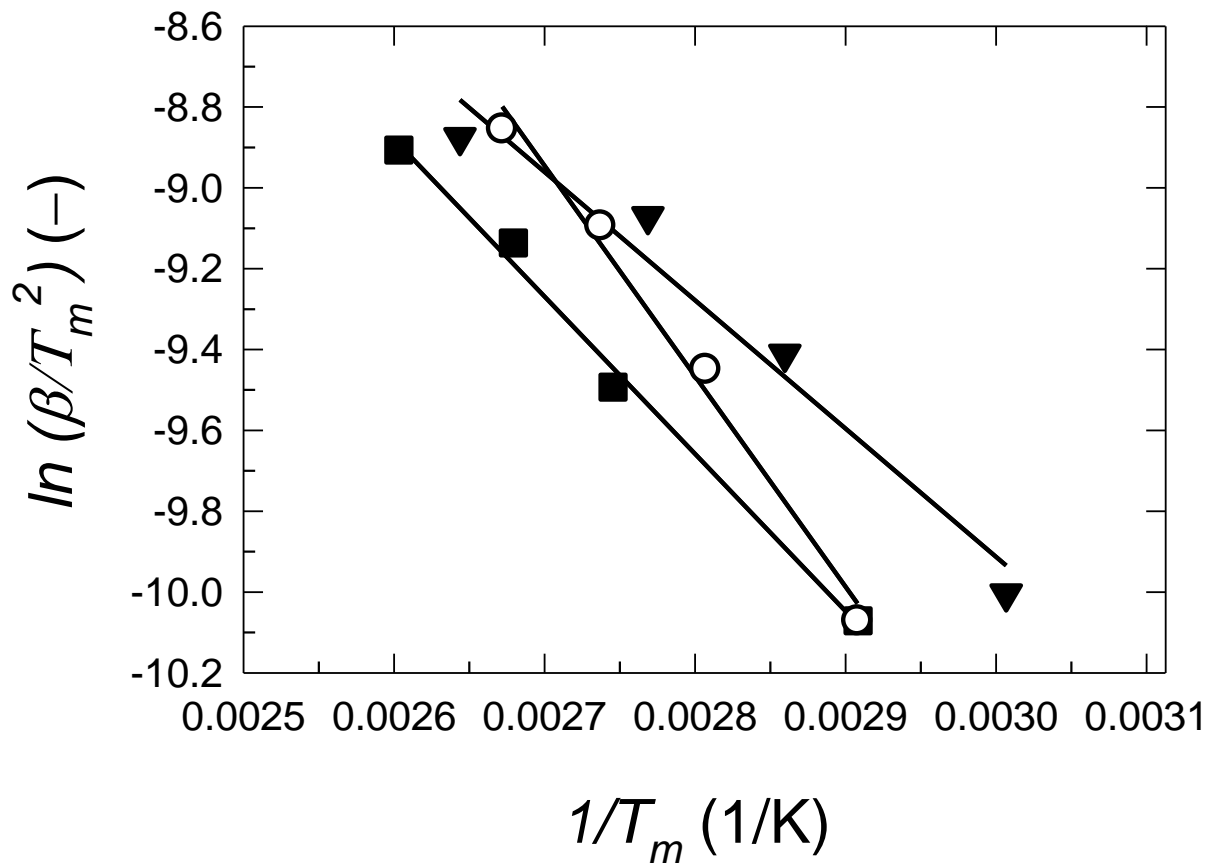


Fig. 7.6. Kissinger plot of studied powders in the temperature range 30-200 °C: empty circle – guar gum, full triangle –  $\kappa$ -carrageenan, full square – xanthan gum;  $\beta$  – heating rate;  $T_m$  – peak temperature on derivative thermogravimetric curve. Full line – linear regression curve.

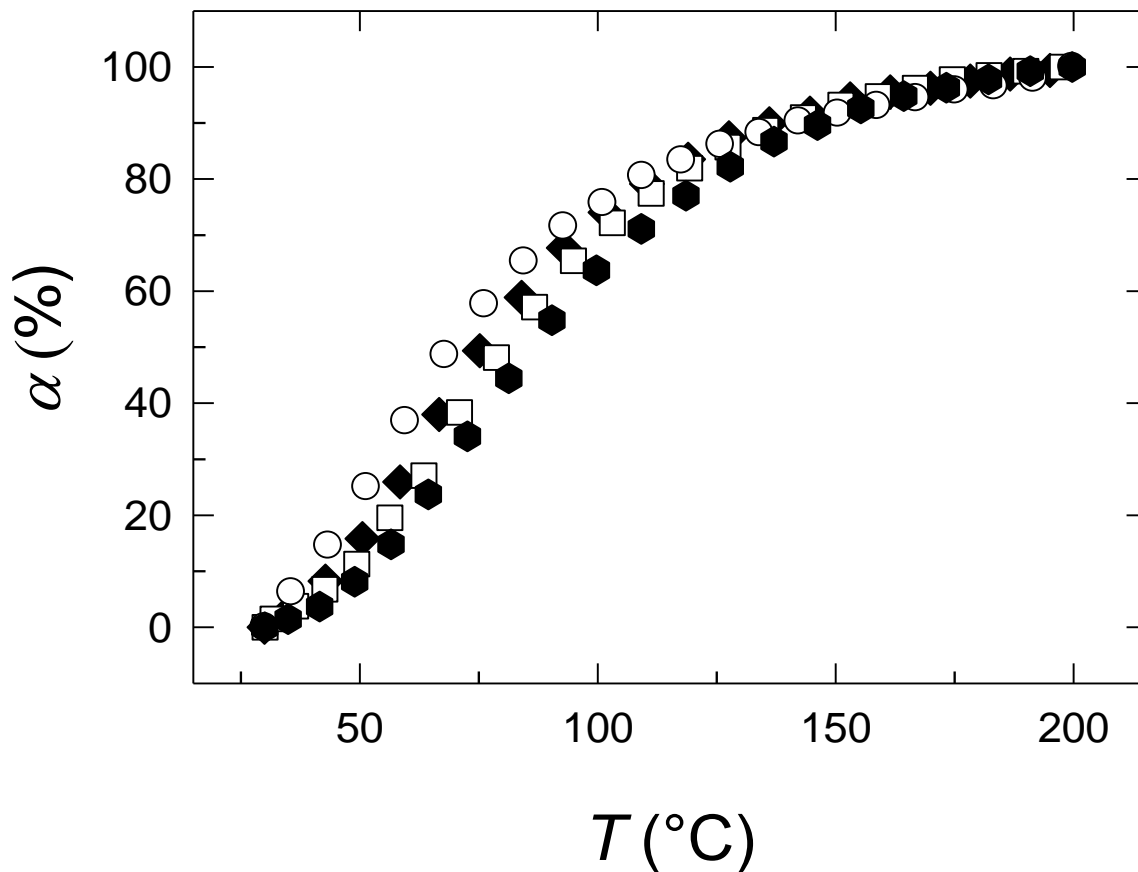


Fig. 7.7. Degree of conversion ( $\alpha$ ) vs. temperature  $T$  (in the temperature range 30-200 °C) at different heating rates for xanthan gum powder: empty circle – heating rate 5 °C/min, full diamond – heating rate 10 °C/min, empty square – heating rate 15 °C/min, full hexagon – heating rate 20 °C/min.

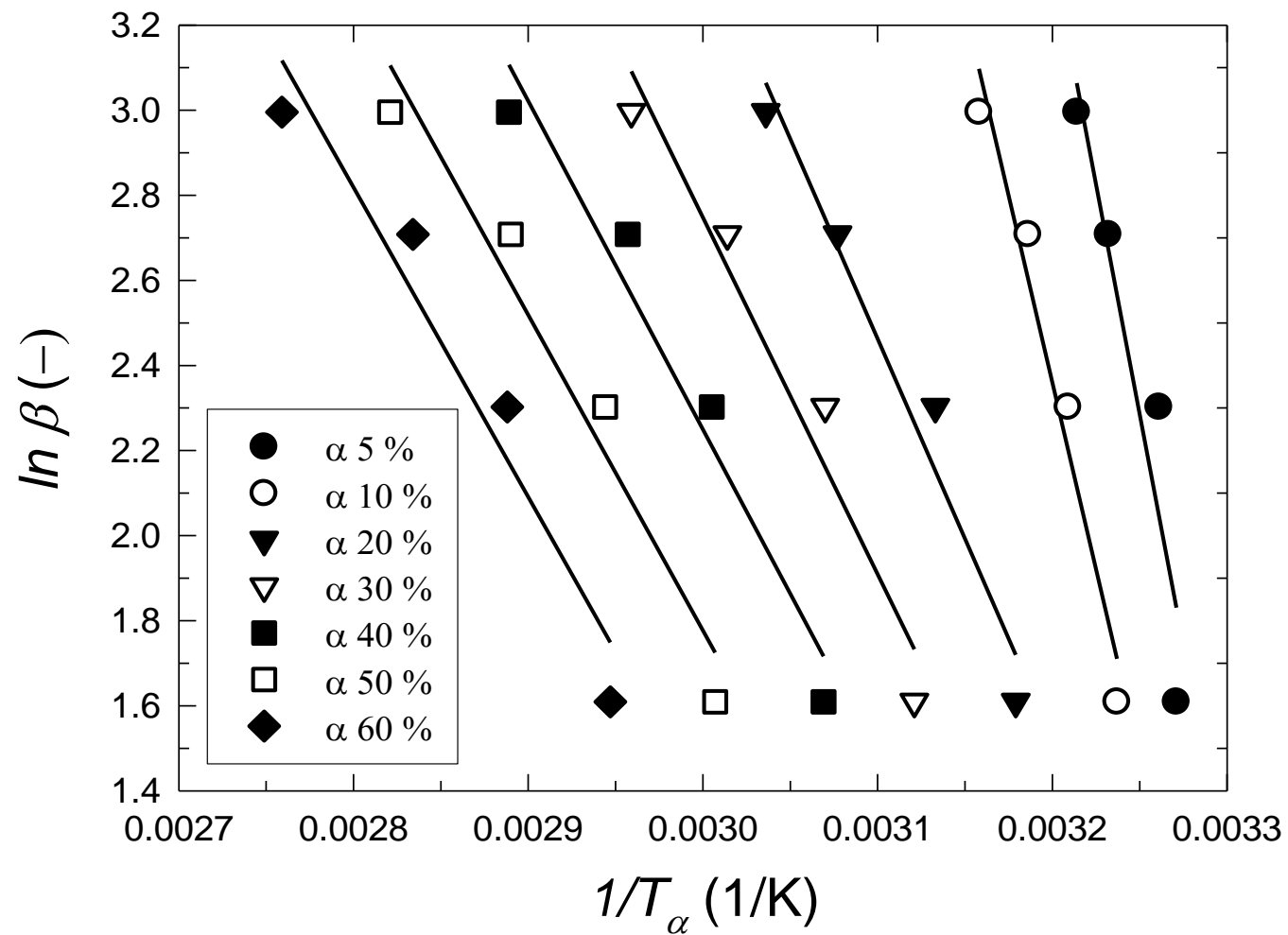


Fig. 7.8. Model-free kinetics plot of  $\kappa$ -carrageenan in the temperature range 30-200 °C:  $\beta$  – heating rate;  $T_\alpha$  – thermodynamic temperature at the degree of conversion  $\alpha$ . Full line – linear regression curve.

## 7.2.4 Arrhenius parameters

Temperature sensitivity of 0.25% to 1.0% (w/w) hydrocolloid solutions both in distilled water and in 0.07M KCl was evaluated by the Arrhenius model (at shear rates  $20 \text{ s}^{-1}$  and  $100 \text{ s}^{-1}$ ). Effect of temperature dependency on the apparent viscosity of 0.5% samples at shear rate  $20 \text{ s}^{-1}$  is presented in Fig. 7.9.

As clear from the data given in Tables 7.10 and 7.11, hydrocolloid samples in water generally exhibited higher values of activation energy ( $E_a$ ) and higher values of pre-exponential factor ( $A$ ), than samples in KCl (except  $E_a$  values for xanthan gum). This behaviour can be explained by the presence of chaotropic cations  $\text{K}^+$  in KCl solution, which partially shield the ionic charges along the polymer chains via electrostatic adsorption (the cations  $\text{K}^+$  diminish the electrostatic repulsion effect). As a result, this leads to a decrease in polymer bulk viscosity. In accordance with this fact, a lower activation energy has to be overcome to achieve the disentanglement of higher-order polymer structure in a salt solvent, and thus, to promote viscous flow of the solution. This is very important technological aspect in the manufacturing of food products modified by the hydrocolloids.

In my study, KCl was chosen to modify physicochemical properties of the solutions due to the specific character of  $\text{K}^+$  ions, as stated above. On the other hand, the electrostatic repulsion effect in distilled water contributed to a stretching state of polymer chains, which resulted in a higher hydrodynamic volume of dissolved polymer and a higher intrinsic viscosity (Ma & Pawlik, 2007; Wang et al., 2015). Therefore, higher activation energy was needed to promote viscous flow of samples in water as compared to samples in KCl solvent.

The values of pre-exponential factor ( $A$ ) determined for hydrocolloids in distilled water as well as in KCl correlate with the values of  $E_a$ . As listed in Tables 7.10-7.11, the values of  $A$  increase with decreasing activation energy, i.e., with increasing concentration of solutions (guar gum, xanthan gum). On the other hand, a decrease of pre-exponential factor with increasing  $E_a$  (at higher concentrations) was typical for  $\kappa$ -carrageenan in distilled water. From a thermodynamic point of view, this relationship is consistent with the theory that pre-exponential factor is related to the entropy of the system. Lower values of  $A$  represent a more ordered (i.e., less chaotic) molecular structure which requires higher energy to be broken down. It is in accordance with the fact that the hydrocolloids in KCl at higher concentrations (except  $\kappa$ -carrageenan due to its gelation) provide higher values of activation energy, as compared with the samples in distilled water owing to higher-order assembly of hydrocolloid structure in salt solution.

Obtained results of the present study confirmed the fact that the activation energy of hydrocolloid solutions, both in water and KCl, decreases with increasing shear rate. It suggests that the energy necessary for reorientation of solvent molecules is substantially reduced by higher shear rate. However, the

energy intake at  $100 \text{ s}^{-1}$  is still relatively high, which indicates a possible reorganisation of hydrocolloid chain structure during the energy input. In the region of higher shear rate values, hydrodynamic forces become of the same order of magnitude as the structural forces, which induces a new structure, and thus a new equilibrium can be attained after some time (Figura & Teixeira). This behaviour can be also related to the fact that the pre-exponential factor  $A$  of the solutions, representing the viscosity at infinite temperature (Busch et al., 2007), is generally decreasing (guar gum, xanthan gum) at higher shear rates, and hence the entropy of the system can be interpreted as a measure of the degree to which structural re-arrangement occurs during the flow (Chandler, 2014). The lower values of pre-exponential factor at higher shear rate are in agreement with the expected restructuring of polysaccharide chains. It suggests that the using of higher shear forces may re-establish a relatively ordered polymer structure during solution shearing process.

In addition, as stated above, the  $E_a$  values of salt solutions are lower in comparison to water samples at the same shear rate which may be explained by the ion-induced assembly of molecular chains in KCl, resulting in a higher temperature sensitivity at higher shear rates. The application of a higher shear stress broke up the original arrangement of hydrocolloid macromolecules which are associated into an incoherent structure (Pruska-Kedzior & Kedzior, 2007). This breakdown of samples' structure into small complexes led to a decrease of their structural resistance to temperature, according to the type of hydrocolloid and solvent used.

The results of the present study show that activation energy of guar gum both in water and in salt solutions was predominantly decreasing with increasing concentration, probably due to higher-order assembly of molecular structure at higher polymer concentrations. The decrease of  $E_a$  could be attributed to entanglement density of guar chain structure; the equilibrium of the density, representing the entanglement stability of the structure, is also decreasing with increasing shear rate (Wang et al., 2015). A new entanglement state results from the balance between the flow-induced disentanglement of the chains and the re-entanglement process governed by Brownian motion (Pruska-Kedzior & Kedzior, 2007). Thus, the activation energy necessary for the viscous flow of the sample was lower at higher shear rates. The observed temperature behaviour can be also related to the unique high viscosity properties of guar gum which provides high viscosity to food products when used even at low concentrations (Gupta et al., 2015; Nor Hayati et al., 2016).

Among all the samples,  $\kappa$ -carrageenan solutions provided the largest values of activation energy, thus exhibited the highest resistance of their molecular structure to the viscous flow. The highest  $E_a$  was determined for 1.0 % (w/w) carrageenan aqueous solution at  $20 \text{ s}^{-1}$ , 85.88 kJ/mol. In other words,  $\kappa$ -carrageenan was the most temperature resistant polymer with the lowest sensitivity of its structure to temperature changes, which is in agreement with

the observations of hydrocolloids behaviour by other authors (Marcotte et al., 2001a; Marcotte et al., 2001b). The values of activation energy in distilled water were substantially increasing with rising concentration of  $\kappa$ -carrageenan. This fact can be related to the specific properties of  $\kappa$ -carrageenan which yield high viscosity solutions even at low concentrations (ranging between 0.1 to 0.5 %). By cooling a salt solution at concentration no less than 0.5 %, the intermolecular association of carrageenan double helices occurs, and a super helical structure is formed (Núñez-Santiago et al., 2011; Şen & Erboz, 2010). In the presence of potassium cations, the solutions of  $\kappa$ -carrageenan (at concentration  $c \geq 0.5$  % w/w) formed firm and brittle gels; the gelation of  $\kappa$ -carrageenan in KCl was caused by coil to helix transition. However, there was no strong dependency of activation energy on polymer concentration in salt solution;  $E_a$  values fluctuated in a relatively narrow range at both shear rates.

Xanthan gum showed the lowest  $E_a$  values of all samples both in water and KCl, i.e., xanthan gum was the least temperature dependent sample. The activation energy of xanthan in 0.07M KCl ranges from 6.1 to 3.8 kJ/mol at  $20 \text{ s}^{-1}$ , and from 4.4 to 2.0 kJ/mol at  $100 \text{ s}^{-1}$ , respectively. Observed low values of activation energy can correspond to flow properties of xanthan solutions which show excellent thermostability over a wide temperature range (Brunchi et al., 2014).

Observed xanthan behaviour is in accordance with the results by Marcotte et al. (2001b) who ascertained that apparent viscosity of xanthan gum (in salt solution) is slightly affected by temperature but particularly affected by shear rate. As in the case of guar gum, activation energy of xanthan gum was mostly decreasing with increasing concentration. Xanthan solutions are highly pseudoplastic and do not form gel itself (Viturawong et al., 2008). For that reason, the formation of a stable molecular structure in the presence of potassium cations can lead to a decrease of  $E_a$  at higher xanthan concentrations. Nevertheless, the Arrhenius model was not suitable to apply to xanthan gum in distilled water, because of lower values of determination coefficient ( $R^2$ ) and due to negative values of activation energy obtained for more concentrated samples.



Table 7.10. Activation energy and pre-exponential factor at 20 s<sup>-1</sup> and 100 s<sup>-1</sup> (upward curves) for samples in distilled water.

Sample	<i>c</i> (% w/w)	Arrhenius equation (20 s <sup>-1</sup> )			Arrhenius equation (100 s <sup>-1</sup> )		
		<i>A</i> (mPa.s)	<i>E<sub>a</sub></i> (kJ/mol)	<i>R</i> <sup>2</sup>	<i>A</i> (mPa.s)	<i>E<sub>a</sub></i> (kJ/mol)	<i>R</i> <sup>2</sup>
Guar gum	0.25	1.09 x 10 <sup>-2</sup>	19.59	0.9816	3.09 x 10 <sup>-2</sup>	16.13	0.9852
	0.50	8.16 x 10 <sup>-4</sup>	26.61	0.9553	4.41 x 10 <sup>-3</sup>	21.73	0.9734
	0.75	9.68	10.18	0.9741	9.68	10.18	0.9878
	1.00	149.5	4.84	0.7541	88.30	3.36	0.7037
κ-carrageenan	0.25	0.34	9.40	0.8650	0.75	7.27	0.7852
	0.50	0.86	8.56	0.5533	1.33	7.19	0.5106
	0.75	3.00 x 10 <sup>-9</sup>	60.78	0.8950	1.58 x 10 <sup>-4</sup>	32.02	0.9178
	1.00	4.03 x 10 <sup>-13</sup>	85.88	0.8949	8.75 x 10 <sup>-7</sup>	46.87	0.9066
Xanthan gum	0.25	12.16	4.82	0.8860	13.81	1.83	0.9397
	0.50	117.1	1.52	0.8191	73.40	-0.51	0.2845
	0.75	669.1	-1.23	0.7429	151.0	-1.01	0.9720
	1.00	1291	-2.21	0.9764	218.5	-1.34	0.9737

Note: *c* – concentration; *A* – pre-exponential factor; *E<sub>a</sub>* – activation energy; *R*<sup>2</sup> – determination coefficient.

Table 7.11. Activation energy and pre-exponential factor at 20 s<sup>-1</sup> and 100 s<sup>-1</sup> (upward curves) for samples in 0.07M KCl.

Sample	<i>c</i> (% w/w)	Arrhenius equation (20 s <sup>-1</sup> )			Arrhenius equation (100 s <sup>-1</sup> )		
		<i>A</i> (mPa.s)	<i>E<sub>a</sub></i> (kJ/mol)	<i>R</i> <sup>2</sup>	<i>A</i> (mPa.s)	<i>E<sub>a</sub></i> (kJ/mol)	<i>R</i> <sup>2</sup>
Guar gum	0.25	3.30 x 10 <sup>-2</sup>	15.11	0.9306	5.96 x 10 <sup>-2</sup>	13.13	0.9770
	0.50	6.81	7.56	0.9188	6.74	5.76	0.9718
	0.75	20.79	7.67	0.9628	20.72	5.21	0.9842
	1.00	94.22	6.45	0.9818	58.88	4.70	0.9947
κ-carrageenan	0.25	2.21 x 10 <sup>-2</sup>	19.99	0.9886	2.94 x 10 <sup>-2</sup>	16.91	0.9820
	0.50	n.c.	n.c.	0.1421	0.63	13.16	0.6818
	0.75	3.70	15.33	0.8681	4.13	9.60	0.9140
	1.00	0.61	20.93	0.5778	0.22	17.58	0.7783
Xanthan gum	0.25	7.98	5.48	0.9401	4.12	4.35	0.9875
	0.50	28.46	5.24	0.8452	15.56	3.54	0.9656
	0.75	42.65	6.07	0.9575	28.96	3.59	0.9771
	1.00	168.5	3.78	0.6130	81.55	2.04	0.8419

Note: *c* – concentration; *A* – pre-exponential factor; *E<sub>a</sub>* – activation energy; *R*<sup>2</sup> – determination coefficient; n.c. – not computed value.

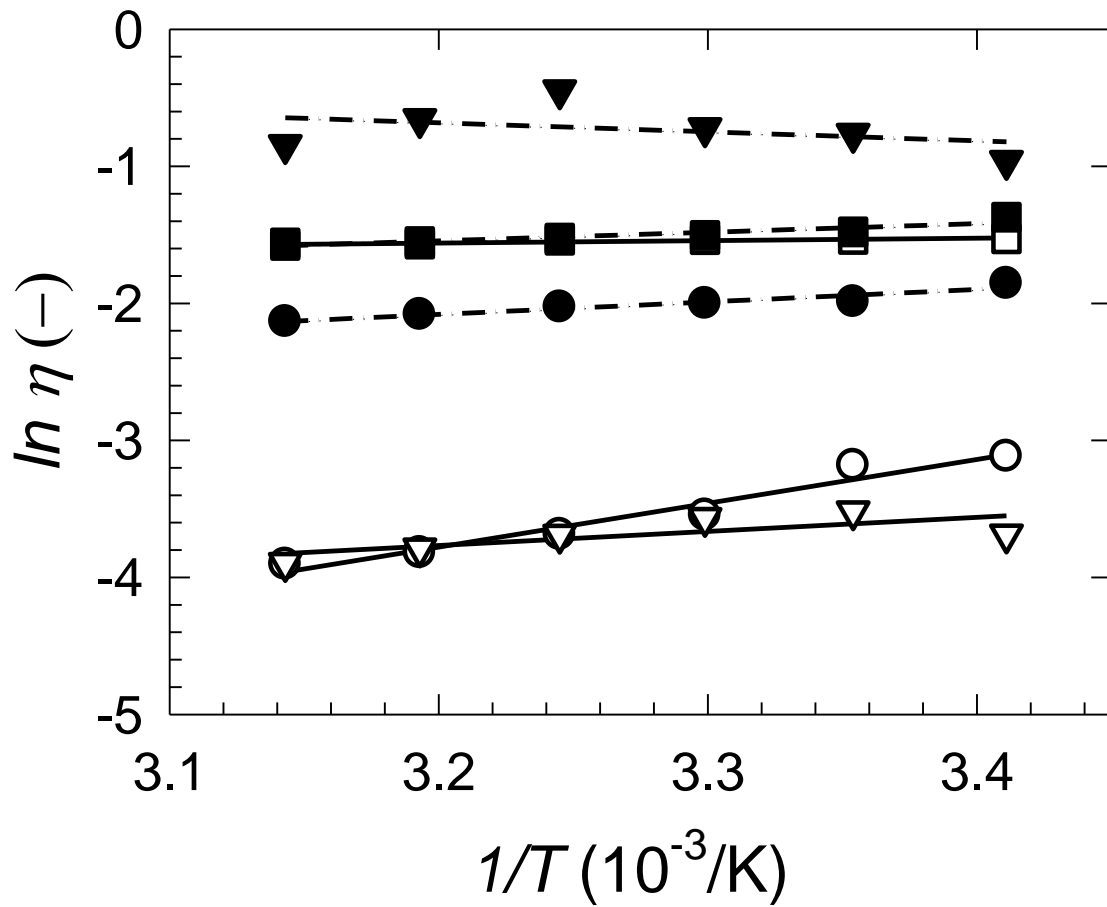


Fig. 7.9. Arrhenius plot of 0.5% (w/w) samples in water (empty symbols) and in 0.07M KCl (full symbols) (viscosities  $\eta$  read at shear rate  $20 \text{ s}^{-1}$ ): circle – guar gum, triangle –  $\kappa$ -carrageenan, square – xanthan gum;  $T$  – temperature. Linear regression curves: full line – in water, dash-dot line – in 0.07M KCl.

## 7.3 Functional properties of gelatin-polysaccharide blends

### 7.3.1 Rheological analysis

The blends of 0.5% (w/w) gelatin/polysaccharide were dissolved in two different salt solvents (0.07M KCl or 0.07 M NaCl) to follow the effects of conformational transition induced by external stimulus, i.e., by the change of temperature and type of solvent.

The electrostatic interactions were the main forces in the formation and stabilization of the prepared biopolyelectrolyte complexes (PECs), although the hydrogen bonds and hydrophobic interactions were also important. From a general point of view, an anionic polysaccharide plays a role of a basis in the electrostatic complexation. As stated by Voron'ko et al. (2016), at high temperatures, when biopolymer macromolecules in solution assume the random coil conformation, hydrophobic interactions contribute to a large extent to complex stabilization. On the other hand, below and at the temperature of gelatin coil to helix conformational transition, the electrostatic interactions and hydrogen bonds play a decisive role in the complex formation. In the presence of a positively charged natural polyelectrolyte (gelatin), the polysaccharide self-assembles with the complementary polyelectrolyte. The complexation with gelatin is provided by the electrostatic interaction between positively charged groups in gelatin and negatively charged groups in the polysaccharide (e.g., sulfate groups in  $\kappa$ -carrageenan) leading to conformational changes of gelatin macromolecules (Derkach et al., 2015a).

There was a detectable change of rheological behaviour of gelatin/polysaccharide blends reflecting the conformational transition (helix-coil) at temperature about 35 °C. The change corresponds to the conformational ordering of hydrocolloid chains in the complex (leading to the enhancement of gelatin/polysaccharide electrostatic complexation) and gelatin gel-sol transition upon heating. Thus, at higher temperatures (above 40 °C), gelatin and polysaccharide in the complex are present in the form of disordered flexible coils. On the other hand, gelatin/polysaccharide complex dissociates during cooling by reverse conformational ordering (coil to helix transition), as reported by Cao et al. (2016) for gelatin/ $\kappa$ -carrageenan complexation.

It is also important to consider the effect of salt concentration on the complexes. The conformational transition temperature of the polysaccharide increases with the addition of salts such as KCl and NaCl. This is due to the reduction of electrostatic complex coacervation of a gelatin/polysaccharide mixture with increasing salt concentration; the coacervation is entirely screened after a certain salt concentration level is reached. For example, the electrostatic complex coacervation of 0.75% gelatin/ $\kappa$ -carrageenan blend is completely screened when KCl concentration is more than 100 mM (Cao et al., 2016). In the present study, the concentration of 0.07M (70mM) KCl and NaCl was used

as sufficiently high to be assumed that the complex coacervation of 0.5% (w/w) blends will be completely screened.

As shown in Tables 7.12-7.13, temperature had an obvious effect on the flow behaviour of studied solutions. The flow curves of the blends read at 35 °C are shown in Fig. 7.10. Temperature dependency of flow behaviour index of the blends is presented in Fig. 7.11. The consistency coefficient ( $k$ ) of guar gum/gelatin and  $\kappa$ -carrageenan/gelatin blends was predominantly decreasing with temperature, whereas the flow behaviour index ( $n$ ) was increasing in the studied temperature range (25-45 °C). However, xanthan gum/gelatin blends exhibited an opposite behaviour of  $n$  versus temperature, as compared to other samples. For xanthan gum/gelatin blend in NaCl, the flow behaviour index was predominantly decreasing, whereas the consistency coefficient increasing with temperature. Both for xanthan gum/gelatin in KCl and NaCl, there was an evident change of  $n$  at temperature about 35 °C, demonstrating a conformational transition of xanthan chains (Fig. 7.11).

Overall, xanthan gum provided more viscous blends at higher temperatures, in contrast to guar gum and  $\kappa$ -carrageenan blends which tend to less pseudoplastic behaviour at elevated temperatures. The blends of xanthan gum also exhibited a significant yield stress ( $\tau_0$ ) within the whole temperature range. Although the values of  $\tau_0$  were predominantly decreasing with temperature, the yield stress was noticeable even at 45 °C, the highest temperature under study (1.647 Pa for the blend in KCl, and 0.973 Pa for the blend in NaCl, respectively). The viscosity stability of xanthan blends at elevated temperatures (relatively high at low-shear conditions) and the non-negligible values of yield stress result from the weak intermolecular associations of xanthan structure, typical even at very low hydrocolloid concentration (Marcotte et al., 2001b).

For  $\kappa$ -carrageenan and gelatin blends, the solutions in NaCl exhibit substantially larger values of yield stress and consistency coefficient, and comparatively lower values of flow behaviour index, than the samples in KCl. This fact can be related to the presence of potassium or sodium cations which effect the gelation properties of the blends. It means that the flow parameters of gelatin/ $\kappa$ -carrageenan blends, including yield stress, are notably affected by the type of salt solvent.

Gelatin/ $\kappa$ -carrageenan blends in NaCl provided a *gel* of high consistency at temperature about 25 °C, whereas the blend in KCl did not undergo a sol to gel transition within the studied temperature range. Therefore, the differences in flow parameters between the blends in KCl and NaCl were substantial, particularly between the values of  $k$  and  $\tau_0$ . This behaviour proves that  $\kappa$ -carrageenan can be largely used as co-gelator of gelatin-based solutions via interaction of charged gelatin with the polysaccharide macroions leading to formation of specific PECs. As stated by Derkach et al. (2015a), the addition of  $\kappa$ -carrageenan to aqueous gelatin solutions affects gelation kinetics of the blends, as well as thermal stability of the system; moreover, gelatin/ $\kappa$ -

carrageenan ratio has a substantial influence on the flow parameters of the blends. In other words, according to the type of solvent used and concentration of the components, the blends of gelatin/ $\kappa$ -carrageenan tend to form a gel. The blends of gelatin with guar gum or xanthan gum in the present study did not undergo a sol to gel transition between 25-45 °C.

Overall, the values of  $k$  and  $n$  are comparatively different for the blends in KCl and NaCl, respectively. The presence of chaotropic cations ( $K^+$ ) and kosmotropic cations ( $Na^+$ ) leads to the reduction of electrostatic complex coacervation of gelatin/polysaccharide system (Cao et al., 2016). However, the mechanism of action of these ions is opposite: the chaotropic electrolytes (KCl) suppress the electrostatic repulsion effect on the polymer chains. Moreover, the chaotropic ions can enhance the dissolution of colloidal aggregates which are ordinarily present in polysaccharide solutions under ambient conditions (Ma & Pawlik, 2007; Wang et al., 2015). On the other hand, the kosmotropic electrolytes (NaCl) promote interactions between water molecules and thus stabilize intramolecular interactions in protein macromolecules such as gelatin (Moelbert et al., 2004).

These specific properties of salt solvents also affect flow behaviour of guar gum/gelatin blends. The effect of  $Na^+$  ions on the hydrocolloid macromolecules seems to tend guar gum/gelatin blends to less pseudoplastic fashion at higher temperatures, as compared to the effect of  $K^+$  ions in the same system showing more pseudoplastic behaviour (higher values of  $k$ , and lower values of  $n$ ).

Table 7.12. Flow parameters of 0.5% (w/w) gelatin/polysaccharide blends in 0.07M KCl (upward curves).

Sample	$T$ (°C)	Herschel-Bulkley model without extrapolation				Ostwald-de Waele model		
		$\tau_0$ (Pa)	$k$ (Pa.s <sup>n</sup> )	$n$	$R^2$	$k$ (Pa.s <sup>n</sup> )	$n$	$R^2$
Guar gum/gelatin	25	-7.008	6.830	0.22	0.9990	1.956	0.38	0.9905
	30	-0.9089	0.8898	0.45	0.9998	0.5246	0.53	0.9982
	35	-0.7405	0.5905	0.51	0.9998	0.3434	0.59	0.9980
	40	-0.6377	0.4812	0.53	0.9997	0.2826	0.61	0.9980
	45	-0.5032	0.3679	0.56	0.9998	0.2265	0.64	0.9984
$\kappa$ -carrageenan/gelatin	25	0.1580	0.0139	0.83	0.9962	0.0438	0.64	0.9895
	30	0.1794	0.0015	1.18	0.9675	0.0201	0.72	0.9425
	35	0.2516	0.0404	0.55	0.9198	-	-	-
	40	0.1044	0.0030	1.07	0.9906	0.0120	0.83	0.9824
	45	0.3453	0.0038	0.89	0.6532	-	-	-
Xanthan gum/gelatin	25	3.282	0.8333	0.36	0.9998	3.264	0.187	0.9931
	30	2.10	1.489	0.27	0.9985	3.177	0.180	0.9961
	35	1.179	1.989	0.23	0.9985	2.953	0.186	0.9978
	40	2.057	1.292	0.28	0.9993	2.919	0.185	0.9963
	45	1.647	1.077	0.32	0.9988	2.281	0.224	0.9959

Note:  $T$  - temperature;  $\tau_0$  - yield stress;  $k$  - consistency coefficient;  $n$  - flow behaviour index;  $R^2$  - determination coefficient. The hyphen means that no relevant value was possible to determine by fitting of the model.

Table 7.13. Flow parameters of 0.5% (w/w) gelatin/polysaccharide blends in 0.07M NaCl (upward curves).

Sample	$T$ (°C)	Herschel-Bulkley model without extrapolation				Ostwald-de Waele model		
		$\tau_0$ (Pa)	$k$ (Pa.s <sup>n</sup> )	$n$	$R^2$	$k$ (Pa.s <sup>n</sup> )	$n$	$R^2$
Guar gum/gelatin	25	-2.823	2.493	0.31	0.9987	0.9213	0.45	0.9927
	30	-0.4414	0.3243	0.58	0.9998	0.2066	0.65	0.9986
	35	-0.2869	0.1849	0.66	0.9998	0.1253	0.72	0.9989
	40	-0.2373	0.1557	0.67	0.9999	0.1086	0.73	0.9991
	45	-0.1773	0.1166	0.70	0.9999	0.0848	0.76	0.9993
$\kappa$ -carrageenan/ gelatin	25	4.80	0.7628	0.56	0.9983	3.093	0.35	0.9867
	30	9.877	0.2149	0.76	0.9977	5.478	0.25	0.9427
	35	3.009	1.083	0.48	0.9992	2.674	0.34	0.9946
	40	2.084	1.044	0.39	0.9889	2.386	0.28	0.9953
	45	0.208	0.0727	0.68	0.9998	0.126	0.59	0.9982
Xanthan gum/gelatin	25	3.30	0.6827	0.38	0.9997	3.112	0.184	0.9913
	30	2.288	0.8347	0.36	0.9985	2.428	0.220	0.9976
	35	1.911	0.940	0.34	0.9987	2.332	0.219	0.9944
	40	1.394	1.184	0.30	0.9990	2.221	0.222	0.9970
	45	0.973	1.375	0.28	0.9992	2.106	0.227	0.9983

Note:  $T$  - temperature;  $\tau_0$  - yield stress;  $k$  - consistency coefficient;  $n$  - flow behaviour index;  $R^2$  - determination coefficient.



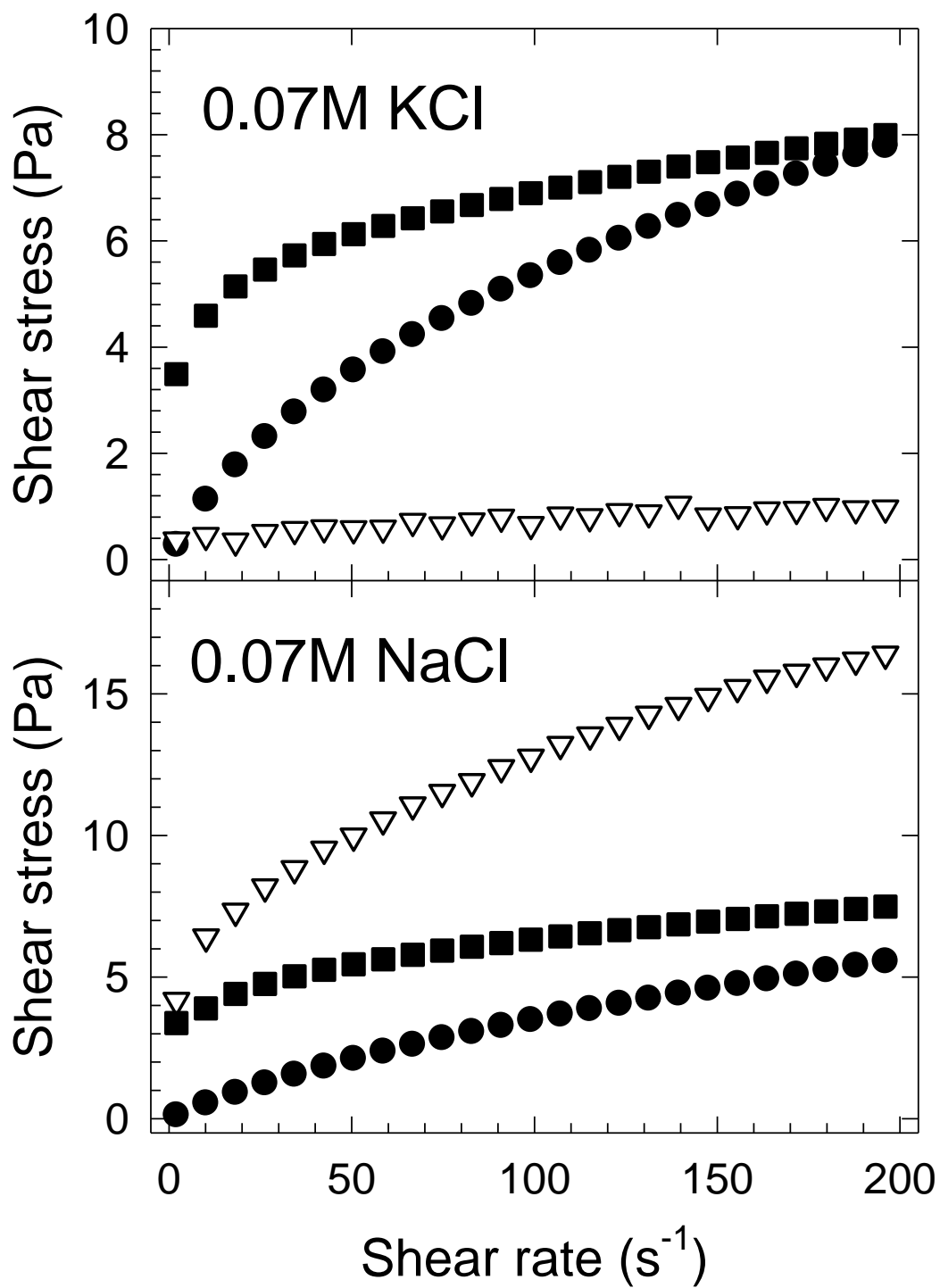


Fig. 7.10. Flow curves of 0.5% (w/w) gelatin/polysaccharide blends in 0.07M KCl and 0.07M NaCl at 35 °C (upward shear rate): full circle – guar gum/gelatin, empty triangle –  $\kappa$ -carrageenan/gelatin, full square – xanthan gum/gelatin.

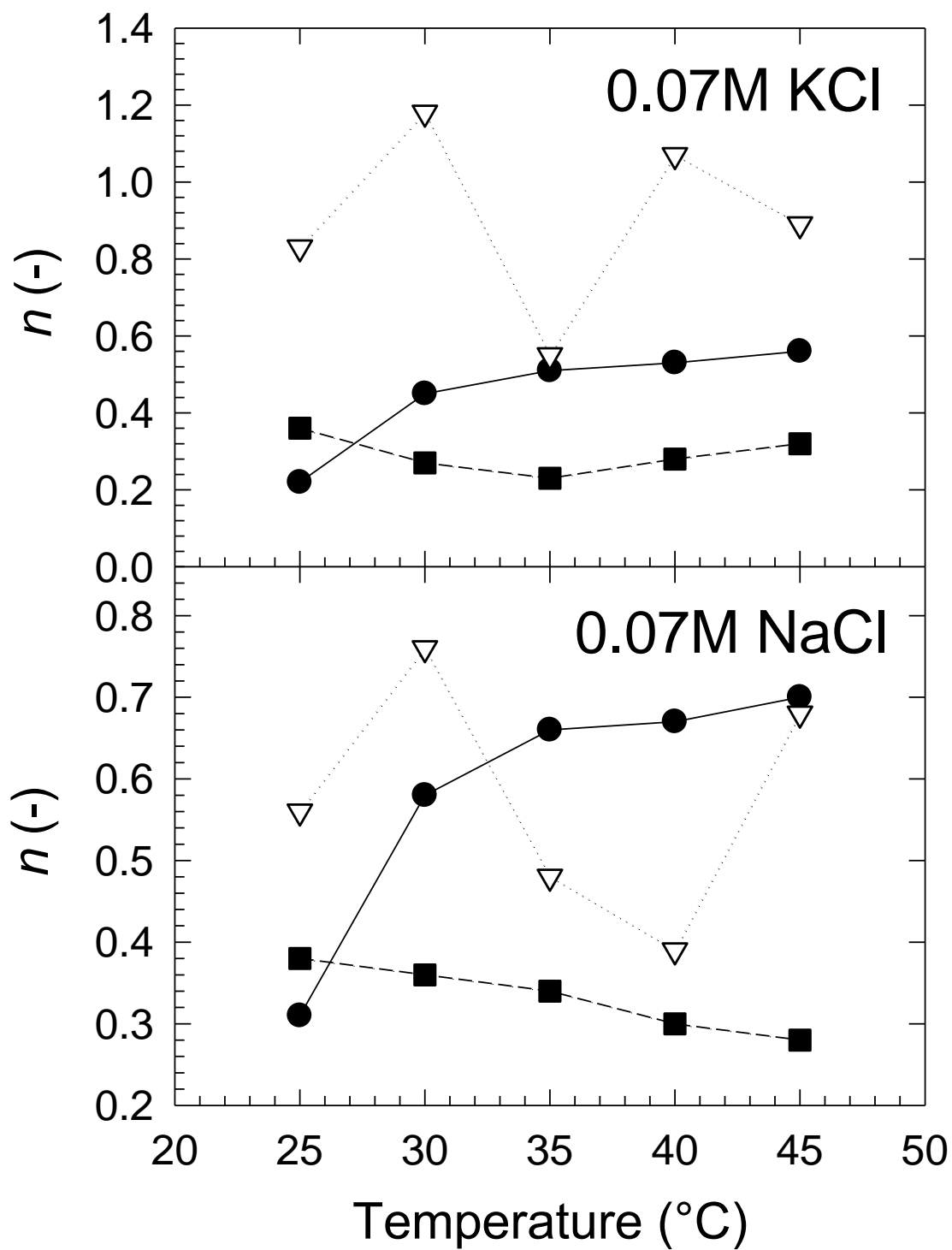


Fig. 7.11. Temperature dependency of flow behaviour index ( $n$ ) (Herschel-Bulkley model) of 0.5% (w/w) gelatin/polysaccharide blends in 0.07M KCl and 0.07M NaCl: full circle – guar gum/gelatin, empty triangle –  $\kappa$ -carrageenan/gelatin, full square – xanthan gum/gelatin.

### 7.3.2 Arrhenius parameters

Temperature dependency of the blends' viscosity was investigated by the Arrhenius model. The Arrhenius plots of the blends read at shear rate of  $20 \text{ s}^{-1}$  are shown in Fig. 7.12. The activation energy ( $E_a$ ), representing an energy barrier of reorientation of water molecules in biopolymer system (Baranowska et al., 2008), was calculated according to the model. The Arrhenius parameters are stated in Table 7.14.

As can be seen from the data, relatively high values of  $E_a$  were determined for blends of guar gum/gelatin both in KCl and NaCl, and for  $\kappa$ -carrageenan/gelatin blend in NaCl; these blends are relatively high temperature-dependent samples indicating a higher resistance of their molecular structure to temperature (i.e., a higher resistance to achieve the structural changes by elevating the temperature). On the other hand, the lowest values of  $E_a$  were calculated for mixtures of xanthan gum with gelatin which were less affected by temperature changes. This fact proves that xanthan gum/gelatin blends have the ability to retain their polymer network and viscosity at higher temperatures which is in compliance with the temperature dependency of apparent viscosity observed for xanthan gum solutions (Marcotte et al., 2001a; Marcotte et al., 2001b). A relatively high difference between the values of  $E_a$  was determined for  $\kappa$ -carrageenan/gelatin blends in KCl and NaCl, respectively. However, the Arrhenius model was not suitable to apply for  $\kappa$ -carrageenan/gelatin blends because of low values of determination coefficient ( $R^2$ ).

Overall, the activation energy of samples in 0.07M NaCl was higher than that of samples in KCl; it means that the blends in NaCl need higher amount of activation energy to promote viscous flow than the samples in KCl, probably due to more complex structure of hydrocolloids in NaCl solution. Samples in KCl provided lower values of  $E_a$  and higher values of pre-exponential factor ( $A$ ), indicating a less stabilized structure, as compared to Arrhenius parameters for NaCl blends. This mode of behaviour was the same for all blends, regardless of the polysaccharide type.

In the same way, the activation energy read at  $20 \text{ s}^{-1}$  was higher than  $E_a$  read at  $100 \text{ s}^{-1}$  for all samples. This is in accordance with the fact that the structure of a hydrocolloid and its change with the shearing plays an important role in the temperature dependency of the solutions. As stated by Marcotte et al. (2001a), the decrease in activation energy of the hydrocolloid solutions is, in varying degree, associated with an increase of the applied shear rate, depending on the hydrocolloid type. The observations indicate that energy necessary for reorientation of water (solvent) molecules in gelatin/polysaccharide blends is obviously influenced by the type of hydrocolloid and salt solution, as well as by the applied shear rate.

Table 7.14. Arrhenius parameters at 20 s<sup>-1</sup> and 100 s<sup>-1</sup> (upward shear rate) of 0.5% (w/w) gelatin/polysaccharide blends in 0.07M KCl and 0.07M NaCl.

Sample	Solvent	Arrhenius equation (20 s <sup>-1</sup> )			Arrhenius equation (100 s <sup>-1</sup> )		
		<i>A</i> (mPa.s)	<i>E<sub>a</sub></i> (kJ/mol)	<i>R</i> <sup>2</sup>	<i>A</i> (mPa.s)	<i>E<sub>a</sub></i> (kJ/mol)	<i>R</i> <sup>2</sup>
Guar gum/gelatin	KCl	2.64x10 <sup>-7</sup>	50.94	0.8438	1.03x10 <sup>-4</sup>	34.02	0.8234
	NaCl	4.52x10 <sup>-8</sup>	53.90	0.8398	2.45x10 <sup>-5</sup>	36.62	0.8682
κ-carrageenan/ gelatin	KCl	n.c.	n.c.	0.2940	n.c.	n.c.	0.0419
	NaCl	3.576x10 <sup>-13</sup>	87.53	0.6613	1.494x10 <sup>-11</sup>	75.30	0.7083
Xanthan gum/gelatin	KCl	7.873	8.926	0.9113	4.995	6.727	0.9747
	NaCl	5.498	9.545	0.9153	4.163	6.992	0.9600

Note: *A* - pre-exponential factor; *E<sub>a</sub>* - activation energy; *R*<sup>2</sup> - determination coefficient; n.c. - not computed value.

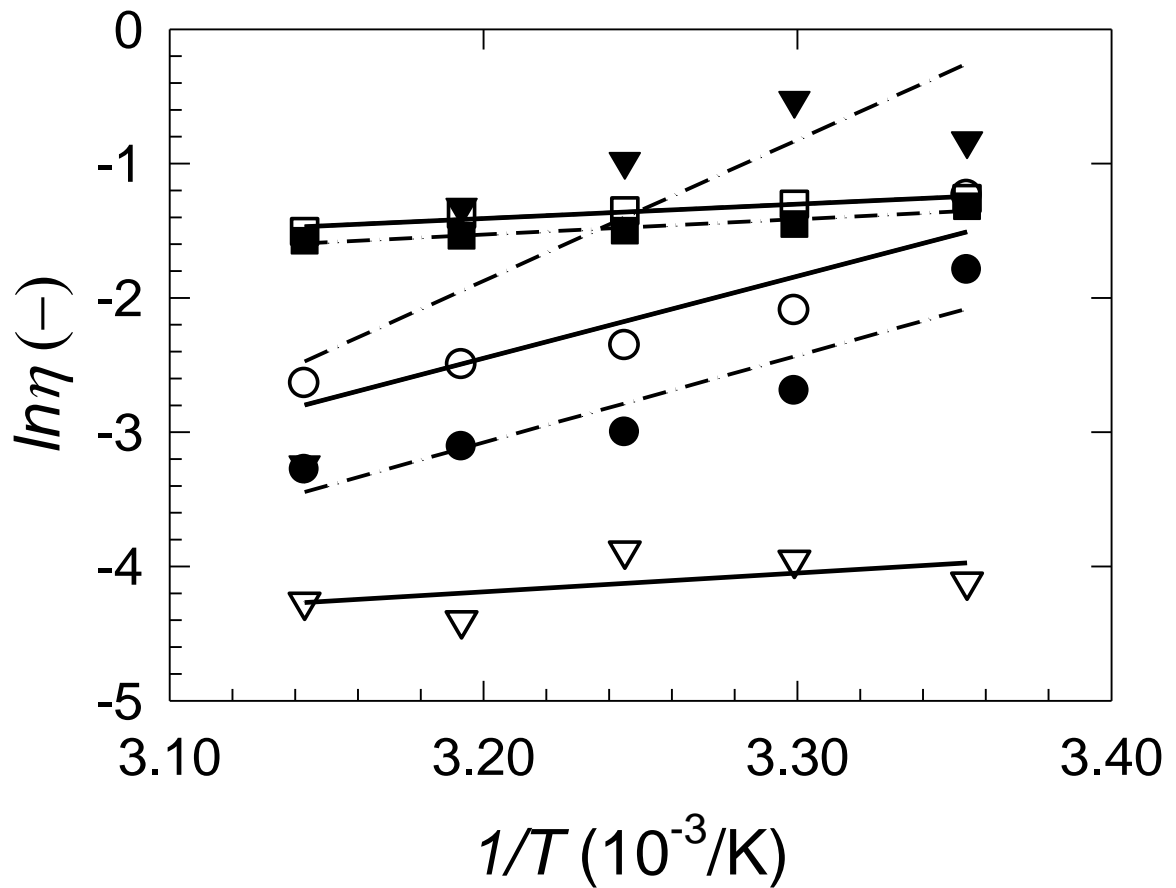


Fig. 7.12. Arrhenius plots of 0.5% (w/w) gelatin/polysaccharide blends in 0.07M KCl (empty symbols) and in 0.07M NaCl (full symbols) at temperature  $T$  (viscosities  $\eta$  read at shear rate  $20 \text{ s}^{-1}$ ): circle – guar gum/gelatin, triangle –  $\kappa$ -carrageenan/gelatin, square – xanthan gum/gelatin. Linear regression curves: full line – in 0.07M KCl, dash-dot line – in 0.07M NaCl.

### 7.3.3 Other analyses

Gelatin/polysaccharide blends were examined by conductivity measurement and zeta potential analysis, which provided an additional information about the conformational properties and stability of the blends.

The effect of conformational transition on the conductivity  $C$  of the blends was tested, depending on temperature. As stated by Cao et al. (2016), pure gelatin solution contributes only negligibly to the conductivity of gelatin/polysaccharide blends. Therefore, the difference in conductivity between pure polysaccharide solution and gelatin/polysaccharide mixture reflects the difference between the polysaccharide in free and complex states. The average values of  $C$  (mS/cm), determined for gelatin/polysaccharide blends, are plotted in Fig. 7.13.

As can be seen from the graph, there is an evident change of conductivity at temperature about 35 °C, both for blends in KCl and NaCl, which can be attributed to the conformational transition of the hydrocolloids. This conformational change entails a steep rise of conductivity above 35 °C. As in the case of rheological behaviour (temperature dependency of  $n$ ), the change in the slope of conductivity can be considered as confirmation of the effect of conformational ordering on the functional properties of gelatin/polysaccharide blends.

Besides, as evident from the graph, the conductivity of the blends in KCl solution was patently higher than in NaCl solution, due to the different character of the ions employed in the PECs. Kosmotropic cations  $\text{Na}^+$  (which stabilize the intramolecular interactions in gelatin) could provide more complex structure of gelatin/polysaccharide blends, as compared with chaotropic ions  $\text{K}^+$ . This fact can be attributed to the different conductivity of the same gelatin/polysaccharide mixtures in different solutions, and can cohere with lower temperature resistance obtained for KCl samples, in comparison to higher temperature resistance of the blends in NaCl (characterized by higher values of  $E_a$  and lower values of  $A$ ), as discussed above.

Potential stability of gelatin/polysaccharide blends was evaluated by zeta potential ( $\zeta$ -potential) analysis. The experimental data of  $\zeta$ -potential, pH-values of the solutions and effective diameter of the particles are summarized in Table 7.15.

$\zeta$ -potential value is dependent on the nature of particle surface and its charge (related to pH), on the electrolyte concentration in the solution and nature of the electrolyte and solvent used. The most important factor for  $\zeta$ -potential analysis is pH-value, which was measured for each tested blend in its natural state. As can be seen in Table 7.15, the pH-value of all blends ranged between 4.60 and 6.60; thus, the  $\zeta$ -potential was determined under moderately or slightly acidic conditions. A zero value of  $\zeta$ -potential indicates the least stable state of a colloidal system at a defined pH, i.e., an isoelectric point of the system (Anonym, 2000; Delgado et al., 2007).

The  $\zeta$ -potential is an electrokinetic potential at the plane of shear, i.e., at the interface between compact and diffusive part of the electric double layer, characterized by charged surface and liquid moving with respect to each other. The sign of  $\zeta$ -potential value is opposite to the charge of ions of outer layer in the electric double layer (Szymczyk et al., 1998). Hence, the analysis of the blends provided information about the electric charge of their double layer or, more specifically, about the electro-potential difference between the medium and the layer of fluid related to the dispersed particles.

The colloidal particles in an aqueous medium prone to interact with each other to form aggregates or clusters by attractive forces or remain dispersed via electrostatic repulsion. The balance between attractive and repulsive forces depends on surface charge of the blends; even an electrostatically stabilized system is possible to coagulate by adding enough electrolyte such as KCl (Anonym, 2000; Gerzhova et al., 2016; Wu et al., 2015). Thus, the  $\zeta$ -potential analysis was used to characterize the influence of antagonistic forces acting in the gelatin/polysaccharide blends on their potential stability.

In the present study, the low values of  $\zeta$ -potential determined for all samples (less than  $\pm 10$  mV) indicate an instability of the blends, which tend to coagulate. It suggests that the electrostatic repulsion (between similarly charged nearby particles in the solution) is weak and the blends do not resist aggregation, because the particles are not small enough, and the attractive forces between them exceed the electrostatic repulsion. The highest  $\zeta$ -potential (in absolute value) was obtained for  $\kappa$ -carrageenan/gelatin blend in NaCl (7.21 mV) with corresponding effective diameter  $d$  of the particles 14 463 nm, exceeding the size limit for dispersed colloidal particles (1  $\mu$ m). On the other hand, the lowest values of  $\zeta$ -potential were determined for guar gum/gelatin blends (around  $\pm 1.0$  mV) with  $d$  about 8 000 nm (in KCl) and 3 000 nm (in NaCl), which represent the least electrostatically stabilized blends under study.

Table 7.15.  $\zeta$ -potential analysis of 0.5% (w/w) gelatin/polysaccharide blends in 0.07M KCl and 0.07M NaCl.

<b>Sample</b>	<b>Solvent</b>	<b><math>\zeta</math>-potential (mV)</b>	<b><math>d</math> (nm)</b>	<b>pH (-)</b>
Guar gum/gelatin	KCl	-0.99 $\pm$ 0.36	7922 $\pm$ 1280	4.83
	NaCl	1.00 $\pm$ 0.20	3226 $\pm$ 919	5.00
$\kappa$ -carrageenan/gelatin	KCl	2.37 $\pm$ 0.84	6385 $\pm$ 478	6.61
	NaCl	-7.21 $\pm$ 0.95	14463 $\pm$ 734	6.44
Xanthan gum/gelatin	KCl	-4.93 $\pm$ 1.02	54020 $\pm$ 9863	4.59
	NaCl	-5.01 $\pm$ 1.72	28891 $\pm$ 6874	4.63

Note:  $d$  - effective diameter;  $\pm$  values indicate standard deviation (for 10 replicate measurements).

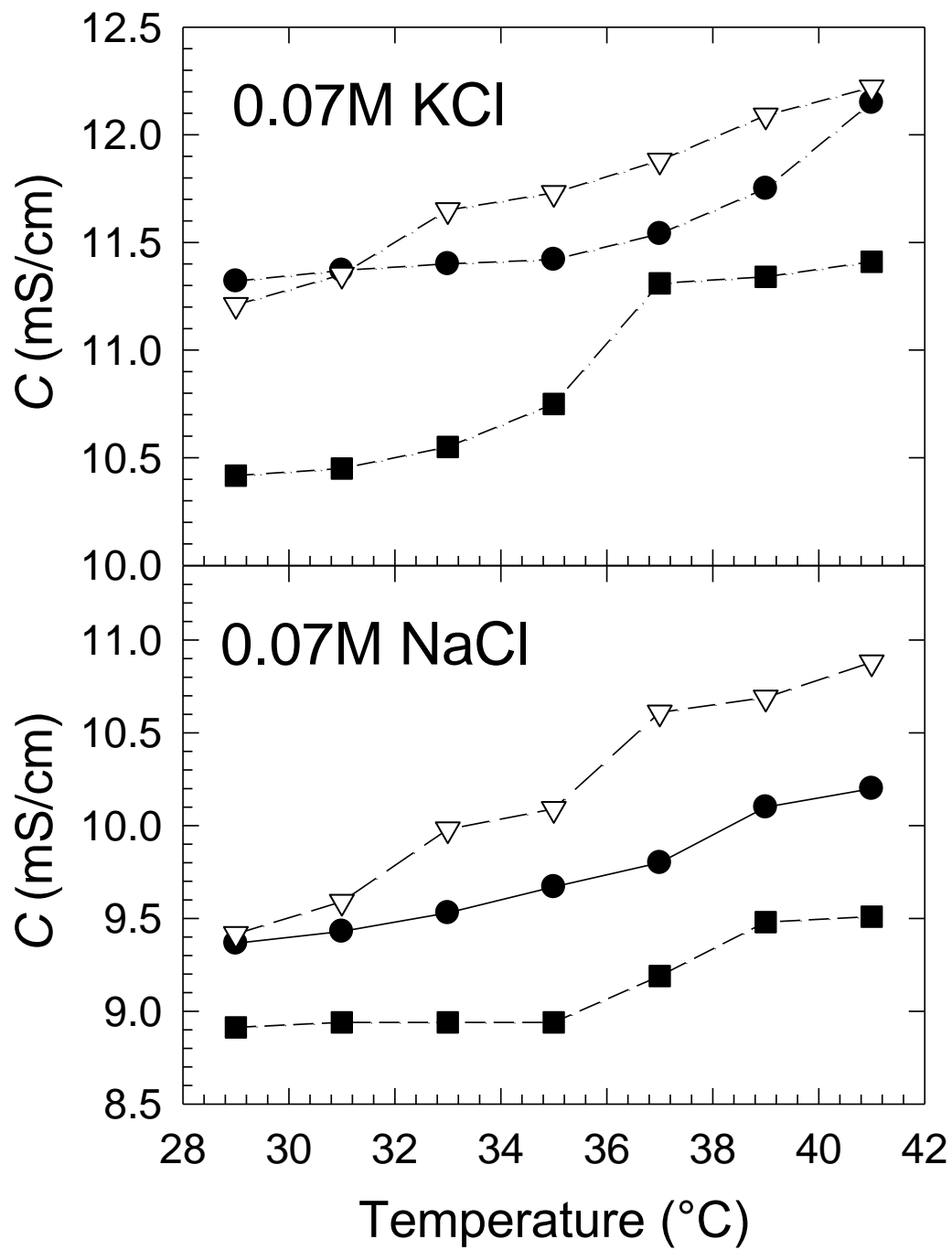


Fig. 7.13. Temperature dependency of conductivity ( $C$ ) of 0.5% (w/w) gelatin/polysaccharide blends in the temperature range 29-41 °C: full circle – guar gum/gelatin, empty triangle –  $\kappa$ -carrageenan/gelatin, full square – xanthan gum/gelatin.



## 8. CONTRIBUTION TO SCIENCE AND PRACTICE

The study of rheological and thermal properties of food hydrocolloids is very perspective area. The research on this field is promising new approaches how to understand the effect of these hydrocolloids on the functional character of food products and how to optimize their amount in selected food matrices.

From a general point of view, the study of flow properties of hydrocolloid solutions (food rheology or, more specifically, macromolecular hydrodynamics) is an effective tool in elucidating various levels of macromolecular structure of different food products. For that reason, accurate description, measurement and classification of the flow behaviour of macromolecular liquids are directly useful in practical processing, and have an immense stimulus to the science of rheology (Macosko, 1994).

The main contributions of this Doctoral Thesis in the field of hydrocolloid rheology can be summarized into the following points:

- Structural change of food hydrocolloids in aqueous and salt solutions (semi-dilute regime) can be detected by appropriate rheological models (Ostwald-de Waele model and Herschel-Bulkley model), i.e., by temperature and concentration dependency of the flow parameters. The transition of hydrocolloid chains (order-disorder transition) with changing temperature obviously influences the flow behaviour of hydrocolloid solutions.
- Conformational ordering of gelatin/polysaccharide blends (polyelectrolyte complexes) induced by temperature changes has an effect on their rheological behaviour and other functional properties (conductivity) of the blends.
- Presence of specific ions (chaotropic cations  $K^+$ , kosmotropic cations  $Na^+$ ) in the solvent used affects the flow behaviour and gelation of the hydrocolloid solutions.

Thermal and temperature dependency of food hydrocolloids can characterize endothermic and exothermic events in these materials, and also the resistance of their molecular structure to the changes in temperature, concentration, shear rate and other physico-chemical factors. The key points determined during the study of hydrocolloids' thermal and temperature properties are stated here:

- The ability of powder samples to bind moisture in varying degrees depends on the chemical and higher-order structure of each polysaccharide studied. The moisture content is related to the values of reaction enthalpy and peak temperature upon thermal treatment of powders.
- In dependence of the kinetic approach used (Friedman model, Kissinger model, and Model-free kinetics), the values of activation energy ( $E_a$ ) of polysaccharide powders vary in a specific range. The largest values of  $E_a$  determined at low conversions (at the onset of thermal treatment) suggest that energy barriers of the powders originate from cooperative disruption of

energetic associations between water molecules and hydrophilic groups on the polymer matrix.

- There was found a reverse dependency between activation energy of polysaccharide solutions and reaction enthalpy of powder samples. The highest resistance of  $\kappa$ -carrageenan solution molecular network to temperature changes was related to the lowest energy intake needed to dissociate the polymeric structure of  $\kappa$ -carrageenan powder sample. Vice versa, xanthan gum with the highest sensitivity of its solution structure to temperature changes provided the largest reaction enthalpy during thermal treatment of powders.

The Doctoral Thesis also offers another point to be discussed in the field of food science:

- Relatively low values of  $\zeta$ -potential and large values of particle diameters obtained for 0.5% (w/w) gelatin/polysaccharide blends indicate that these polyelectrolyte complexes are electrostatically unstable systems which tend to coagulate.

## CONCLUSION

At the present time, there is a large number of food hydrocolloids and natural hydrogels with excellent water holding capacity. They are being used as functional foods and food additives. These materials are becoming more and more popular because of being safe, biodegradable and biocompatible, and due to their ability to change the functional properties of specific food products in a favourable way. They can be used as emulsifying and gelling agents, stabilizers, thickeners, fat replacers, etc. The increasing importance of these additives has motivated the scientists to study their physico-chemical properties in order to find their property-based applications, and was also a great motivation for the author of the present study.

This Doctoral Thesis was focused on the rheological and thermal properties of several food hydrocolloids (shear-thinning polysaccharides and gelatin) which find the growing use in the food industry.

Rheological analysis of polysaccharides solutions in distilled water and 0.07M KCl provided information about their hydrodynamic properties as a function of polymer concentration, type of solvent and temperature. Flow parameters of the solutions were described by suitable rheological models (Ostwald-de Waele and Herschel-Bulkley models). The transition from double helical polysaccharide structure to conformation of single coils at temperature about 30 °C (in salt solution) and the disentanglement process of polymer coils (in distilled water) were proved by the temperature dependency of the Kraemer constant ( $k_K$ ). The intrinsic viscosity of the solutions was dependent on the hydrocolloid type and solvent used. Overall, the intrinsic viscosity at lower shear rate (20 s<sup>-1</sup>) was higher than that at higher shear rate (100 s<sup>-1</sup>) owing to the breakdown of the original molecular structure. The differences of  $k_K$  in the studied temperature range (20-45 °C) were relatively small. However, for all polysaccharides, based on the  $k_K$  results, KCl seems to be a better solvent as compared to distilled water, especially for  $\kappa$ -carrageenan.

The same rheological approach was used for gelatin/polysaccharide blends, dissolved in 0.07M KCl and 0.07M NaCl. The functional properties of the blends were influenced by the conformational transition of hydrocolloid chains. A noticeable change of flow parameters upon heating, determined about 35 °C, corresponds to the order-disorder transition of the hydrocolloids, as well as to the gel-sol transition of gelatin. The flow behaviour and gelation properties of the blends were affected by the type of hydrocolloid and solvent used. The effect of Na<sup>+</sup> ions on the macromolecules of guar gum/gelatin blends can be characterized by less pseudoplastic behaviour of the blends at higher temperatures (above 35 °C), as compared to the effect of chaotropic K<sup>+</sup> ions. Xanthan gum both in KCl and NaCl blends showed more pseudoplastic behaviour at elevated temperatures, in comparison to guar gum and  $\kappa$ -carrageenan blends.

Thermal properties of powder polysaccharides were assessed by thermal analysis techniques (TGA and DTA). The powders were able to bind moisture to different extent, dependent on the chemical and higher-order structure of the polysaccharides, as well as on their conditioning. On the basis of the latter water binding ability, samples showed different values of reaction enthalpy and peak temperature. The order-disorder phase transition (endothermic process) occurred in the temperature range 50-85 °C. Different kinetic models (Friedman model, Kissinger model, and Model-free kinetics), were used to assess the kinetics of phase transition and water evaporation, providing information about the energy barriers which has to be overcome during thermal treatment of the powders. Model free kinetics revealed a significant decrease in activation energy ( $E_a$ ) with increasing degree of conversion ( $\alpha$ ), in the highest extent between 5 and 20 % of  $\alpha$ , probably due to the release of water molecules from polymer matrix at the onset of powder thermal treatment. Temperature dependency of polysaccharide solutions was evaluated using the Arrhenius model. Higher values of activation energy ( $E_a$ ) and pre-exponential factor ( $A$ ) determined for samples in water can be explained by a more complicated (less ordered) structure of these solutions, in comparison to samples dissolved in 0.07M KCl.  $\kappa$ -carrageenan solutions were exhibiting the most temperature resistant flow behaviour, based on the highest values of  $E_a$ . On the other hand, xanthan gum was the least temperature dependent hydrocolloid, as proved by the lowest  $E_a$  values of all samples.

In the field of rheology and thermal analysis, other research of hydrocolloids examined in this study and further development of food additives of desirable functional properties can be expected. New investigation will bring a better understanding of hydrocolloid performance in specific food applications, such as functional food, polyelectrolyte complexes, etc. Future research will also enable the optimisation of hydrocolloid concentration and combination in different food matrices in regard to the storage and manufacturing conditions.

## REFERENCES

- AI, Y. & JANE, J. (2015). Gelatinization and rheological properties of starch. *Starch/Stärke*. Vol. 67, p. 213-224. ISSN 1521-379X.
- ANONYM (2000). *Instruction manual for ZetaPlus Zeta Potential Analyzer*. New York: Brookhaven Instruments Corporation.
- APPELQVIST, I. A. M., COOKE, D., GIDLEY, M. J. & LANE, S. J. (1993). Thermal properties of polysaccharides at low moisture: 1 - An endothermic melting process and water-carbohydrate interactions. *Carbohydrate Polymers*. Vol. 20, p. 291-299. ISSN 0144-8617.
- BARANOWSKA, H. M., SIKORA, M., KOWALSKI, S. & TOMASIK, P. (2008). Interactions of potato starch with selected polysaccharide hydrocolloids as measured by low-field NMR. *Food Hydrocolloids*. Vol. 22, p. 336-345. ISSN 0268-005X.
- BEHLAU, L. & WIDMANN, G. (2003). *Collected Applications: Thermal Analysis. Food Handbook*. Mettler-Toledo.
- BeMILLER, J. N. (2011). Pasting, paste, and gel properties of starch-hydrocolloid combinations. *Carbohydrate Polymers*. Vol. 86, p. 386-423. ISSN 0144-8617.
- BERČIČ, G. (2017). The universality of Friedman's isoconversional analysis results in a model-less prediction of thermodegradation profiles. *Thermochimica Acta*. Vol. 650, p. 1-7. ISSN 0040-6031.
- BILANOVIC, D., STAROSVETSKY, J. & ARMON, R. H. (2015). Cross-linking xanthan and other compounds with glycerol. *Food Hydrocolloids*. Vol. 44, p. 129-135. ISSN 0268-005X.
- BLAŽEK, A. (1972). *Termická analýza*. 1st ed. Praha: SNTL. ISBN 04-626-72.
- BOCK, J., VARADARAJ, R., SCHULZ, D. N. & MAURER, J. J. (1994). Solution Properties of Hydrophobically Associating Water-Soluble Polymers. In: DUBIN, P., BOCK, J., DAVIS, R., SCHULZ, D. N. & THIES, C. (eds.). *Macromolecular Complexes in Chemistry and Biology*. 1st ed., p. 33-50. Berlin: Springer Verlag. ISBN 978-3-642-78471-2.
- BOGRACHEVA, T. Y., WANG, Y. L., WANG, T. L. & HEDLEY, C. L. (2002). Structural Studies of Starches with Different Water Contents. *Biopolymers*. Vol. 64, p. 268-281. ISSN 0006-3525.
- BRENNER, T., TUVIKENE, R., PARKER, A., MATSUKAWA, S. & NISHINARI, K. (2014). Rheology and structure of mixed kappa-carrageenan/iota-carrageenan gels. *Food Hydrocolloids*. Vol. 39, p. 272-279. ISSN 0268-005X.
- BRUNCHI, C.-E., MORARIU, S. & BERCEA, M. (2014). Intrinsic viscosity and conformational parameters of xanthan in aqueous solutions: Salt addition effect. *Colloids and Surfaces B: Biointerfaces*. Vol. 122, p. 512-519. ISSN 0927-7765.

BOURBON, A. I., PINHEIRO, A. C., RIBEIRO, C., MIRANDA, C., MAIA, J. M., TEIXEIRA, J. A. & VICENTE, A. A. (2010). Characterization of galactomannans extracted from seeds of *Gleditsia triacanthos* and *Sophora japonica* through shear and extensional rheology: Comparison with guar gum and locust bean gum. *Food Hydrocolloids*. Vol. 24, iss. 2–3, p. 184-192. ISSN 0268-005X.

BUSCH, R., SCHROERS, J. & WANG, W. (2007). Thermodynamics and Kinetics of Bulk Metallic Glass. *MRS Bulletin*. Vol. 32, iss. 8, p. 620-623. ISSN 0883-7694.

CAI, J., XU, D., DONG, Z., YU, X., YANG, Y., BANKS, S. W. & BRIDGWATER, A. V. (2018). Processing thermogravimetric analysis data for isoconversional kinetic analysis of lignocellulosic biomass pyrolysis: Case study of corn stalk. *Renewable and Sustainable Energy Reviews*. Vol. 82, p. 2705-2715. ISSN 1364-0321.

CAO, Y., FANG, Y., NISHINARI, K. & PHILIPS, G. O. (2016). Effects of conformational ordering on protein/polyelectrolyte electrostatic complexation: Ionic binding and chain stiffening. *Scientific Reports - Nature*. Vol. 6, p. 1-11. ISSN 2045-2322.

CEVOLI, C., BALESTRA, F., RAGNI, L. & FABBRI, A. (2013). Rheological characterisation of selected food hydrocolloids by traditional and simplified techniques. *Food Hydrocolloids*. Vol. 33, p. 142-150. ISSN 0268-005X.

CHANDLER, H. D. (2014). An activation energy approach to analysing non-Newtonian slurry viscosities with application to a suspension of starch in a carboxymethylcellulose solution. *Powder Technology*. Vol. 268, p. 368-372. ISSN 0032-5910.

CHEN, Y., LIAO, M. & DUNSTAN, D. E. (2002). The rheology of K<sup>+</sup>-κ-carrageenan as a weak gel. *Carbohydrate Polymers*. Vol. 50, iss. 2, p. 109-116. ISSN 0144-8617.

CHIVERO, P., GOHTANI, S., YOSHII, H. & NAKAMURA, A. (2015). Effect of xanthan and guar gums on the formation and stability of soy soluble polysaccharide oil-in-water emulsions. *Food Research International*. Vol. 70, p. 7-14. ISSN 0963-9969.

CORAL, D. F., PINEDA-GÓMEZ, P., ROSALES-RIVERA, A. & RODRIGUEZ-GARCIA, M. E. (2009). Determination of the gelatinization temperature of starch presented in maize flours. In: SERQUIS, A., BOLCATO, P. & BALSEIRO, C. (ed.). *XIX Latin American Symposium on Solid State Physics. Journal of Physics: Conference Series*. Vol. 167, p. 280-284. New York: Curran Associates, Inc. ISBN 978-1-61738-316-8.

DELGADO, A. V., GONZÁLEZ-CABALLERO, F., HUNTER, R. J., KOOPAL, L. K. & LYKLEMA, J. (2007). Measurement and interpretation of electrokinetic phenomena. *Journal of Colloid and Interface Science*. Vol. 309, iss. 2, p. 194-224. ISSN 1095-7103.

DERKACH, S. R., ILYIN, S. O., MAKLAKOVA, A. A., KULICHIKHIN, V. G. & MALKIN, A. Y. (2015a). The rheology of gelatin hydrogels modified by  $\kappa$ -carrageenan. *LWT - Food Science and Technology*. Vol. 63, p. 612-619. ISSN 0023-6438.

DERKACH, S., ZHABYKO, I., VORON'KO, N., MAKLAKOVA, A. & DYAKINA, T. (2015b). Stability and the rheological properties of concentrated emulsions containing gelatin- $\kappa$ -carrageenan polyelectrolyte complexes. *Colloids and Surfaces A: Physicochemical and Engineering Aspects*. Vol. 483, p. 216-223. ISSN 0927-7757.

DIGENIS, G. A., GOLD, T. B. & SHAH, V. P. (1994). Crosslinking of gelatin capsules and its relevance to their *in vitro-in vivo* performance. *Journal of Pharmaceutical Sciences*. Vol. 83, iss. 7, p. 915-921. ISSN 0022-3549.

DRANCA, I. & VYAZOVKIN, S. (2009). Thermal stability of gelatin gels: Effect of preparation conditions on the activation energy barrier to melting. *Polymer*. Vol. 50, p. 4859-4867. ISSN 0032-3861.

DUNSTAN, D. E., CHEN, Y., LIAO, M. L., SALVATORE, R., BOGER, D. V. & PRICA, M. (2001). Structure and rheology of the  $\kappa$ -carrageenan/locust bean gum gels. *Food Hydrocolloids*. Vol. 15, p. 475-484. ISSN 0268-005X.

FANG, Y., LI, L., INOUE, C., LUNDIN, L. & APPELQVIST, I. (2006). Associative and segregative phase separations of gelatin/K-carrageenan aqueous mixtures. *Langmuir*. Vol. 22, p. 9532-9537. ISSN 0743-7463.

FESSAS, D. & SCHIRALDI, A. (2001). Water properties in wheat flour dough I: classical thermogravimetry approach. *Food Chemistry*. Vol. 72, p. 237-244. ISSN 0308-8146.

FESSAS, D. & SCHIRALDI, A. (2000). Starch gelatinization kinetics in bread dough. *Journal of Thermal Analysis and Calorimetry*. Vol. 61, p. 411-423. ISSN 1388-6150.

FIGURA, L. O. & TEIXEIRA, A. A. (2007). *Food Physics: Physical Properties - Measurement and Applications*. Berlin, Heidelberg, New York: Springer-Verlag. ISBN 978-3-540-34194-9.

FU, Z., WANG, L., ZOU, H., LI, D. & ADHIKARI, B. (2014). Studies on the starch-water interactions between partially gelatinized corn starch and water during gelatinization. *Carbohydrate Polymers*. Vol. 101, p. 727-732. ISSN 0144-8617.

GARCÍA-OCHOA, F., SANTOS, V. E., CASAS, J. A. & GÓMEZ, E. (2000). Xanthan gum: production, recovery, and properties. *Biotechnology Advances*. Vol. 18, iss. 7, p. 549-579. ISSN 0734-9750.

GARREC, D. A., GUTHRIE, B. & NORTON, I. T. (2013). Kappa carrageenan fluid gel material properties. Part 1: Rheology. *Food Hydrocolloids*. Vol. 33, iss. 1, p. 151-159. ISSN 0268-005X.

GERZHOVA, A., MONDOR, M., BENALI, M. & AIDER, M. (2016). Study of total dry matter and protein extraction from canola meal as affected by the

pH, salt addition and use of zeta-potential/turbidimetry analysis to optimize the extraction conditions. *Food Chemistry*. Vol. 201, p. 243-252. ISSN 0308-8146.

GÓMEZ-MASCARAQUE, L. G., LAGARÓN, J. M., LÓPEZ-RUBIO, A. (2015). Electrospayed gelatin submicroparticles as edible carriers for the encapsulation of polyphenols of interest in functional foods. *Food Hydrocolloids*. Vol. 49, p. 42-52. ISSN 0268-005X.

GORODYLOVÁ, N., ŠULCOVÁ, P., DOHNALOVÁ, Ž., BOSACKA, M. & FILIPEK, E. (2015). Application of DTA/TG method for investigation of solid state reaction mechanisms. In: ŠULCOVÁ, P. & DOHNALOVÁ, Ž. (eds.). *Sborník příspěvků termoanalytického semináře TAS 2015*. 1st ed., p. 90-94. Pardubice: Univerzita Pardubice. ISBN 978-80-7395-888-6.

GRYSZKIN, A., ZIEBA, T., KAPELKO, M. & BUCZEK, A. (2014). Effect of thermal modifications of potato starch on its selected properties. *Food Hydrocolloids*. Vol. 40, p. 122-127. ISSN 0268-005X.

GUPTA, S., SAURABH, CH., VARIYAR, P. S. & SHARMA, A. (2015). Comparative analysis of dietary fiber activities of enzymatic and gamma depolymerized guar gum. *Food Hydrocolloids*. Vol. 48, p. 149-156. ISSN 0268-005X.

GYAWALI, R. & IBRAHIM, S. A. (2016). Effects of hydrocolloids and processing conditions on acid whey production with reference to Greek yogurt. *Trends in Food Science & Technology*. Vol. 56, p. 61-76. ISSN 0924-2244.

HOMER, S., KELLY, M. & DAY, L. (2014). Determination of the thermo-mechanical properties in starch and starch/gluten systems at low moisture content – A comparison of DSC and TMA. *Carbohydrate Polymers*. Vol. 108, p. 1-9. ISSN 0144-8617.

IQBAL, M. S., MASSEY, S., AKBAR, J., ASHRAF, C. M. & MASIH, R. (2013). Thermal analysis of some natural polysaccharide materials by isoconversional method. *Food Chemistry*. Vol. 140, p. 178-182. ISSN 0308-8146.

JANALÍK, J. (2010). *Viskozita tekutin a její měření* [online]. Ostrava: Vysoká škola báňská - Technická univerzita Ostrava [cit. 2017-12-24]. Available from: <http://docplayer.cz/14903740-Viskozita-tekutin-a-jeji-mereni.html>

JAIN, A. A., MEHRA, A. & RANADE, V. V. (2016). Processing of TGA data: Analysis of isoconversional and model fitting methods. *Fuel*. Vol. 165, p. 490-498. ISSN 0016-2361.

JING, N. (2005). Model free kinetics. In: Anonym (ed.). *UserCom*. Vol. 1, p. 6-8. Mettler-Toledo.

KEJNAR, Z. (2009). *Kinetické modely degradace v termální analýze*, diploma thesis. Zlín: Univerzita Tomáše Bati ve Zlíně.

KELESSIDIS, V. C., MAGLIONE, R., TSAMANTAKI, C. & ASPIRTAKIS, Y. (2006). Experimental study and predictions of pressure losses of fluids modeled as Herschel–Bulkley in concentric and eccentric annuli in laminar,



transitional and turbulent flows. *Journal of Petroleum Science and Engineering*. Vol. 53, p. 203-224. ISSN 0920-4105.

KUPSKÁ, I., LAPČÍK, L., LAPČÍKOVÁ, B., ŽÁKOVÁ, K. & JUŘÍKOVÁ, J. (2014). The viscometric behaviour of sodium hyaluronate in aqueous and KCl solutions. *Colloids and Surfaces A: Physicochemical and Engineering Aspects*. Vol. 454, p. 32-37. ISSN 0927-7757.

KLOUŽKOVÁ, A., ZEMENOVÁ, P., KLOUŽEK, J. & PABST, W. (2012). *Termická analýza* [online]. Praha: Vysoká škola chemicko-technologická v Praze [cit. 2017-12-30]. Available from:

<http://tresen.vscht.cz/sil/sites/default/files/Termick%C3%A1%20anal%C3%BDza.pdf>

KUMBÁR, V., NEDOMOVÁ, Š., PYTEL, R., KILIÁN, L. & BUCHAR, J. (2017). Study of rheology and friction factor of natural food hydrocolloid gels. *Potravinárstvo: Slovak Journal of Food Sciences*. Vol. 11, iss. 1, p. 203-209. ISSN 1337-0960.

LI, Q., HE, D., CHEN, W. & NI, L. (2005). Preparation, Characterization and Anticoagulant Activity of Guar Gum Sulphate. *Journal of Macromolecular Science, Part A: Pure and Applied Chemistry*. Vol. 42, iss. 8, p. 1085-1094. ISSN 1520-5738.

LI, J. & NIE, S. (2016). The functional and nutritional aspects of hydrocolloids in foods. *Food Hydrocolloids*. Vol. 53, p. 46-61. ISSN 0268-005X.

LI, X., WU, W., WANG, J. & DUAN, Y. (2006). The swelling behavior and network parameters of guar gum/poly(acrylic acid) semi-interpenetrating polymer network hydrogels. *Carbohydrate Polymers*. Vol. 66, p. 473-479. ISSN 0144-8617.

LIU, H., YU, L., XIE, F., & CHEN, L. (2006). Gelatinization of cornstarch with different amylose/amylopectin content. *Carbohydrate Polymers*. Vol. 65, p. 357-363. ISSN 0144-8617.

MA, X. & PAWLIK, M. (2007). Intrinsic viscosities and Huggins constants of guar gum in alkali metal chloride solutions. *Carbohydrate Polymers*. Vol. 70, iss. 1, p. 15-24. ISSN 0144-8617.

MACOSKO, C. W. (1994). *Rheology. Principles, Measurements, and Applications*. New York: Wiley-VCH. ISBN 1-56081-579-5.

MAGNY, B., ILIOPOULOS, I. & AUDEBERT, A. (1994). Aggregation of Hydrophobically Modified Polyelectrolytes in Dilute Solution: Ionic Strength Effects. In: DUBIN, P., BOCK, J., DAVIES, R., SCHULZ, D. N. & THIES, C. (eds.), *Macromolecular complexes in chemistry and biology*. Berlin: Springer-Verlag. 1st ed., p. 51-62. ISBN 978-3-540-57166-7.

MANNION, R. O., MELIA, C. D., LAUNAY, B., CUVELIER, G., HILL, S. E., HARDING, S. E. & MITCHELL, J. R. (1992). Xanthan/locust bean gum interactions at room temperature. *Carbohydrate Polymers*. Vol. 19, p. 91-97. ISSN 0144-8617.

MARCOTTE, M., TAHERIAN, A. R. & RAMASWAMY, H. S. (2001a). Rheological properties of selected hydrocolloids as a function of concentration and temperature. *Food Research International*. Vol. 34, p. 695-703. ISSN 0963-9969.

MARCOTTE, M., TAHERIAN, A. R., TRIGUI M. & RAMASWAMY, H. S. (2001b). Evaluation of rheological properties of selected salt enriched food hydrocolloids. *Journal of Food Engineering*. Vol. 48, p. 157-167. ISSN 0260-8774.

McKENNA, B. M. & LYNNG, J. G. (2003). Introduction to food rheology and its measurement. In: McKENNA, B. M. (ed.). *Texture in food. Volume 1: Semi-solid foods*. 1st ed., p. 131-160. Cambridge: Woodhead Publishing Ltd. ISBN 1-85573-673-X.

MOELBERT, S., NORMAND, B. & DE LOS RIOS, P. (2004). Kosmotropes and chaotropes: modelling preferential exclusion, binding and aggregate stability. *Biophysical Chemistry*. Vol. 112, p. 45-57. ISSN 0301-4622.

MOHAMMADI, M., SADEGHNIA, N., AZIZI, M., NEYESTANI, T. & MORTAZAVIAN, A. M. (2014). Development of gluten-free flat bread using hydrocolloids: Xanthan and CMC. *Journal of Industrial and Engineering Chemistry*. Vol. 20, iss. 4, p. 1812-1818. ISSN 1226-086X.

NOR HAYATI, I., WAI CHING, C. & ROZAINI, M. Z. H. (2016). Flow properties of o/w emulsions as affected by xanthan gum, guar gum and carboxymethyl cellulose interactions studied by a mixture regression modelling. *Food Hydrocolloids*. Vol. 53, p. 199-208. ISSN 0268-005X.

NÚÑEZ-SANTIAGO, M. C., TECANTE, A., GARNIER, C., DOUBLIER, J. L. (2011). Rheology and microstructure of  $\kappa$ -carrageenan under different conformations induced by several concentrations of potassium ion. *Food Hydrocolloids*. Vol. 25, 32-41. ISSN 0268-005X.

PAVLÍNEK, V., STĚNIČKA, M. & MRLÍK, M. (undated). *Reologie potravin a kosmetických prostředků* [online]. [cit. 2017-12-24].

Available from: <http://kosmetika.ft.utb.cz/EntityDisplayTab.aspx?id=4>

PELC, D., MARION, S., POŽEK, M. & BASLETIĆ, M. (2014). Role of microscopic phase separation in gelation of aqueous gelatin solutions. *Soft Matter*. Vol. 10, p. 348-356. ISSN 1744-6848.

PELLETIER, E., VIEBKE, C., MEADOWS, J. & WILLIAMS, P. A. (2001). A Rheological Study of the Order-Disorder Conformational Transition of Xanthan Gum. *Biopolymers*. Vol. 59, p. 339-346. ISSN 0006-3525.

PICULELL, L., BORGSTRÖM, J., CHRONAKIS, I. S., QUIST, P. & VIEBKE, C. (1997). Organisation and association of  $\kappa$ -carrageenan helices under different salt conditions. *International Journal of Biological Macromolecules*. Vol. 21, iss. 1-2, p. 141-153. ISSN 0141-8130.

PLASHCHINA, I. G., MURATALIEVA, I. R., BRAUDO, E. E. & TOLSTOGUZOV, V. B. (1986). Studies of the gel formation of  $\kappa$ -carrageenan

above the coil-helix transition temperature range. *Carbohydrate Polymers*. Vol. 6, iss. 1, p. 15-34. ISSN 0144-8617.

PRUSKA-KEDZIOR, A. & KEDZIOR, Z (2007). Rheological Properties of Food Systems. In: SIKORSKI, Z. E. (ed.). *Chemical and Functional Properties of Food Components*. 3rd ed., p. 209-244. Boca Raton: CRC Press, Taylor and Francis Group, LLC. ISBN 978-0-8493-9675-5.

RAMAJO-ESCALERA, B., ESPINA, A., GARCÍA, J. R., SOSA-ARNAO, J. H. & NEBRA S. A. (2006). Model-free kinetics applied to sugarcane bagasse combustion. *Thermochimica Acta*. Vol. 448, p. 111-116. ISSN 0040-6031.

RAZI, M. M., KELESSIDIS, V. C., MAGLIONE, R., GHIASS, M. & GHAYYEM, M. A. (2014). Effect of Guar Gum Polymer and Lime Powder Addition on the Fluid Loss and Rheological Properties of the Bentonite Dispersions. *Journal of Dispersion Science and Technology*. Vol. 35, p. 1793-1800. ISSN 0193-2691.

RHEIN-KNUDSEN, N., ALE, M. T., AJALLOUEIAN, F., YU, L. & MEYER, A. S. (2017). Rheological properties of agar and carrageenan from Ghanaian red seaweeds. *Food Hydrocolloids*. Vol. 63, p. 50-58. ISSN 0268-005X.

ROOS, Y. H. (1995). Chapter 4 - Water and Phase Transitions. In: ROOS, Y. H. (ed.). *Phase Transitions in Foods*. 1st ed., p. 73-107. San Diego: Academic Press. ISBN 978-0-12-595340-5.

ROUSSENOVA, M., ENRIONE, J., DIAZ-CALDERON, P., TAYLOR, A. J., UBBINK, J. & ALAM, M. A. (2012). A nanostructural investigation of glassy gelatin oligomers: molecular organization and interactions with low molecular weight diluents. *New Journal of Physics*. Vol. 14, iss. 3, p. 1-18. ISSN 1367-2630.

SABOKTAKIN, M. R. (2012). Biomedical Properties Study of Modified Chitosan Nanoparticles for Drug Delivery Systems. In: LIANG, X.-J. (ed.). *Nanopharmaceutics: The Potential Application of Nanomaterials*. P. 129-172. World Scientific Publishing Company, Ltd. ISBN 978-981-4368-66-7.

SADDAWI, A., JONES, J. M., WILLIAMS, A. & WÓJTOWICZ, M. A. (2010). Kinetics of the Thermal Decomposition of Biomass. *Energy & Fuels*. Vol. 24, iss. 2, p. 1274-1282. ISSN 0887-0624.

SAHA, D. & BHATTACHARYA, S. (2010). Hydrocolloids as thickening and gelling agents in food: a critical review. *Journal of Food Science and Technology*. Vol. 47, p. 587-597. ISSN 0975-8402.

SARBON, N. M., BADI, F. & HOWELL, N. K. (2015). The effect of chicken skin gelatin and whey protein interactions on rheological and thermal properties. *Food Hydrocolloids*. Vol. 45, p. 83-92. ISSN 0268-005X.

SCHORSCH, C., GARNIER, C. & DOUBLIER, J. (1997). Viscoelastic properties of xanthangalactomannan mixtures: comparison of guar gum with locust bean gum. *Carbohydrate Polymers*. Vol. 34, p. 165-175. ISSN 0144-8617.

SEN, M. & ERBOZ, E. N. (2010). Determination of critical gelation conditions of  $\kappa$ -carrageenan by viscosimetric and FT-IR analyses. *Food Research International*. Vol. 43, p. 1361-1364. ISSN 0963-9969.

SHAO, P., QIN, M., HAN, L. & SUN, P. (2014). Rheology and characteristics of sulfated polysaccharides from chlorophytan seaweeds *Ulva fasciata*. *Carbohydrate Polymers*. Vol. 113, p. 365-372. ISSN 0144-8617.

SILVA, D. M., NUNES, C., PEREIRA, I., MOREIRA, A. S. P., DOMINGUES, M. R. M., COIMBRA, M. A. & GAMA, F. M. (2014). Structural analysis of dextrans and characterization of dextrin-based biomedical hydrogels. *Carbohydrate Polymers*. Vol. 114, p. 458-466. ISSN 0144-8617.

SZYMCZYK, A., FIEVET, P., MULLET, M., REGGIANI, J. C. & PAGETTI, J. (1998). Comparison of two electrokinetic methods - electroosmosis and streaming potential - to determine the zeta-potential of plane ceramic membranes. *Journal of Membrane Science*. Vol. 143, p. 189-195. ISSN 0376-7388.

THOMBARE, N., JHA, U., MISHRA, S. & SIDDIQUI, M. Z. (2016). Guar gum as a promising starting material for diverse applications: A review. *International Journal of Biological Macromolecules*. Vol. 88, p. 361-372. ISSN 0141-8130.

TOMASIK, P. (2004). Saccharides and Polysaccharides: An Introduction. In: TOMASIK, P. (ed.), *Chemical and Functional Properties of Food Saccharides*. P. 1-18. Boca Raton, London, New York, Washington, D.C.: CRC Press LLC. ISBN 0-8493-1486-0.

TOMŠIČ, M., PROSSNIGG, F. & GLATTER, O. (2008). A thermoreversible double gel: Characterization of a methylcellulose and  $\kappa$ -carrageenan mixed system in water by SAXS, DSC and rheology. *Journal of Colloid and Interface Science*. Vol. 322, iss. 1, p. 41-50. ISSN 1095-7103.

TOPPING, D. (1993). Physiological Aspects of Food Hydrocolloids. In: NISHINARI, K. & DOI, E. (eds.). *Food Hydrocolloids. Structures, Properties, and Functions*. P. 477-484. New York: Springer Science+Business Media, LLC. ISBN 978-1-4613-6059-9.

VARELA, P. & FISZMAN, S. M. (2011). Hydrocolloids in fried foods. A review. *Food Hydrocolloids*. Vol. 25, iss. 8, p. 1801-1812. ISSN 0268-005X.

VIEBKE, C., AL-ASSAF, S. & PHILLIPS, G. O. (2014). Food hydrocolloids and health claims. *Bioactive Carbohydrates and Dietary Fibre*. Vol. 4, iss. 2, p. 101-114. ISSN 2212-6198.

VIEBKE, C., PICULELL, L. & NILSSON, S. (1994). On the mechanism of gelation of helix-forming biopolymers. *Macromolecules*. Vol. 27, p. 4160-4166. ISSN 0024-9297.

VIEBKE, C., WILLIAMS, P. A. (2000). Determination of molecular mass distribution of  $\kappa$ -carrageenan and xanthan using asymmetrical flow field-flow fractionation. *Food Hydrocolloids*. Vol. 14, p. 265-270. ISSN 0268-005X.

VITURAWONG, Y., ACHAYUTHAKAN, P. & SUPHANTHARIKA, M. (2008). Gelatinization and rheological properties of rice starch/xanthan mixtures: Effects of molecular weight of xanthan and different salts. *Food Chemistry*. Vol. 111, p. 106-114. ISSN 0308-8146.

VORON'KO, N. G., DERKACH, S. R., VOVK, M. A. & TOLSTOY, P. M. (2016). Formation of  $\kappa$ -carrageenan–gelatin polyelectrolyte complexes studied by <sup>1</sup>H NMR, UV spectroscopy and kinematic viscosity measurements. *Carbohydrate Polymers*. Vol. 151, p. 1152-1161. ISSN 0144-8617.

VYAZOVKIN, S. (2002). Thermal Analysis. *Analytical Chemistry*. Vol. 74, p. 2749-2762. ISSN 0003-2700.

VYAZOVKIN, S., BURNHAM, A. K., CRIADO, J. M., PÉREZ-MAQUEDA, L. A., POPESCU, C. & SBIRRAZZUOLI, N. (2011). ICTAC Kinetics Committee recommendations for performing kinetic computations on thermal analysis data. *Thermochimica Acta*. Vol. 520, p. 1-19. ISSN 0040-6031.

VYAZOVKIN, S. & WIGHT, C. A. (1999). Model-free and model-fitting approaches to kinetic analysis of isothermal and nonisothermal data. *Thermochimica Acta*. Vol. 340-341, p. 53-68. ISSN 0040-6031.

WAGNER, M. (2009). *Collected Applications: Thermal Analysis. Thermal Analysis in Practice*. Mettler-Toledo.

WANG, S., HE, L., GUO, J., ZHAO, J. & TANG, H. (2015). Intrinsic viscosity and rheological properties of natural and substituted guar gums in seawater. *International Journal of Biological Macromolecules*. Vol. 76, p. 262-268. ISSN 0141-8130.

WILLIAMS, P. A., DAY, D. H., LANGDON, M. J., PHILLIPS, G. O. & NISHINARI, K. (1991). Synergistic interaction of xanthan gum with glucomannans and galactomannans. *Food Hydrocolloids*. Vol. 4, iss. 6, p. 489-493. ISSN 0268-005X.

WILLIAMS, P. A. & PHILLIPS, G. O. (2009). Introduction to food hydrocolloids. In: PHILLIPS, G. O. & WILLIAMS, P. A. (eds.). *Handbook of Hydrocolloids*. 2nd ed., p. 1-22. Cambridge: Woodhead Publishing. ISBN 978-1-84569-414-2.

WU, C., WANG, L., HARBOTTLE, D., MASLIYAH, J. & XU, Z. (2015). Studying bubble–particle interactions by zeta potential distribution analysis. *Journal of Colloid and Interface Science*. Vol. 449, p. 399-408. ISSN 1095-7103.

ZOBEL, H. F. & STEPHEN, A. M. (2006). Starch: Structure, Analysis, and Application. In: STEPHEN, A. M., PHILLIPS, G. O. & WILLIAMS, P. A. (eds.). *Food Polysaccharides and their Applications*. 2nd ed., p. 25-86. Boca Raton: CRC Press. ISBN 978-0-8247-5922-3.

## LIST OF FIGURES

Fig. 2.1. Flow curves of shear stress $\tau$ versus shear rate $\dot{\gamma}$ (with a yield stress $\tau_p$ ) representing different fluids: 1 – Newtonian fluid; 2 – shear-thinning (pseudoplastic) fluid; 3 – shear-thickening (dilatant) fluid; 4 – real plastic fluid; 5 – Bingham ideal plastic fluid; 6 – Eyring model of fluid (Janalík, 2010).....	17
Fig. 3.1. A typical TGA curve of a polysaccharide thermally treated under air conditions. The numbers denote the following components or processes: 1 – volatile components (moisture); 2 – decomposition (dehydration); 3 – combustion of formed carbon black; 4 – residue (ash) (Behlau & Widmann, 2003).....	21
Fig. 4.1. Chemical structure of guar gum (Thombare et al., 2016).....	26
Fig. 4.2. Idealized structure of $\kappa$ -carrageenan. G represents galactose, AG means anhydrogalactose (Sen & Erboz, 2010). ....	27
Fig. 4.3. Chemical structure of xanthan gum. Me – methyl group (Saboktakin, 2013).....	28
Fig. 4.4. Spatial structure of gelatin. The numbers refer to the partial renaturation process in gelatin: 1 – forming of the “collagen fold” conformation after cooling an aqueous gelatin solution; 2 - association of polypeptide chains into a spatial network which is stabilized by lateral inter-chain hydrogen bonding within the helical regions (Roussanova et al., 2012). ....	29
Fig. 7.1. Concentration dependent flow curves of guar gum solutions at 25 °C (increasing shear rate): circle – 0.25 w.%, triangle – 0.50 w.%, square – 0.75 w.%, diamond – 1.0 w.%.....	48
Fig. 7.2. Kraemer plot of studied hydrocolloids samples in water (empty symbols) and in 0.07M KCl (full symbols) at 25 °C (viscosities read at shear rate 20 s <sup>-1</sup> ): circle – guar gum, triangle – $\kappa$ -carrageenan, square – xanthan gum. Linear regression curves: full line – in water, dash-dot line – in 0.07M KCl.....	54
Fig. 7.3. Temperature dependency of the Kraemer constant ( $k_K$ ) of studied samples in water and in 0.07M KCl (at shear rate 20 s <sup>-1</sup> ): circle – guar gum, triangle – $\kappa$ -carrageenan, square – xanthan gum.....	55
Fig. 7.4. TGA curves of powder samples (conditioned at room conditions) in the range 30-600 °C (heating at 10 °C/min).....	61
Fig. 7.5. DTA curves of powder samples (conditioned at room conditions) in the range 30-200 °C (heating at 10 °C/min).....	62

- Fig. 7.6. Kissinger plot of studied powders in the temperature range 30-200 °C: empty circle – guar gum, full triangle –  $\kappa$ -carrageenan, full square – xanthan gum;  $\beta$  – heating rate;  $T_m$  – peak temperature on derivative thermogravimetric curve. Full line – linear regression curve..... 67
- Fig. 7.7. Degree of conversion ( $\alpha$ ) vs. temperature T (in the temperature range 30-200 °C) at different heating rates for xanthan gum powder: empty circle – heating rate 5 °C/min, full diamond – heating rate 10 °C/min, empty square – heating rate 15 °C/min, full hexagon – heating rate 20 °C/min. .... 68
- Fig. 7.8. Model-free kinetics plot of  $\kappa$ -carrageenan in the temperature range 30-200 °C:  $\beta$  – heating rate;  $T_\alpha$  – thermodynamic temperature at the degree of conversion  $\alpha$ . Full line – linear regression curve..... 69
- Fig. 7.9. Arrhenius plot of 0.5% (w/w) samples in water (empty symbols) and in 0.07M KCl (full symbols) (viscosities  $\eta$  read at shear rate 20 s<sup>-1</sup>): circle – guar gum, triangle –  $\kappa$ -carrageenan, square – xanthan gum; T – temperature. Linear regression curves: full line – in water, dash-dot line – in 0.07M KCl..... 75
- Fig. 7.10. Flow curves of 0.5% (w/w) gelatin/polysaccharide blends in 0.07M KCl and 0.07M NaCl at 35 °C (upward shear rate): full circle – guar gum/gelatin, empty triangle –  $\kappa$ -carrageenan/gelatin, full square – xanthan gum/gelatin..... 81
- Fig. 7.11. Temperature dependency of flow behaviour index (n) (Herschel-Bulkley model) of 0.5% (w/w) gelatin/polysaccharide blends in 0.07M KCl and 0.07M NaCl: full circle – guar gum/gelatin, empty triangle –  $\kappa$ -carrageenan/gelatin, full square – xanthan gum/gelatin..... 82
- Fig. 7.12. Arrhenius plots of 0.5% (w/w) gelatin/polysaccharide blends in 0.07M KCl (empty symbols) and in 0.07M NaCl (full symbols) at temperature T (viscosities  $\eta$  read at shear rate 20 s<sup>-1</sup>): circle – guar gum/gelatin, triangle –  $\kappa$ -carrageenan/gelatin, square – xanthan gum/gelatin. Linear regression curves: full line – in 0.07M KCl, dash-dot line – in 0.07M NaCl. .... 85
- Fig. 7.13. Temperature dependency of conductivity (C) of 0.5% (w/w) gelatin/polysaccharide blends in the temperature range 29-41 °C: full circle – guar gum/gelatin, empty triangle –  $\kappa$ -carrageenan/gelatin, full square – xanthan gum/gelatin..... 88

## LIST OF TABLES

Table 7.1. Flow parameters of hydrocolloid solutions in distilled water at 25 °C (upward curves).....	45
Table 7.2. Flow parameters of hydrocolloid solutions in 0.07M KCl at 25 °C (upward curves).....	46
Table 7.3. Effect of temperature on the flow parameters of Herschel-Bulkley model (without extrapolation) for 0.25% (w/w) solutions.....	47
Table 7.4. Intrinsic viscosity and Kraemer constant at 20 s <sup>-1</sup> and 100 s <sup>-1</sup> for samples in distilled water. ....	52
Table 7.5. Intrinsic viscosity and Kraemer constant at 20 s <sup>-1</sup> and 100 s <sup>-1</sup> for samples in 0.07M KCl. ....	53
Table 7.6. Thermal analysis of powders (conditioned at room conditions) in the temperature range 30-200 °C at different heating rates. ....	59
Table 7.7. Thermal analysis of powders at constant moisture level (adjusted at different conditions) in the temperature range 30-200 °C at heating rate 10 °C/min.....	60
Table 7.8. Thermal stability (burning profile) of powders (conditioned at room conditions) in the temperature range 200-400 °C at heating rate 10 °C/min.....	63
Table 7.9. Activation energy of powders (conditioned at room conditions) calculated by kinetic models in the temperature range 30-200 °C. ....	66
Table 7.10. Activation energy and pre-exponential factor at 20 s <sup>-1</sup> and 100 s <sup>-1</sup> (upward curves) for samples in distilled water. ....	73
Table 7.11. Activation energy and pre-exponential factor at 20 s <sup>-1</sup> and 100 s <sup>-1</sup> (upward curves) for samples in 0.07M KCl.....	74
Table 7.12. Flow parameters of 0.5% (w/w) gelatin/polysaccharide blends in 0.07M KCl (upward curves).....	79
Table 7.13. Flow parameters of 0.5% (w/w) gelatin/polysaccharide blends in 0.07M NaCl (upward curves).....	80
Table 7.14. Arrhenius parameters at 20 s <sup>-1</sup> and 100 s <sup>-1</sup> (upward shear rate) of 0.5% (w/w) gelatin/polysaccharide blends in 0.07M KCl and 0.07M NaCl. ....	84
Table 7.15. ζ-potential analysis of 0.5% (w/w) gelatin/polysaccharide blends in 0.07M KCl and 0.07M NaCl. ....	87



## LIST OF SYMBOLS AND ABBREVIATIONS

$A$	pre-exponential factor
$a$	exponential constant of Mark-Houwink equation
$C$	conductivity
$c$	concentration
$c^*, c^{**}$	critical concentrations
$d$	effective diameter
$E_a$	activation energy
$f(\alpha)$	reaction model
$H_0$	null hypothesis
$H_1$	alternative hypothesis
$\Delta H$	reaction enthalpy
$K$	constant of Mark-Houwink equation
$k$	consistency coefficient
$k_i$	rate constant
$k_K$	Kraemer constant
$\Delta m_w$	weight loss (moisture content)
$n$	flow behaviour index
$n_i$	reaction order
$R$	molar gas constant
$R^2$	determination coefficient
$T$	temperature
$T_g$	gelation temperature
$T_m$	peak temperature on derivative thermogravimetric curve
$T_{mid}$	midpoint transition temperature
$T_p$	peak temperature
$T_\alpha$	temperature at the degree of conversion $\alpha$
$t$	time
w. %	weight percent (w/w)
$\alpha$	degree of conversion (conversion rate)
$\alpha_m$	degree of conversion corresponding to $T_m$ (Kissinger model)
$\beta$	heating rate
$\gamma$	shear rate
$\gamma_{crit}$	critical shear rate
$\eta$	dynamic viscosity
$\eta_0$	constant viscosity (below critical shear rate, or at zero $\gamma$ )
$\eta_\infty$	viscosity at infinite shear rate
$\eta_r$	relative viscosity
$\eta_{sp}$	specific viscosity
$[\eta]$	limiting viscosity number (intrinsic viscosity)
$[\eta]_K$	intrinsic viscosity according to the Kraemer equation

$\tau$	shear stress
$\tau_0$	yield stress
ANOVA	analysis of variability
EGA	evolved gas analysis
DSC	differential scanning calorimetry
DTA	differential thermal analysis
PECs	biopolyelectrolyte complexes
RH	relative humidity
TA	thermal analysis
TBU	Tomas Bata University
TGA	thermogravimetric analysis
XRD	X-ray diffraction

## LIST OF PUBLICATIONS

### Articles in international journals with impact factor (Web of Science)

VALENTA, T., LAPČÍKOVÁ, B. & LAPČÍK, L. (2018). Determination of kinetic and thermodynamic parameters of food hydrocolloids/water interactions by means of thermal analysis and viscometry. *Colloids and Surfaces A: Physicochemical and Engineering Aspects*. Vol. 555, p. 270-279. ISSN 0927-7757.

LAPČÍKOVÁ, B., VALENTA, T. & LAPČÍK, L. (2017). Rheological Properties of Food Hydrocolloids based on Polysaccharides. *Journal of Polymer Materials*. Vol. 34, iss. 3, p. 631-645. ISSN 0970-0838.

LAPČÍK, L., VAŠINA, M., LAPČÍKOVÁ, B. & VALENTA, T. (2016). Study of bread staling by means of vibro-acoustic, tensile and thermal analysis techniques. *Journal of Food Engineering*. Vol. 178, p. 31-38. ISSN 0260-8774.

### Articles in journals indexed in Scopus database

LAPČÍKOVÁ, B., VALENTA, T., LAPČÍK, L., FUKSOVÁ, M. (2018). Thermal aging of edible oils: spectrophotometric study. *Potravinárstvo: Slovak Journal of Food Sciences*. Vol. 12, iss. 1, p. 372-378. ISSN 1337-0960.

VALENTA, T., LAPČÍKOVÁ, B., LAPČÍK, L., LI, P. (2017). The effect of conformational transition of gelatin-polysaccharide polyelectrolyte complex on its functional properties. *Potravinárstvo: Slovak Journal of Food Sciences*. Vol. 11, iss. 1, p. 587-596. ISSN 1337-0960.

### Conference proceedings

VALENTA, T., LAPČÍKOVÁ, B., LAPČÍK, L. (2016). Thermal properties of food hydrocolloids. In: JAMPÍLEK, J. & MARVANOVÁ, P. (eds.). *8<sup>th</sup> Central European Conference "Chemistry towards Biology"*. *Book of Abstracts*. P. 162. Brno: University of Veterinary and Pharmaceutical Sciences Brno. ISBN 978-80-7305-777-0.

# Curriculum Vitae

## Personal Data:

Name: Ing. Tomáš Valenta  
Date of birth: 19.7.1986  
Place of birth: Zlín  
Address: třída Svobody 1033  
763 02 Zlín – Malenovice  
Nationality: Czech  
Phone: +420 774 354 058  
E-mail: [tvalenta@utb.cz](mailto:tvalenta@utb.cz)  
Affiliation: Tomas Bata University in Zlín, Faculty of Technology, Department of Food Technology  
Supervisor: doc. Mgr. Barbora Lapčíková, Ph.D.,  
lecturer and academic scientific researcher

## Education:

Since September 2014 **Full-time Ph.D. study** at TBU in Zlín, Faculty of Technology, Department of Food Technology. Degree course: Food Technology. Thesis topic: *The study of foodstuff rheological and thermal properties*

2009 – 2011 **Master's Degree** at TBU in Zlín, Faculty of Technology. Degree course: Technology, Hygiene and Economics of Food Production. Diploma topic: *Antibiotic resistance of bacterial strains Escherichia coli and its importance in food chain*

2006 – 2009 **Bachelor's Degree** at TBU in Zlín, Faculty of Technology. Degree course: Chemistry and Food Technology. Bachelor topic: *Enzymatic hydrolysis of carbohydrates and proteins*

2002 – 2006 **Gymnázium T. G. Masaryka** (grammar school in Zlín).  
Final exams in Czech, German, Chemistry and Biology (May 2006)

### **Work on projects:**

- 2018 IGA/FT/2018/003  
The role of additives and other functional substances in food production
- 2017 IGA/FT/2017/004  
The use of additives and other functional substances in selected food products
- 2016 IGA/FT/2016/003  
The application of additives and other functional substances during the production of selected foodstuffs
- 2015 IGA/FT/2015/004  
The study of the function of selected additives and biologically active substances in foodstuffs

### **Conferences:**

30. – 31.3.2017 XIV. Scientific Conference with International Participation „Bezpečnost’ a kontrola potravin“, Piešťany
- 28.8. – 1.9.2016 8<sup>th</sup> Central European Conference „Chemistry towards Biology“, Brno

### **Seminars, courses:**

- 19.6.2018 Rheological seminar with the presentations of the companies Alpha Technologies, Netzsch and Schill+Seilecher, TBU, Zlín
13. – 14.11.2017 Training course „Jak psát a řídit projekt ve vědě a výzkumu“, TBU Job Centre, Zlín

26.9.2017 Seminar „Termická analýza Mettler-Toledo 2017“, Prague

21.5.2015 Lecture about grant program „Horizont 2020“, TBU Library, Zlín

**Language skills:** English (level B2)  
German (level B1)  
Chinese (level A1)

2016 – 2018 Chinese Language and Culture Course (public course), Faculty of Humanities, TBU in Zlín

**Computer skills:** MS Office (Word, Excel, PowerPoint)  
TA-60 software (Shimadzu, Japan)  
SigmaPlot (Systat Software, USA)

**Other skills:** Food Handler Card of the worker in the food industry

**Interests:** Arts and history  
Creative writing



# **The study of foodstuff rheological and thermal properties**

Studium reologických a termických vlastností potravin

Doctoral Thesis

Edition: published electronically

Typesetting by: Author

This publication has not undergone any proofreading or editorial review.

Publication year: 2018